IMPACT OF CLIMATE AND LAND USE LAND COVER CHANGE ON STREAMFLOW: A CASE STUDY OF YADOT RIVER WATERSHED, GENALE DAWA BASIN, ETHIOPIA.

MSc. THESIS

ABAY MUSTEFA ABDULE

HAWASSA UNIVERSITY, HAWASSA, ETHIOPIA

OCTOBER, 2021

IMPACT OF CLIMATE AND LAND USE LAND COVER CHANGE ON STREAMFLOW: A CASE STUDY OF YADOT RIVER WATERSHED GENALE DAWA BASIN, ETHIOPIA.

ABAY MUSTEFA ABDULE

A THESIS SUBMITTED TO THE DEPARTMENT OF WATER RESOURCES AND IRRIGATION ENGINEERING, INSTITUTE OF TECHNOLOGY, SCHOOL OF GRADUATE STUDIES

HAWASSA UNIVERSITY

HAWASSA, ETHIOPIA

IN PARTIAL FULFILLMENT OF THE REQUIREMENTS FOR THE DEGREE OF MASTER OF SCIENCE IN WATER RESOURCE ENGINEERING AND MANAGEMENT

OCTOBER, 2021

SCHOOL OF GRADUATE STUDIES

HAWASSA UNIVERSITY

ADVISORS' APPROVAL SHEET

(Submission Sheet -1)

This is to certify that the thesis entitled **"Impact of Climate and Land Use Land Cover Change on Stream flow (A Case Study of Yadot River Watershed Genale Dawa Basin, Ethiopia)"** submitted in partial fulfillment of the requirement for Degree of Master of Science in Water Resource Engineering and Management, the graduate program of the department /School of Biosystems and Water Resources Engineering has been carried out Abay Mustefa ID.NO.WREMK/001/08, under my/our supervision. Therefore, I/we recommend that the student has fulfilled the requirement and hence hereby can submit the thesis to the department.

Abraham Woldemichael (PhD)	_________________________	_____________
Major advisor	Signature	Date
Alemayehu Muluneh(PhD)	_________________________	_____________
Co-advisor	Signature	Date

SCHOOL OF GRADUATE STUDIES

HAWASSA UNIVERSITY

EXAMINERS' APPROVAL SHEET-1

(Submission Sheet -2)

We, the undersigned members of the Examining Board of the Final MSc Open Defense by **Abay Mustefa** have read and evaluated his /her thesis entitled **"Impact of Climate and Land Use Land Cover Change on Stream flow (A Case Study of Yadot River Watershed Genale Dawa Basin, Ethiopia)"** and examined the candidate.

This is, therefore, to certify that the thesis has been accepted in partial fulfillment of requirement for the degree of Master of Science in Water Resource Engineering and Management.

Abraham Woldemichael (PhD)	___________________	___________________
Major Advisor	Signature	Date
Alemayehu Muluneh (PhD)	___________________	_________________
Co-advisor	Signature	Date
Tewodros T (PhD)	___________________	___________________
Chair man	Signature	Date
Mulugeta D. (PhD)	___________________	___________________
Name of Internal Examiner	Signature	Date
Habtamu H. (PhD)	___________________	______________
Name of External Examiner	Signature	Date
___________________________	___________________	___________________
SGS Approval	Signature	Date

Final approval and acceptance of the thesis is contingent upon the submission of the final copy of the thesis to the School of Graduate Studies (SGC) through the Department /School of graduate committee (DGC/SGS) of the candidate's department.

Stamp of SGS Date: ___________________

Declaration

I hereby declare that this MS thesis is my original work and has not been presented for a degree in any other university, and all sources of material used for this thesis / dissertation have been duly acknowledged.

Name: _Abay Mustefa

Signature: __________________

Date of Submission: _____________________

Email: Abayfx2007@gmail.com

DEDICATION

This work is dedicated to my lovely wife Fanu Amare**,** for nursing me with affection, love and for her dedication in all success of my life.

ACKNOWLEDGEMENT

I would like to express my sincere gratitude to my major advisor Dr. Abraham W/Michael and Co-Advisor Dr. Alemayehu Muluneh for their patient, continuous guidance, encouragement and motivation from the start of proposal writing to the completion thesis work. I won't to really thank Dr. Wakjira Takala Dibaba for helping and guiding me to carry out my Msc thesis.

I extend my appreciation and special thanks to Ministry of Agriculture (MoA) for scholar and sponsoring me with financial support in order to finish thesis work. Special thanks also go to Agarfa Agricultural Technical Vocation Education and Training College (ATVET) for providing all other facilities whenever required during the study.

My acknowledgments extended to the National Meteorological Agency of Ethiopia (NMA) and Ministry of Water, Irrigation and Energy (MoWIE) particularly hydrology Department for providing me relevant data including hydro-meteorological and soil shape file required for my study free of payment.

Lastly, but not least, I would like heart-felt thanks to my wife Fanu Amare , my baby Abenezer Abay and to all my family for their consistent love, care and encouragement which served me as a sources of strength throughout the study period.

Above all, I would like to sincere thank the Almighty God, who made it possible, to begin and finish this work successfully. This day what God have done for me is really beyond what I can imagine

TABLE CONTENTS

ACKNOWLEDGEMENT I
LIST OF TABLE V
LIST OF FIGURE VI
LIST OF ABBREVIATION AND ACRONYMS IX
ABSTRACT X
1. INTRODUCTION 1
1.1. Background of the Study 1
1.2. Statement of the Problem 3
1.3. Objectives 4
1.3.1.General objective 4
1.3.2. Specific objectives 4
1.4. Research Questions 4
1.5. Significance of the Study 4
1.6. Scope of the Study 5
2. LITERATURE REVIEW 6
2.1. The Concept and Definition of Land Use Land Cover 6
2.2. Land Use Land Cover Changes in Ethiopia 6
2.3. Land Use Land Cover Change Impact on Stream Flow 8
2.4. Land Use Land Cover Change Prediction 9
2.5. Application of Remote Sensing for Land Use Land Cover Change 11
2.6. Concept and Definition of Climate Change 12
2.7. Climate Change in Ethiopia 13
2.8. Climate Change Impacts on Stream Flow 14
2.9. Projection of Future Climate 16
2.9.1. Global Climate Model (GCM) 16
2.9.2. Downscaling Techniques (Methods) 17
2.10. Climate Scenarios 18
2.10.1. CORDEX-Africa Domain 19
2.10.2. Regional Climate Model (RCM) 20
3.2.1.1. Comparisons of SRES and RCP climate scenarios 21

3.2.1.2. Representative Concentration Pathways (RCP) 21
2.11. Hydrological Model 23
2.11.1. Type of Hydrological Model 24
2.11.2. Application of SWAT Model 25
3. MATERIALS AND METHODS.. 27
3.1. Description of Study Area.. 27
3.1.1. Location 27
3.1.2. Climate 28
3.1.3. Land Use Land Cover.. 30
3.1.4. Soil.. 30
3.2. Data Collection Methods and Procedures 31
3.2.1. Data Collection... 31
3.2.1.1. Digital Elevation Model.. 31
3.2.1.2. Land Use Land Cover Data 32
3.2.1.3. Soil Map Data 33
3.2.1.4. Hydro – Meteorological Data 33
3.2.1.5. Checking Hydro-Meteorological Data quality 34
3.2.2. Land Use Land Cover Change Detection 37
3.2.2.1. Image Processing and Date of Acquisition... 37
3.2.2.2. Image Classification 37
3.2.2.3. Accuracy Assessment 39
3.2.3. Land Use Land Cover Change Detection Analysis 40
3.2.4. Land Use Land Cover Prediction and Model Validation 40
3.2.4.1. Land Use Land Cover prediction.. 40
3.2.4.2. Validating LULC Prediction Model 41
3.2.5. Near-term and Mid-term Climate Projection 42
3.2.5.1. GCMs and RCMs used for this study 42
3.2.5.2. Bias Correction of Future Climate Data 43
3.2.6. Impact of Climate and LULC Change on Stream flow 45
3.2.6.1. Climate Change Impact Simulation Using SWAT Model...................... 45
3.2.6.2. Description of SWAT Model.. 45
3.2.6.3. Data Input for SWAT Model 47
3.2.7. SWAT Model Setup 47

3.2.7.1. Watershed Delineation 47
3.2.7.2. Hydrological Response Unit (HRU) 48
3.2.7.3. Sensitivity Analysis 48
3.2.7.4. Model Calibration 49
3.2.7.5. Model Validation 50
3.2.7.6. Model Performances Evaluation 50
4.RESULTS AND DISCUSSION 52
4.1. Land Use Land Cover Classification Accuracy Assessment 52
4.2. Land Use Land Cover Change Analysis 54
4.3. LULC Change Transition Probability Matrix between 1985 to 2015 57
4.4. Future Land Use Land Cover Change prediction 60
4.4.1.Validation of CA-Markov Model 60
4.4.2. Predicted future Land Use Land Cover 61
4.5. LULC Transition Probability Matrix between 2015 to 2055 64
4.6. Future Climate Projection 68
4.6.1. Precipitation Projection under RCP4.5 and RCP 8.5 scenarios 68
4.6.2. Temperature Projection under RCP4.5 and RCP 8.5 Scenarios 72
4.7. Calibration and Validation of SWAT Model 76
4.7.1. Sensitivity Analysis 76
4.7.2. Calibration of SWAT Model 77
4.7.3. Validation of Model 78
4.8. Independent and Combined effect of Climate and LULCC on Stream Flow 80
4.8.1. Past Land Use Land Cover Change Impact on Stream flow 80
4.8.2. Future Land Use Land Cover Change Impact on Stream flow 82
4.8.3. Impact of Climate Change on Stream flow 83
4.8.4. Combined Impact of Climate and LULC Change on Stream flow 86
5. SUMMARY CONCLUSIONS AND RECOMMENDATION 91
5.1. Summary and Conclusions 91
5.2. Recommendation 93
6. REFERENCE 94
7. APPENDICES 111

LIST OF TABLES

Table 3.1: Summary of Homogeneity test climate data with 5% (α = 0.05) significance level 36
Table 3.2: Land sat images used for LULC change analyses and their characteristics 37
Table 3.3: Summaries of GCM and RCM climate model used in the study 43
Table 3.4: Performance ratings of recommended statistics for monthly stream flow 51
Table 4.1: Confusion Matrix for LULC Classification 1985... 52
Tables 4.2: Confusion Matrix for LU/LC Classification of 2000.. 53
Table 4.3: Confusion Matrix for LU/LC Classification of 2015 53
Table 4.4: The area coverage of LULC, percent, and rate of changes in the Ydaot watershed between 1985, 2000 and 2015 55
Table 4.5: Transition Area Matrix (ha) between 1985-2000 and 200-2015 period in Yadot watershed. 58
Table 4.6: Comparison of actual and projected LULC 2015... 60
Table 4.7: The k-index values of the simulated LULC map of 2015 60
Table 4.8: The area coverage of LULC, percent, and rate of changes in the Ydaot watershed between 2015, 2035 and 2055 63
Table 4.9: Transition Area Matrix (ha) between 2015 - 2035 and 2035 - 2055 period in Yadot Watershed 66
Table 4.10: Sensitive Flow Parameters, their rank and fitted value 77
Table 4.11: Model Performance Evaluation Statistics for calibration and validation 79
Table 4.12: Mean Annual and Seasonal changes of stream flow results for past LULC change. 80
Table 4.13: Mean Annual and Seasonal change of stream flow results for future LULC change. 82
Table 4.14: Mean annual and seasonal change of flow under RCP4.5 and RCP8.5 scenarios for climate change only from baseline period 84
Table 4.15: Mean Annual and Seasonal change of flow under RCP4.5 and RCP8.5 scenarios for combined climate and LULC change from baseline period.. 87

LIST OF FIGURES

Figure 3.1: Location map of Yadot Watershed.. 27
Figure 3.2: Mean Monthly Rainfall Distributions of the Stations (1985-2015) 29
Figure 3.3: Mean areal rainfalls of the watershed from (1985-2015)...................................... 29
Figure 3.4: Average Monthly Max, Min and Mean Temp in the period of (1985-2015)......... 30
Figure 3.6: Digital Elevation Model of Yadot watershed.. 32
Figure 3.7: Double Mass Curves for the Stations... 35
Figure 3.8: Homogeneity tests of annual rainfall data of individual rain gauge stations 36
Figure 3.9: Pettitt's Homogeneity test of Annual Stream flow.. 36
Figure 4.1: LULC Map of Yadot Watershed in the period 1985, 2000, and 2015................... 56
Figure 4.2: Gain, Loss and Persistence area of LULC class in (1985 -2000) and (2000-2015)59
Figure 4.3: Simulated and observed LULC Map of 2015 61
Figure 4.4: Predicted LULC Map of the year 2035 and 2055 62
Figure 4.5: Gain, Loss and Persistence area of LULC class in (2015 -2035) and (2035-2055)67
Figure 4.6: Mean monthly precipitation under RCP4.5 for near and mid future compared to baseline period. 68
Figure 4.7: Percentage changes of monthly rainfall for near-term and midterm under RCP 4.5 scenarios from baseline period 69
Figure 4.8: Mean monthly precipitation under RCP8.5 for near and mid future compared to baseline period 70
Figure 4.9: Percentage changes of monthly rainfall for near-term and midterm under RCP 8.5 scenarios from baseline period 71
Figure 4.10: Mean monthly maximum and minimum temperatures of near and mid future period with respect to baseline period under RCP 4.5 scenarios... 72
Figure 4.11: Mean monthly and seasonal changes in maximum and minimum temperature (°C) for near and midterm from baseline period under RCP 4.5 scenarios..................................... 73
Figure 4.12: Mean monthly maximum and minimum Temperature of near-term and midterm with respect to baseline period under RCP8.5 scenarios... 74
Figure 4.13: mean monthly and seasonal changes in maximum and minimum temperature (°C) for near and midterm from baseline period under RCP 8.5 scenarios..................................... 75

Figure 4.14: Calibration result for average monthly stream flow (1988-2002)........................ 78
Figure 4.15: Scatter plots of observed and simulated stream flow for Calibration (1988-2002). 78
Figure 4.16: Validation result for average monthly stream flow (2003-2008)......................... 79
Figure 4.17: Scatter plot of observed and simulated stream flow for Validation (2003-2008) 79
Figure 4.18: Mean monthly stream flow results for the past three land use land cover 81
Figure 4.19: Mean monthly flow for near and midterm under RCP4.5 and RCP8.5 scenarios from the baseline period. 85
Figure 4.20: Percentage change of flow for near and midterm future under RCP4.5 and RCP8.5 scenarios compared to baseline period.. 85
Figure 4.21: Mean monthly stream flow for near and midterm under RCP4.5 and RCP8.5 scenarios compared to baseline period. 88
Figure 4.22: Percentage change of flow for near-term and midterm under RCP4.5 and RCP8.5 scenarios compared to baseline period. 89

LIST OF TABLES IN APPENDIX

Tables 1: Mean Monthly Flow for Only LULC under Baseline and future Period................ 111

Tables 2: Major soil type of the watershed.. 111

Tables 3: Meteorological data used for SWAT model (1985-2015) for Delo Mena Station . 111

Tables 4: Mean monthly flow for Climate Change only simulation under RCP4.5 and RCP8.5 112

Tables 5: Mean Monthly Flow for Combined Simulation under RCP4.5 and RCP8.5.......... 112

Tables 6: Projected maximum and minimum Temperature for near and midterm underRCP4.5 and RCP8.5 scenarios 113

Tables 7: Projected mean monthly and % of rainfall under RCP4.5 and RCP8.5.................. 114

LIST OF ABBREVIATION AND ACRONYMS

AR5	Fifth Assessment Report
CCLM4.8	Climate Limited Area Model Version 4.8
CMIP5	Coupled Model Inter-Comparison Project Phase 5
CORDEX	Coordinated Regional Climate Downscaling Experiment
DEM	Digital Elevation Model
EC-EARTH	EC-EARTH Consortium
ERDAS	Earth System Data Analysis System
GIS	Geographic Information System
HadGEM2-ES	Hadley Global Environment Model 2- Earth System
LULC	Land Use Land Cover
MOWIE	Ministry of Water, Irrigation and Electricity
MPI-ESM-LR	Max Planck Institute for meteorology (MPI-M)
NSE	Nash and Sutcliffe Simulation Efficiency
RACMO22T	KNMI, Regional Atmospheric Climate Model, version 22
IPCC	Inter Government Panel on Climate Change
RCA4	Rossby Centre Regional Atmospheric Model Version 4
RCM	Regional Climate Model
RCP	Representative Concentration Pathways
RMSE	Root Mean Square Error
SRES	Special Report on Emission Scenarios
SWAT	Soil and Water Assessment
SWAT-CUP	SWAT- Calibration Uncertainty program

ABSTRACT

Both climate and land use land cover (LULC) change are the main factors that influence hydrological regimes by altering the magnitude of ground water recharge and river flow. Thus, for predicting future stream flow both climate and LULC changes projection should be accounted. In this study, Cellular Automata (CA)-Markov in IDRISI software was used to predict the future LULC scenarios and the ensemble mean of three regional climate models (RCMs) in the coordinated regional climate downscaling experiment (CORDEX)-RCM daily precipitation and temperature for Ethiopia under RCP 4.5 (medium emission scenarios) and RCP 8.5(higher emission scenarios) were used for the future climate scenarios. Power transformation and variance scaling method were used to correct bias the RCMs outputs, with respect to the observed precipitation and temperature. The separate and combined impact of climate and LULC change on stream flow was analyzed using SWAT hydrological model. The calibrated and validated for stream flow simulation using SWAT-CUP with a method of SUFI2.The performance of the model was assessed through calibration and validation process and resulted R2 = 0.8 and ENS = 0.73 during calibration and R2 = 0.83 and ENS = 0.77 during validation on monthly base simulation. The results of the ensemble mean of the three RCMs (CCLM4.8, RACMO22T and EC-EARTH) output show parallel precipitation and temperature increasing trends in the future under RCP4.5 and RCP8.5 scenarios but vary on monthly basis. The increases in mean annual maximum and minimum temperatures are higher for higher emission scenarios than medium emission scenarios. The LULC results showed that both in the past and future period, agricultural and settlement are significantly increased while forest land and scrub/bush lands continuously declined conversely grass/range lands and wood land show decline in the past and increased from 2015 to 2035 and again decreased from 2035 to 2055 in the future period. The past LULC caused an increased mean annual flow by 1.26%, and wet season flow by 2.68% but dry season flow decreased by 2.22% while the future LULC 2015 to 2055 will cause mean annual flow increased by 1.19%, and wet season flow by 2.9% but by decreased for dry season flow by 3.14%. The mean annual flow is projected to increase under both climate and combined scenarios by 7.63% (8.13%) and 5.76% (6.26%) in the near (2021-2050), while in the midterm (2051 – 2080) flow increased by 5.76% (6.26) and 6.07% (6.72%) at the outlet of the watershed under RCP4.5 and RCP8.5 scenarios, respectively. Generally, results of future stream flow projection indicated that the combined change of climate and LULC have relatively higher than the climate changed alone. Such studies enhance better understanding of the various impacts of climate and LULC change scenarios on stream flow, which can be used for better adaptation and mitigation of water resources management problem in the watershed by Appling different water and soil conservation measures.

Key Words: Climate Change, Land use/land cover change, CA-Markov, RCP, RCM

1. INTRODUCTION

1.1. Background of the Study

Climate and land Use land Cover change have significant impacts on the hydrology of the watershed through changing processes such as precipitation, evapotranspiration and infiltration, thus affecting the rainfall-runoff processes (Yin *et al*., 2017) and the amount of available water resources (Li *et al*., 2012). Stream flow, as a primary component of the hydrology and widely believed to be affected mainly by climate and land use land cover changes (Ning *et al*., 2016 and Wuletawu *et al*., 2019).

Changes in climate and land use land cover are the two inseparable linked global environmental challenges the world faces today (IPCC, 2019). Since the beginning of the industrial revolution in the mid-eighteenth century, the contribution of human activity to climate change has increased dramatically, by increasing the concentration of greenhouse gases (GHGs) in the atmosphere. The rise in temperature and precipitation patterns are prominent features of change in climate that directly impact almost all other hydrological responses (Azari *et al.*, 2016). Therefore, understanding and quantifying their respective influence is of great importance for water resources management and socio-economic activities as well as policy and planning for sustainable development (Yang *et al*., 2017).

Water resources are currently under severe pressure because of impacts of climate change and human activities, which include land-use change, increasing population growth, and economic development (IPCC, 2013). Climate change due to human activity has led to changes in precipitation patterns and increased the frequency of heavy precipitation events which have been significant effects on the ecological system (Belay *et al*., 2017) and affects streamflow through changes in temperature, precipitation, and evaporation (Ahn and Merwade, 2014; Guo *et al*., 2019). Land use land cover change can significantly alter canopy interception, infiltration and evapotranspiration, which may eventually change the runoff volume, peak flow and flow routing time (Zhang *et al*., 2017and Umair *et al*., 2019). However, the relative impacts of land use land cover and climate change may vary from place to place due to the rate and extent of changes in climate and land-use. Therefore, it is crucial to the long-term water resource planning and management to better understand the potential impacts of climate and land use land cover changes on the runoff and stream flow in the basins.

In recent years, many studies examined the combined impact of land use land cover and climate change on hydrologic processes (Koch *et al*., 2015; Hyandye *et al*., 2018; Aboelnour *et al*., 2019). The findings from different studies consistently highlight the water balance components including streamflow, surface runoff, groundwater, and evapotranspiration are likely to be impacted by future land use and climatic changes. Determining the individual or combined hydrological consequences of climate and land use land cover changes is a key for implementing effective measures for adaptation of climate change and understanding the patterns of water use under different land use land cover policies (Wang *et al*., 2018; Clerici *et al.*, 2019; Trolle *et al*., 2019). For example, some studies have found that the hydrological processes are impacted more by climate change than land-use change (Dagnenet *et al*., 2018; Aboelnour *et al*. , 2019), and other studies have indicated that the impacts of land-use change are more significant as compared to the impacts of climate change (M wangi *et al*. , 2016; Yin et al. , 2017). On the other hand, enhancing land use land cover will mitigate the negative effects of climate change (Tekalegn *et al*., 2018; Mulatu *et al*., 2019). This suggests that the combined effect of climate and LULC change on hydrological responses requires site specific investigation.

There are many effective models that can continuously simulate stream flow, erosion or nutrient loss from a watershed. From those hydrologic models the Soil and Water Assessment Tool (SWAT) has been widely applied to understand the relationship between climate and LULC change on hydrology (Chang *et al.*, 2015, Natkhin *et al*., 2015). This study aims to assess the impacts of climate and land use land cover changes on stream flows of Yadot river watershed using SWAT Hydrological model and downscaled hydro climatic data from CORDEX-RCMs output under RCP4.5 and RCP8.5 climate scenarios within Genale Dawa basin of Ethiopia. Integrating remote sensing-based high resolution satellite image of temporal land use land cover classification with hydrological modeling would significantly improve the accuracy in simulating the impacts of the LULC change on the hydrologic regime.

1.2. Statement of the Problem

Yadot watershed is one of the watersheds draining in to river basin of Genale Dawa, and it is under threat due to the growing population and increasing demand of water mainly for irrigation and other development activities. The watershed is intensively cultivated and there is high expansion of settlement in the watershed. The watershed is undergoing climate and land use land cover change due to expansion of agricultural land and unplanned and unrestricted settlement as a result of rapid population growth, deforestation (fire), improper land use and rapid immigration which has an impact on hydrologic response of the watershed. Among these changes in climate and land use land cover have a significant impact on the hydrologic regime by affecting stream flow and volume of rivers flow and evapotranspiration. Therefore, understanding watershed hydrology is crucial for effective and sustainable water resource planning, development and management activities.

Most of the study in the basin focused on the impact of either climate change (Tufa & Sarma 2021; Tesfaye *et al*., 2019) or land use land cover change (Mesfin, 2018) on stream flow response. There was a clear general lack of modeling on the combined impact of land use land cover and climate change on watershed hydrology. In terms of land use land cover and climate change, major participants that alter a stream flow in a study area are urbanization, agricultural and deforestation activities. This continuous change in land use land cover and climate has impacted the water balance of the watershed by changing the magnitude of the components of stream flow which are surface runoff and ground water flow, which results increasing the extent of the water management problem. Therefore, a properly managed rivers watershed can provide fresh drinking water, food, hydropower and recreation. However, there were no comprehensive studies which projected the future impact of climate and land use land cover changes on the hydrologic regime of the basin. Therefore this study tried to bridge this knowledge gap by assessing the impacts of current and future land use land cover and climate change on stream flow of Yadot Watershed.

1.3. Objectives

1.3.1. General objective

The general objective of this study is to assess the impact of climate and land use land cover change on stream flow using SWAT hydrological model and downscaled hydro climatic data from CORDEX-RCMs output under RCP4.5 and RCP8.5 climate scenarios: A Case Study of Yadot River Watershed Genale Dawa Basin, Ethiopia.

1.3.2. Specific objectives

- To detect the past and predict the future land use land cover changes in the Yadot Watershed.
- To assess the projected climate change for the near and midterm in Yadot watershed
- To evaluate the independent and combined effect of climate and land use land cover changes on stream flow in the Yadot Watershed.

1.4. Research Questions

- How are the past and future land-use/land cover changes over time in Yadot Watershed from 1985 to 2055?
- What are the projected changes in precipitation and temperature in the Yadot Watershed in the near and midterm period?
- What is the trend of the past and future land-use/land cover change impact on stream flow?
- What is the combined effect of Land-use/land cover and climate change to the stream flow from near to midterm period in the study area?

1.5. Significance of the Study

The land use land cover and climate change has a significant impact on the natural resources, of the watershed, socio economic and the future potential impacts of these natural resources with respect to the changing environment. However, to determine the effects of climate and land use land cover change on stream flow, it is important to have an understanding of the climate and land use land cover change patterns and the hydrological processes of the watershed. Therefore, the finding research will strongly assist governments and decision/policy makers in planning, formulate and implement effective and appropriate response strategies to minimize the undesirable land use land cover and climate change impacts and any other development activities in a watershed.

The significance of a research conducted in the proposed study area is sound because it adds initiatives in watershed management by enhancing the understanding of impacts of various environment (land use land cover changes) and climate change scenarios which, consequently indicate a potential for measurable changes in the conditions that control water yields including rainfall, temperature and stream flow. In generally, this study will be expected to fill the gaps in incorporating the impact of land use/land cover and climate change on stream flow particular in Yadot River watershed.

1.6. Scope of the Study

This study is a step to understand the combined impact of climate and land use land cover change on stream flow response of the watershed by using different historical and future land use land cover and meteorological data available for climatic analysis in SWAT flow model. This study is limited to look at climate and land use land cover changes impact on stream flow in both historical and future period within in a Yadot River watershed Genale Dawa.

2. LITERATURE REVIEW

2.1. The Concept and Definition of Land Use Land Cover

The terms land use land cover often has been confusing and used interchangeably in the literature and also in daily practice. Thus is it important to define and understand the meaning of these terms. Land cover change refers to modification of the existing land cover or complete conversion of land cover to a new cover type (Wu *et al*., 2013). Land use refers to the intended use or management of the land cover type by human beings. Thus, land use involves both the manner in which the biophysical attributes of land are manipulated and intent underlining that manipulation (the purpose for which the land is used e.g., agriculture, grazing), which are more subtle changes that affect the character of the land cover without changing its overall classification (Di Gregorio, 2016).

Both conversion and modifications of land use land cover have important environmental consequences through their impacts on soil and water, biodiversity and contribute to watershed degradation (Obahoundje *et al*., 2017). Generally, knowing of impacts of land use land cover change on the natural resources like water resources depends on understanding of the past land use practices, current land use land cover patterns, and projection of future land use land cover, as affected by population size and distribution, economic development, technology, and other factors

2.2. Land Use Land Cover Changes in Ethiopia

In Ethiopia, land is used for agriculture, pasture, as forest area, buildings and infrastructure sites or for recreational purposes. With the Rapid population growth and slow modern agricultural technological adoption practices in the country increase pressure in deforestation for more production which means conversion of forest to agricultural land and expansion of urban settlements. The dynamic nature of land use arising from an increasing population at an alarming rate in Ethiopia (Haile and Assefa, 2012). Most land use land cover changes in Ethiopia are caused by human drivers mainly due to population growth (Temesgen *et al*., 2014). The anthropogenic activities result in an expansion of agricultural land and urbanization thereby deforestation.

Accordingly, some remnant stands of natural forests are mainly restricted to religious sites, along rivers and streams, and on peaks of hills where crop cultivation is difficult in the highlands of Ethiopia (Warra *et al.*, 2013). This is due to the rapid expansion of agriculture and rural and urban settlement. Land use land cover changes in Ethiopia, particularly in the highland areas caused by a combination of various factors though it depends on the conditions of the area (Hassen *et al*., 2015). Because of population pressures, economic factors and policy issues, settlements, farmland and degraded lands have been expanding while grasslands and forest areas have been diminishing largely (Binyam *et al*., 2015; Hassen *et al*., 2015). Study by (Ebrahim and Mohamed, 2018) reported that farmlands and settlement areas were expanded at the expense of forest area, shrub lands, and grasslands over the study period between 1957 and 2014 in Gelda watershed, Lake Tana Watershed of Ethiopia.

Most of these studies indicate that croplands have expanded at the expanse of natural vegetation including forests and scrublands; for example (Minichil *et al*., 2016; Temesgan *et al*., 2018; Gudeta, 2016) in Blue Nile basin of Ethiopia. Study on land use and land cover change in the Bale mountain eco-region of Ethiopia showed that forest cover decreased from 20.8 % in 1985 to 20.6 %, 18.8 % and 17.5 % in 1995, 2005 and 2015 respectively. Grass land and shrub land also decreased continuously. But farmland and urban settlement increased continuously. Farm land and urban settlement expansion were found to be major drivers of land use and land cover change (Sisay *et al*. 2016). Similarly, (Yesuph and Dagnew, 2019) reported the consistent increase in farmland and settlement area at the expense of Afro-alpine and sub-Afro-alpine vegetation areas between 1973 and 2017 in Beshillo Watershed of Blue Nile Basin, Northeastern Highlands of Ethiopia.

The observed land use and land cover changes were driven by population growth, agriculture land and rural settlement expansion, and growing demand of forest for extraction of fuel and construction materials (Birhan and Assefa, 2018). The main reason behind higher number of land less in Ethiopia as reported by Fasil (2012) is population growth which converted large areas of grass land or forest land into crop or wood land. In the Gilgel Gibe watershed in the south western part of Ethiopia agricultural land and urban area increased continuously in 1987, 2001 and 2010 all these years (Wakjira *et al*., 2016). Especially in the highlands of Ethiopia, agricultural practices and human settlement have a long history and recently a highland population pressure including depletion of natural resources and unsustainable practices (Leal *et al*, 2021). Therefore, rapid increase in deforestation as well as poor practices of managing farmlands accelerating soil erosion and land degradation in the Ethiopian highlands (Hassen *et al*., 2015).

2.3. Land Use Land Cover Change Impact on Stream Flow

Land use land cover changes have major impacts on hydrological processes, such as runoff and ground water flow (Asmamaw, 2013). It is obvious that land use land cover can affect both the degree of infiltration and runoff following rainfall events, while the degree of land cover can affect rates of evaporation. It was reported by (Amare, 2013) that land use land cover changes affected the stream flow of Gilgel Abbay Watershed, Ethiopia. the study by (Yitea and Van, 2015) identified that there was an increase of stream flow by 16.26m^3/s during wet months and decreased by 5.41 m^3/s from 1986 to 2015 reported that the growth of population and its effect on the land use land cover change has been influencing the hydrology of the Melka Kuntrie basin, in the Upper Awash River basin by changing the magnitude of stream flow and groundwater flow. The land use in 2003, which was mostly converted to agriculture land from forest, grass, or shrub land compared to 1986 land use and the result shows that increased stream flow in the main rainy season, while the stream flow in dry or small rainy season indicted inconsistency from month to month. This result is in line with the finding of (Welde, 2016) which indicated the increment in bare land and agricultural land resulted in increased annual and seasonal stream flow and sediment yielded in volumes in Tekeze Dam watershed.

The study by (Abebe, 2020) analysis has shown that the cultivated land has increased from 60.69% to 67.17% and urban land from 2.3% to 3.36% between 1998 and 2016. Whereas the grassland area has decreased from 11.42% to 5.33%, plantation forest from1.84% to 0.9%, and bare land from 3.58% to 2.56%. Result in the increase means annual stream flow 150.3 m^3/sec to 165.6m3/sec for 1998 and 2016 due to land use change in Megech Dam Watershed, respectively. Rapid population growth increases the crops land by decreases the forest land which results increase in stream flow because of soil moisture demand (Asmamaw, 2013). (Gebrie, 2016) concluded that the land use land cover change have a great influence on stream flow especially during wet season than dry season. Increasing land use conversion (especially for urbanization, deforestation, grassland depletion) can potentially lead to an increase in stream flow and flood frequency (Rajib and Merwade, 2017).

The conversion of the land surface from native cover to managed cropland has an effect on the evapotranspiration, infiltration and overland runoff characteristics of a watershed. The increased removal of native vegetation and soil compaction decreases soil infiltration capacity. Hence, this leads to an increase in stream flow. As the watershed becomes more developed, it also becomes more hydrological active, changing the flood volume and runoff components as well as the origin of stream flow (Tesfa, 2015). The decrease of forest land and grass land was accompanied by the increase in agricultural and built up areas and this change in land use land cover increased surface runoff during wet seasons and reduced base flow during the dry seasons (Getachew and Melesse, 2012).

During storm events, greater surface runoff can exceed the flow carrying capacity of the stream within the watershed which may increase the risk of potential flooding. Understanding how land use land cover change influence stream flow will enable planners to formulate policies to decrease the effect of future land use change on stream flow. Surface runoff is extremely limited under grass or forest vegetation compared with agricultural land. Therefore different types of land use land cover have an impact to increase or decrees stream flow. Quantifying the impacts of land use land cover change practices on the hydrological response of a watershed has been an area of interest for the hydrologists in recent years as this information could serve as a basis for developing sound watershed management interventions (Abdi *et al.,* 2014).

2.4. Land Use Land Cover Change Prediction

Markov Chain Model was presented by a Russian mathematician named Andrei A. Markov in 1970. Markov chain analysis is a convenient tool for modeling land use land cover (LULC) change when changes and processing in the land use land cover (LULC) are difficult to describe. Markov is a stochastic model which requires pairs of LULC images (Clark labs, 2012; Eastman, 2012). Markov chains are stochastic processes (Halmy *et al*., 2015) and the matrices to show changes between land use categories (based on the basic core principle of continuation of historical development) (Koomen and Borsboom-van Beurden, 2011) and are often used in modeling and simulation changes and trends of LULC (Halmy *et al*., 2015; Mishra and Rai, 2016; Parsa *et al*., 2016). The homogeneous Markov model for prediction of land use changes can be mathematically presented as follows (Subedi *et al*., 2013):

$$L_{(t+1)} = P_{ij} * L_{(t)} \text{ ---------------------------------- } 1$$

$$P_{ij} = \left\{ \begin{matrix} P11 & p12 & \ldots\ldots p1n \\ P21 & p22 & \ldots\ldots P2n \\ \ldots & \ldots & \ldots \\ \ldots & \ldots & \ldots \\ Pn1 & Pn2 & \ldots\ldots..pnn \end{matrix} \right\} \ldots\ldots\ldots\ldots\ldots\ldots\ldots\ldots\ldots\ldots\ldots\ldots.2$$

$((0 \leq Pij \angle 1) \sum_{j=1}^{m} Pij = 1(i, j = 1, 2, \ldots\ldots. n)$ Where *L(t)* and *L(t+1)* represent land use status at time *t* and *t + 1* respectively. *Pij* is the transition probability matrix in a state; *Pn* is the number of LULC categories

Cellular Automat (CA) is a spatial dynamic model which predicts transitions among any number of LULC categories (Li *et al*., 2015). The CA-Markov analysis was used to test run a pair of land cover images and outputs a transition probability matrix and a transition areas matrix. The transition probability matrix explains the probability that each land cover category changed to every other category. The transition areas matrix is the number of pixels that are expected to change from each land cover type to every other land cover type over the specified number of time units. CA consists of a grid or a raster space, a set of states characterizing the grid cells and a definition for the neighborhood arrangement of cells, a set of transition rules determine the state transitions for each of the cells as a function of the position of neighboring cells and a sequence of discrete time steps then updates composition and configuration of all the cell simultaneously (Arsanjani *et al*., 2013; Mishra and Rai, 2016; Parsa *et al*., 2016).

The basic principle of CA is that the land use changes for any location (cells) can be explained by the current state and changes in neighboring cells (Koomen and Borsboom-van Beurden, 2011). Mathematically, CA model (Al-sharif and Pradhan, 2013) is expressed as

$S_{(t,t+1)} = f(S(t), N)$---3

Cellular Automat –Markov (CA-Markov) is a robust model which integrates the ability of Markov and CA models (Li *et al*., 2015). Cellular automata added into a Markov model lead to probable spatial transitions occurring in particular area over a period time (Subedi *et al*., 2013). In other words, the quantity of changes from the Markov Chain model then is made geo-referred and spatial through cellular automata (Mishra and Rai, 2016). The CA-Markov model uses Markov Chain analysis outputs, particularly the transition area file, to apply a contiguity filter to enable the development of other land use characteristics from two LULC into (combined one LULC) one a later time period (Parsa *et al*., 2016). CA-Markov model is considered a robust approach because of the quantitative estimation and the spatial and temporal dynamic it has for modeling the LULC dynamic (Mishra and Rai, 2016; Parsa *et al*., 2016)**.** In this study, IDRISI Selva v.17 is used to predict the future LULC of study area on CA-Markov model.

2.5. Application of Remote Sensing for Land Use Land Cover Change

Remote Sensing is the science and art of obtaining information about an object, area or phenomenon through an analysis of the data acquired by a device which is not in contact with the object, area or phenomenon under investigation (Reddy, 2008). Remote Sensing (RS), integrated with Geographic Information System (GIS) provides an effective tool for analysis of land use and land cover changes (Afera *et al*., 2018). It is observed that, Remote Sensing and GIS is the most modern technology widely used in natural resource management and monitoring and is a helpful tool in detecting and analyzing spatiotemporal land use/land cover dynamics and evaluation of land use and land cover changes at watershed levels (Ermias *et.al*., 2013). Some of the application of remote sensing technology in mapping and studying of the land use and land cover changes are; map and classify the land use and land cover, assess the spatial arrangement of land use and land cover, allow analysis of time-series images used to analyze landscape history, report and analyze results of inventories including inputs to Geographic Information System (GIS), provide a basis for model building.

(Andualem *et al.* 2018) applied remote sensing to detect the land use of Upper Rib watershed. Their result implies the huge reduction in grassland and increment in cropland (13.78%) for over an 11year period. This was due to the increased population with great interests in agricultural land. Asirat, (2018) also applied Remote Sensing and GIS for evaluating land use land cover dynamics in Upper Blue Nile and reported the increment in cropland and grassland, while a reduction in forest and scrubland. The changes were due to an increment in the human and livestock population in the area. To monitor the rapid changes of land cover, to classify the types of land cover, and to obtain timely land cover information, multi temporal remotely sensed images are considered effective data sources. Remote sensing and GIS technique have been used extensively to provide accurate and timely information describing the extent of LULC over time. Change detection analysis, employing both GIS and remotely sensed data, has been used to assess forest depletion (Soni *et al.*, 2015; Afera *et al.*, 2018) in the Yadot watershed.

2.6. Concept and Definition of Climate Change

A simple definition climate is the average weather condition of a region over a long period of time. According to IPCC (2013) climate change can be defined as a change in the state of the climate that can be identified by their change and variability of its properties and that persists for an extended period, typically decades or longer. Also (IPCC, 2013) defines climate change as a change in the state of the climate that can be identified by changes in the mean and/or the variability of its properties and persist for an extended period typically a decade or even longer either due to anthropogenic or natural forcing. Climate change is the most serious problem that the whole world is facing today. It is now widely accepted that climate change is already happening and further change is inevitable;

The total increase of 0.78^0C in global temperature from the second half of the 19 century to 1^{st} decade of 20^{th} century (IPCC 2013) There is also change in precipitation over the global land areas, particularly Northern Hemisphere has visible increase in precipitation after 1951 (Hartmann *et al.* 2013). Between the start and end of 20^{th} century, the global surface temperature was increased roughly by 0.74^0C (Shongwe *et al.*, 2015). The average global land and ocean surface temperature data calculated shows a warming of 0.85^0C in the period of1880 to 2012 (Shongwe *et al.*, 2015). The IPCC's latest findings, global average temperatures will probably raise a further 1.1 to 6.4ºC this century, depending on the extent of continued greenhouse gas emissions. Concentration of carbon dioxide (CO_2), methane (CH_4) and nitrous oxide (N_2O) increase since 1750 by 40%, 150% and 20%, respectively (IPPC, 2014). The IPCC 5th Assessment Report (AR5) concluded that most of the observed increase in global average temperature since the mid-20th century is very likely due to the observed increase in anthropogenic greenhouse gas concentrations.

2.7. Climate Change in Ethiopia

Like most of Africa countries, Ethiopia has become warmer over the past century and human induced climate change will bring further warming over the next century at unprecedented rates, (Charles et al., 2011). For the past four decades, the average annual temperature in Ethiopia has been increasing by 0.37°C every ten years, which is slightly lower than the average global temperature rising (Osima *et al.*, 2018: Emerta and Aragie, 2013). According to (Emerta and Aragie, 2013) the greater part of the temperature rise was observed during the second half of the 1990’s and temperature rise is more pronounced in the dry and hot spots of the country, which are located in the northern, northeastern, and eastern parts of the country.

According to Kassie *et al*., (2014), Ethiopia’s mean annual temperature is showing a significant warming trend leading to increasing rates of evapotranspiration and crop water requirements, further adding to the already frequent water stress of crops. Future projections show that the mean maximum temperature will increase from 2 to 2.3°C until 2030 and from 2.2 to 2.7 °C until 2050, while the mean minimum temperature will rise between 0.8 and 0.9°C until 2030 and between 1.4 and 1.7°C until 2050, all in conjunction with a surge of hot days and nights and a decrease of cold days and nights (Gebre *et al*., 2015). According to many studies, the precipitation projection in the next future shows an increase and decrease. Climate change is one of the most investigated issues of Ethiopian climate since its rain-fed agriculture is largely dependent on the amount and regular onset of seasonal precipitation (Gebre *et al*., 2013).

Climate change affects various dimensions of Ethiopia’s economy including hydro-power generation; the country’s health, education and industry sectors; and public spending on productive investments. However, estimating the impact of climate variability on agriculture is more straightforward and easy to quantify (Emerta and Aragie, 2013). Ethiopia is a country where about 80% of the population is engaged in the agricultural sector and the main source of income for rural communities. With growing populations, industrialization, climate change and its variability the situation becomes more and more tense (Goitom, 2014). The IPCC 2014 findings indicate that developing countries, such as Ethiopia, will be more vulnerable to climate change. It may have far reaching implications to Ethiopia for various reasons, mainly as its economy largely depends on agriculture. Large share of Ethiopia's population is very vulnerable to climate change and preparing adaptation options as part of the entire program is very crucial in particular to its inter-annual variability (Bekele *et al*., 2014; Headey *et al*., 2014). Ethiopia's economy depends heavily on agriculture and faces increasing population growth. Ethiopia's agricultural sector contributes 47% of the country's gross national product and more than 80% of its exports. Most of the global climate models project an increase in precipitation in both the dry and wet seasons.

2.8. Climate Change Impacts on Stream Flow

The changes in stream flow characteristics resulting from climate change depend on individual watershed aspects. The impact of climate change on stream flows, soil moisture, ground water and other hydrological parameters essentially involves taking projections of climatic variables (e.g., precipitation, temperature, humidity, mean sea level pressure) at a global scale. According to (Anwar et al., 2016) Stream flow projections for future time periods showed that mean annual stream flow may increase by 7.1, 9.7, and 10.1 % at 2020s, 2050s, and 2080s, respectively, from the baseline period for A2 scenario, whereas for B2 scenario, it will be expected to increase by 6.8, 7.9, and 6.4 % for 2020s, 2040s, and 2080s, respectively in the upper Gilgel Abay Catchment, Blue Nile Basin. (Megersa *et al*., 2021) study in Upper Wabe Bridge watershed found in the Wabe Shebele basin reveals that annual stream flow shows increase trends under RCP 4.5 and RCP 8.5 scenarios in both (2041–2070 and 2071–2099) projection periods. The mean seasonally stream flow decreases in the Belg (short rainy) season by −10.91% and increases in the Kiremt (rainy) season by 17.4%. Hence, the increment trend in stream flow during the Kiremt season will have the utmost significance for the requirement of storage and rainwater harvesting structures for irrigation development during dry season.

(Andargachew and Fantahun 2017) in Gumara catchment, in the Lake Tana Basin-Upper Blue Nile Basin showed that Seasonal and annual flow volume increases in all future time horizons as compared to the base period. Seasonally, the maximum increment was shown in the major parts of the rainy season (Kiremit) and small rainy season (Belg) in which the flow volume increases by 144.65% for A2a scenario and 101.58% for B2a scenario. Moreover, the annual increment showed systematic trends and the increment reaches up to 17.65% for both scenarios at the end of 21st century. (Tesfaye *et al*., 2019) Awata River Watershed, Genale Dawa Basin conclude the average total annual flow at the outlet of the watershed might increase up to 7.3% for the RCP4.5 scenario and 7.0% for the RCP8.5 scenario for the 2018-2047 periods and for 2048-2077 periods it might increase up to 7.7% for RCP4.5 scenario and 7.9% for the RCP8.5 scenario. In conclusion increase in average total annual, seasonal and monthly flow volume is observed for periods which show a corresponding increase in mean annual, seasonal and monthly precipitation during scenario developments.

Several studies conducted in parts different parts of Africa showed that understanding the impacts of climate change is vital especially in regions where the social and ecological systems are highly dependent on climate and water resources. For example, (Aich *et al.* 2014) assessed the impact of climate change on stream flow in four large representative river basins (Niger, Upper Blue Nile, Oubangui and Limpopo basin) and found a statistically significant increase in stream flow for the period 2070 to 2099 compared to the baseline period 1970 to 1999. Study by (Amisigo, 2018) Results obtained the impact assessment showed that future mean annual stream flow into the Volta Lake could increase by about 17% and 16% under the A1B and A2 scenarios, respectively**.** However, stream flows from a few sub basins in the Black and White Volta basins are projected to decrease due to climate change. The climate change is less likely to pose the threat on average water availability. However, temporal variation in river flows is expected to increase in the future (Devkota and Gyawali, 2015).

According to Liersch *et al.* (2018) also showed that climate change may decrease stream flow in the Upper Blue Nile River for the months June and July, but an increase for the period August to November. For example at the local scale (Tufa and Sarma 2021) evaluated climate change-induced impact on stream flow and sediment yield at Genale Watershed, Ethiopia using the SWAT model and statistically downscaled CORDEX-RCM and showed that the increase in discharge in March, April, May, August, September under RCP4.5. However, the same study (Tufa and Sarma 2021) reported more pronounced increase in the same months under RCP8.5 scenarios. Average monthly change of stream flow for the RCP4.5 and RCP8.5 was running from -16.47% to 6.58% and -3.6% to 8.27%, respectively, of 2022–2080.

The study (Mesgana *et al*., 2017) on potential impact of climate change on the streamflow of four major river basins in Ethiopia: Awash, Baro, Genale, and Tekeze show that the ensemble mean of 10 GCMs indicate the temperature in those area increase by about 2.3 °C (3.3 °C) in 2050s (2080s), whereas the mean annual precipitation is projected to increase by about 6% (9%) in 2050s (2080s). This results in about 3% (6%) increase in the projected annual streamflow in Awash, Baro, and Tekeze rivers whereas the annual streamflow of Genale river is projected to increase by about 18% (33%) in the 2050s (2080s). However, such projected increase in the mean annual streamflow due to increasing precipitation over Ethiopia contradicts the decreasing trends in mean annual precipitation observed in recent decades. Therefore in Ethiopia suitable planning and sustainable utilization of water resources development based on climate change impact is very critical

2.9. Projection of Future Climate

2.9.1. Global Climate Model (GCM)

Global Climate Models (GCMs) are the primary tools for understanding the global climate and its projected change under different forcing scenarios. One of the best tools for simulating current and future predictions of climate change scenarios is a global climate model (GCM) (Tang, Xu and Xu, 2012). Many GCMs illustrate global climate in 3D-grid with horizontal resolution from 2.5^0 latitudes by 3.75^0 longitudes for atmospheric component to 1.25^0 latitudes by 1.25^0 longitudes for oceanic component. However, the coarse resolution of GCMs precludes them from capturing the effects of local forcing like terrain effect and land-sea contrasts that modulate the signal at a finer scale (Rummukainen, 2010).

Global climate models also known as general circulation models (GCMs) have significant implications for climate at global and regional scales by indicating that rising concentration of greenhouse gases. According to many research results GCMs are the vital resources used to perform climate change experiments regionally, globally and very fine scale up to point climate pattern from which climate change scenarios are derived; but they have main drawbacks because of their course resolution. A significant spatial scale problem exists between the scale of the GCMs (200-400km) and the scales of interest for impacts and adaptation studies which are often only tens of kilometres or less (Evans, 2011). Their resolution is thus quite coarse relative to the scale of exposure units in most impact assessments. The GCMs simulation skill decreases from climate variables to hydrological variables while the hydrological importance increases along the same direction (Xu, 1999). Further (Xu, 1999) has identified three different gaps in using the GCMs for water resources studies. These are: (i) The spatial and temporal scale mismatches, (ii) The vertical level mismatches, and (iii) The accuracy mismatch (IPCC-TGICA, 2007).

2.9.2. Downscaling Techniques (Methods)

Downscaling is the process of translating the climate projections from coarse resolution GCMs to finer resolutions RCMs (Patte *et al*., 2014). Downscaling is dependent on the ability of GCMs to successfully project the climate change signal; it is limited to where that signal is clear. Downscaling process is an agent that establishes relationship between climate variables on a local scale (predicted) and large-scale atmospheric variables (predictors) (Wilby and Dawson, 2013). Downscaling used to increase the temporal resolution (e.g. from monthly to daily values of precipitation and temperature) or the spatial resolution (e.g., from a GCM grid cell size down to the weather station scale). One of the most important parts of downscaling is its ability to identify and analyze extreme events (Domínguez *et al*., 2013). Downscaling approaches are generally categorized as dynamical, using regional climate models, and statistical, using empirical relationships. Dynamic and statistical downscaling is used for developing local or regional scales information from the global climate scenarios applying global climate model.

Statistical downscaling techniques, which employ a statistical relationship between the large-scale climatic data and local variations derived from historical data (Chen, Brissette and Leconte, 2012). Statistical downscaling involves the establishment of empirical relationships between historical and/or current large-scale atmospheric and local climate variables. Statistical downscaling is based on statistical relationships linking regional climate variables to large scale atmospheric variables (predictors). Such links are determined during an observational period, tested with independent data outside this period, and used for computing future climate projections (Pizzigalli *et al*., 2012). Advantages of statistical modeling also include the opportunity to use “ensemble” GCM results. On the downside, the main disadvantage of this approach is that it requires long historical meteorological weather station data to construct an appropriate link with large-scale variables.

Dynamical downscaling usually involves a nested or higher spatial resolution of 10-50 km of regional climate model (RCM) through the inclusion of more realistic topography and land use/vegetation (Chen, Brissette and Leconte, 2012). In dynamic downscaling systematic errors will occur due to RCMs, require statistical corrections to provide realistic output. Therefore dynamical downscaling often includes statistical modeling in the form of bias correction. Dynamical downscaling utilizing higher resolution regional climate models (RCMs) that respond to the output of GCMs. The GCM output is provided as boundary conditions, which are the values at the edges of the spatial domain of the RCM.

The main drawbacks are the requirement of powerful computing capacities and the dependency on initial and boundary conditions. There is also still a lack of readily available climate scenario ensembles for most regions in the world, although the number of publically available ensemble archives from European projects on similar grid size is increasing, e.g., CORDEX (Evans, 2011). The goal of dynamic downscaling, i.e., to extract local-scale information from large-scale GCM data, is achieved by developing and using the limited area models (LAMs) or regional climate models (RCMs) (Tang, Xu and Xu, 2012).

2.10. Climate Scenarios

Climate scenarios are plausible representations of the future that are consistent with assumptions about future emissions of greenhouse gases and other pollutants and with our understanding of the effect of increased atmospheric concentrations of these gases on global climate. Scenarios have been used by decision makers and planners to analyze the situations where outcomes are uncertain (Bjørnæs, 2015). In climate change research, they have become an important element as they allow researchers to understand the long-term consequences (van Vuuren *et al*., 2011) and describe plausible pathways of climatic condition and other aspects of future (Moss *et al*., 2010). The goal of working with scenarios is not to predict the future but to better understand uncertainties and alternative futures, in order to consider how robust different decisions or options may be under a wide range of possible futures (Wayne, 2013). Future greenhouse gas concentrations are an unknown because we cannot predict what activities humans will engage in that will reduce or increase them. The choice of climate scenarios and related non-climatic scenarios is important because it can determine the outcome of climate impact assessment (IPCC-TGICA, 2007). A range of scenarios can be used to identify the sensitivity of an exposure unit to climate change and to help policy makers decide on appropriate policy responses and recently, the new scenarios called Representative Concentration Pathways (RCP) were developed and used for preparing fifth assessment report (AR5) of IPCC released in 2015.

2.10.1. CORDEX-Africa Domain

World climate Research program has initiated Global Coordinated Regional Downscaling Experiment with the intention of producing an ensemble of high resolution climate change projections by downscaling GCM simulations from Coupled Model Inter-comparison Project Phase 5 (CMIP5) data archive (Taylor *et al*., 2012) on 25Km and 50Km grid spacing for 14 regions of the Globe. Africa was selected as the first target region for the CORDEX activity: see (Jones *et al*., 2011) for more details on CORDEX Climate Projection Frame-work. CORDEX-Africa RCMs generate an ensemble of high resolution historical and future climate projections at regional scale by downscaling different GCMs forced by RCPs based on the Coupled Inter-comparison Project Phase 5 (CMIP5).

Output form CORDEX-Africa domain have been used for impact studies especially over east Africa such as one carried out by (Ngaina, *et al*., 2015) they found out that all the CORDEX models performed well in simulating rain fall over east Africa and predicted high variation of minimum and maximum temperature for both RCP4.5 and RCP8.5. However, temperature increase was found to be higher during long rainy season while increase in rainfall was found to be higher during short rainy season. Nikulin *et al*., (2012) evaluates the ability of ten RCMs over Africa and concludes that all RCMs simulate the seasonal mean and annual cycle quite accurately. Likewise, it is verified that the mean of multi-model outputs do better than individual simulation. Hernández-Díaz *et al*., (2013) strengthens the achievement of (Nikulin *et al*., 2012). They successfully reproduce the overall features of geographical and seasonal distribution over most Africa. A further study carried out in the southern Africa on extreme precipitation events and future climate, found out that the simulated climate output correlates well with the observation of station data (Pinto *et al*., 2016).

2.10.2. Regional Climate Model (RCM)

Regional climate models (RCMs) have become important tools for providing detailed estimates of future climate change, to support a range of studies concerned with the regional impacts of climate change on natural ecosystems, society and even government and large utility planning (Abbasa *et al*., 2016). The spatial resolution of Regional Climate Models (RCMs) provides more reliable results on the regional scale as compared to General Circulation model (GCMs) which provide a new opportunity for climate change effects analysis (Nikulin *et al.*, 2018). The regional climate model requires the driving force of the global climate model to downscale the global climate data to the local area. Many studies of regional effects of different global warming levels are based on ensembles of coarse-resolution global models, however, for impact assessment and adaptation planning, high-resolution regional climate information is necessary (Osima *et al.*, 2018).

Africa is one of the most vulnerable continents to weather and climate variability ((IPCC, 2007). Due to its vulnerability to climate variability, the significant impacts of projected climate change, and the general lack of climate projections based on Regional Climate Downscaling tools, Africa was selected as the first target region for the CORDEX activity: see Jones et al., (2011) for more details on CORDEX Climate Projection Frame-work. The CORDEX downscaled Regional Climate Model (RCM) has relatively fine scale or resolutions (50km x 50km). (Teutschbein and Seibert, 2012) provided a recent review on the use of RCMs for hydrological models. They recommend that a bias correction is necessary for using the outputs in any hydrological models as RCMs are susceptible to systematic model errors caused by imperfect conceptualization, discretization and spatial averaging within grid cells. These biases are typically due to the occurrence of too many wet days with low-intensity rain or incorrect estimation of extreme temperature in RCM simulations

3.2.1.1. Comparisons of SRES and RCP climate scenarios

Reducing of income alterations between world regions technology is the main driving force for demographic and economic development is assumed in all SRES scenarios. In four scenarios change in technological, demographic and economic are driving force of the future the greenhouse gas and Sulphur emission. The four RCP scenarios used in CMIP5 lead to radiative forcing values that range from 2.6 to 8.5 W m^{-2} at 2100, a wider range than that of the three SRES scenarios used in CMIP3 (IPCC, 2013). The SRES scenarios do not assume any policy to control climate change, unlike the RCP scenarios. RCP4.5 and SRES B1 have similar radiative forcing at 2100, and comparable time evolution (within 0.2W m^{-2}). The radiative forcing of SRES A2 is lower than RCP8.5 throughout the 21st century, mainly due to a faster decline in the radiative effect of aerosols in RCP8.5 than SRES A2, but they converge to within 0.1 W m^{-2} at 2100 (IPCC,2013). RCPs represent pathways of radiative forcing, not linked with exclusive socio-economic assumption in contrary to Special Report on Emission Scenarios (SRES). Any single radiative forcing pathway can result from a diverse range of socio-economic and technological development scenarios (Van Vuuren *et.al*, 2011). Two key differences between the new RCPs and the previous scenarios (1) there are no fixed sets of assumptions related to population growth, economic development, or technology associated with any RCP. (2) The RCPs are spatially explicit and provide information a global grid at a resolution of approximately 60 kilometers. This gives the spatial and temporal information about the location of various emissions and land use changes. This is an important improvement as the location of some emissions affects their warming potential

3.2.1.2. Representative Concentration Pathways (RCP)

Representative concentrations pathways (RCPs) have been defined as a basis for long term and near term climate modeling experiments in the climate modeling community (Van Vuurent *et al*., 2011). The definitions of the RCPs allows for a parallel development of new socioeconomic, technical, and policy scenarios that provide insights into the impact of policy decisions on the future climate (Van Vuurent *et al.*, 2011). RCPs are time and space dependent trajectories of concentrations and emission of greenhouse gases and pollutants resulting from human activities, including changes in land use. Different types of emission scenarios are used in climate studies to assess the long-term impact of atmospheric greenhouse gases and pollutants based on assumptions of population growth, economic development level, etc. A new generation of scenarios was developed and later used within CMIP5 of the intergovernmental Panel on climate change (IPCC) Fifth assessment Report (RR5) published on 2013-2014. The latest scenarios developed by the research community are denoted by Representative Concentration Pathways (RCPs); (Van Vuuren *et al*., 2011). The Fifth Assessment Report of IPCC, the scientific community has defined a set of four new scenarios, denoted RCPs. The RCPs represent the four range of GHG emissions scenario include a severe mitigation scenario (RCP2.6), two intermediate scenarios (RCP4.5 and RCP6.0), and one scenario with very high GHG emissions (RCP8.5). Each RCPs defines a specific emissions trajectory and subsequent radiative forcing *(Wayne, 2013)*

RCP2.6 (Low emissions) is developed by the IMAGE modeling team of the PBL Netherlands Environmental Assessment Agency (Wayne, 2013). Radiative forcing level first reaches a value of around 3.1 W/m^2 by mid-century, and returns to 2.6 W/m^2 by the end of 21^{st} centuries (van Vuuren, Stehfest, *et al*., 2011). In order to reach such radiative forcing levels, greenhouse gas emissions are reduced substantially, over time (Characteristics quoted from van Vuuren *et al*., 2011). The important assumption in this scenario is that cropping area increases faster than current trends, while grassland area remains constant. Forest vegetation continues to decline at current trends.

RCP4.5 (Intermediate emissions) developed by the GCAM modeling team at the Pacific Northwest National Laboratory‘s Joint Global Change Research Institute (JGCRI) in the United States. It is the stabilization scenario (Wayne, 2013) in which radiative forcing stabilizes at $4.5W/m^2$ (approximately 650 ppm CO2-equivalent) in 2100 without ever exceeding that value (Thomson *et al*., 2011). The RCP4.5 stabilization scenario is a cost-minimizing pathway. The major assumptions of this scenario are the global population reaches a maximum of 9 billion by 2065 and then declines to 8.7 billion in 2100, declines in energy consumption, increase in fossil fuel consumption, substantial increase in renewable energy and nuclear energy use, decreasing use of croplands and grasslands due to yield increases and large increase in forest area due to strong reforestation programs as a mitigation strategy (Wise *et al*.,. 2009).

RCP6.0 (Intermediate emissions) developed by the AIM modeling team at the National Institute for Environmental Studies (NIES) in Japan. It is stabilization scenario were radiative forcing stabilizes at 6.0 W/m^2 in the year 2100 without exceeding that value in prior years (Masui *et al*., 2011). In this scenario, the GHG emissions will be the highest in 2060 and then decline thereafter. The primary assumptions of this RCP are increase in energy demand, shift from coal based to gas based production technologies, increase in use of non-fossil fuel energy type and increase in population and economic growth in urban area, expansion of cropland and forest area, and decrease in grassland (Masui *et al*., 2011).

RCP8.5 (High Emission Scenarios) consistent with a future with no policy changes to reduce emissions (Bjørnæs, 2015). It was developed by Integrated Assessment Framework by the International Institute for Applied System Analysis (IIASA) in Australia using MESSAGE model (Wayne, 2013) and characterized by increasing greenhouse gas emissions that lead to high greenhouse gas concentrations over time (Riahi *et al*., 2011). This scenario is highly energy intensive with total consumption continuing to grow throughout the century reaching well over three times current levels. Oil use grows rapidly until 2070 after which it drops even quickly. Land use continues current trends with crop and grass areas increasing and forest area decreasing which is driven by an increase in population, a world population of 12 billion by 2100, lower rate of technology development, heavy reliance on fossil fuel, high energy intensity and no implementation of climate policies (Riahi *et al*., 2011).

2.11. Hydrological Model

Hydrological modeling is a powerful technique of hydrological system investigation for both the research hydrologist and practicing water resources engineers involved in the planning and development of integrated approach for the management of water resources. Hydrological modeling methods are widely used to quantify the effects of climate and land use land cover change (Tekalegn *et al.,* 2018). A hydrological model involves the application of mathematical equations to model the physical response of a watershed to meteorological events in a watershed area (Rwigi, 2014). Hydrological model uses mathematical estimations of stream flow as a function of basin characteristics with rainfall and drainage area being the most important input element in addition to soil characteristics, land cover, topography of the watershed, soil water content and availability of an aquifer therefore hydrological models are vital and necessary for water and environment management (Abdulkareem *et. al.*, 2018).

They have been developed for many different reasons and therefore have many different forms. However, hydrological models are in general designed to meet one of the two primary objectives. Among the objectives of hydrological models, getting a better understanding of the hydrologic processes and how changes occur in a watershed, predicting hydrological processes and providing important information for studying potential impacts of changes like LULC are the major ones (Kassa, 2007).

2.11.1. Type of Hydrological Model

A. **Lumped models:** parameters in these hydrologic models typically do not vary spatially within the basin and thus, basin response is evaluated only at the outlet, without explicitly accounting for the response of individual sub-basins. This model empirically based on integrating over some time and space scales. The high non-linear response of watersheds appears linear. Parameters of lumped models often do not represent physical features of hydrologic processes and usually involve a certain degree of empiricism. Though they are conceptually simple and easy to program and apply, they require substantial calibration data and they are not useful outside of the range of calibration. Examples include WATBAL, SRM, HYRROM, SWM4, IHACRES, and others.

B. **Distributed models**: Parameters of distributed models are fully allowed to vary in space at a resolution usually chosen by the user. These are broken down into small time and space increments. The physical processes occurring in the watershed may be explicitly simulated and then integrated to produce the watershed response. Examples in this category are MIKE-SHE, Wetspa, CASC2D, WATFLOOD, and others. They can be used to analyze changing conditions such as land use changes, project alternatives, and climate change and they are extendible beyond the calibration range. However, they are data intensive and code development is difficult. Distributed models generally require large amounts of (often unavailable) data for parameterization in each grid cell. However, the governing physical processes are modeled in detail, and if properly applied, they can provide the highest degree of accuracy.

C. Semi-distributed models: parameters of semi-distributed models are partially allowed to vary in space by dividing the basin into a number of smaller sub-basins. They are a mixture of empirical and physically -based approaches. They lie between lumped and distributed models. They have the advantage of increased spatial resolution and better process descriptions over simple lumped parameter models and have computational advantage over fully distributed, physics-based models. Some of the examples a Semi-distributed model includes SWAT, HEC-HMS, HPV, TOPMODEL, and others.

2.11.2. Application of SWAT Model

The applicability of Soil and Water Assessment Tool (SWAT) model in the impact of land use land cover dynamics on stream flow and sediment yield from Upper Awash basin from Koka Dam was used for analyzing sediment yield. Therefore, 45.05 m^3/s of stream flow and 57.06 Mtone annual sediment yield were entered to Koka dam during 1990 and 66.56 m^3/s of stream flow and 47.36 Mtone annual sediment yield was extracted from the upper awash basin during 2013 land use land cover data. In addition, urban area was increased by 166%, while plantation area appeared to be highly increased. The result obtained shows that there is 47.75 % increment of stream flow and 17 % decrement of sediment yield in 2013 as compared to 1990 land use/land cover data by (Tarik, 2017).

Dagenent *et al* (2017) Analysis of the combined and single effects of LULC and climate change on the streamflow of the Upper Blue Nile River Basin (UBNRB): Using statistical trend tests, remote sensing land cover maps and the SWAT model. The results show an increase of evapotranspiration by up to 0.84%, 59.8% and 55.5% under LULC, climate and combined climate and LULC change by the end of the 21st century under RCP8.5 compared to the baseline period, respectively. Furthermore, both stream-flow and lateral flow are projected to increase by up to 12.85% (9.9%), 28.5% (20.03%) and 26.4% (29.12%) under LULC, climate and combined climate and LULC change scenarios, respectively. As predicted, the shift in magnitude in RCP8.5 emissions is greater than RCP2.6 and RCP4.5.

Birhan et al., (2021) Applied SDSM and SWAT model for modeling projected impacts of climate and land use/land cover changes on hydrological responses in the Lake Tana Basin, upper Blue Nile River Basin, Ethiopia. As predicted, the shift in magnitude in RCP8.5

emissions is greater than RCP2.6 and RCP4.5. The impacts of climate change on water balances are relatively higher than the combined effects of changes in climate and LULC. Future LULC shifts, on the other hand, change comparatively offsetting hydrological components.

Aich *et al*., (2014) this study aims to compare impacts of climate change on stream flow in four large representatives African river basins: the Niger, the Upper Blue Nile, the Ouban-gui and the Limpopo. Eco-hydrological model SWIM (Soil and Water Integrated Model)

Accordingly, the study concluded Kinati *et al*., (2019) SWAT model can be used investigate the Effect of Land Use Land Cover and Climate Change on River Flow and Soil Loss in Didessa River Basin, South West Blue Nile, Ethiopia Future climate changes under RCP scenarios enhanced river discharge and soil loss in the river basin. Average monthly river flow increased by 4.9, 5.7 and 10.6 m3/s due to LULCC between1986 and 2001, 2001 and 2015, and in the long-term between 1986 and 2015, respectively.

3. MATERIALS AND METHODS

3.1.Description of Study Area

3.1.1. Location

The Yadot river watershed is located in Bale Zone, Oromia Regional State South-eastern part of Ethiopia. The watershed is located in Genale-Dawa basin at the upper most parts of the Deyu sub basin. Geographically, the Yadot watershed is located between 6° 18’N and 6°51’N latitudes and 39°49’E and 39°58’E longitudes in South Eastern part of Ethiopia shown on (Figure 3.1). Yadot River originates from an elevation of 4,373 meters above mean sea level, in the Bale Mountains and drains to an elevation of 946 meters above mean sea level at the outlet of the watershed, and total area of the watershed is 735.6 km^2.Yadot River is gauged and its minimum and maximum flows are known and the river is perennial but the flow is decreased during winter season and increased during summer season.

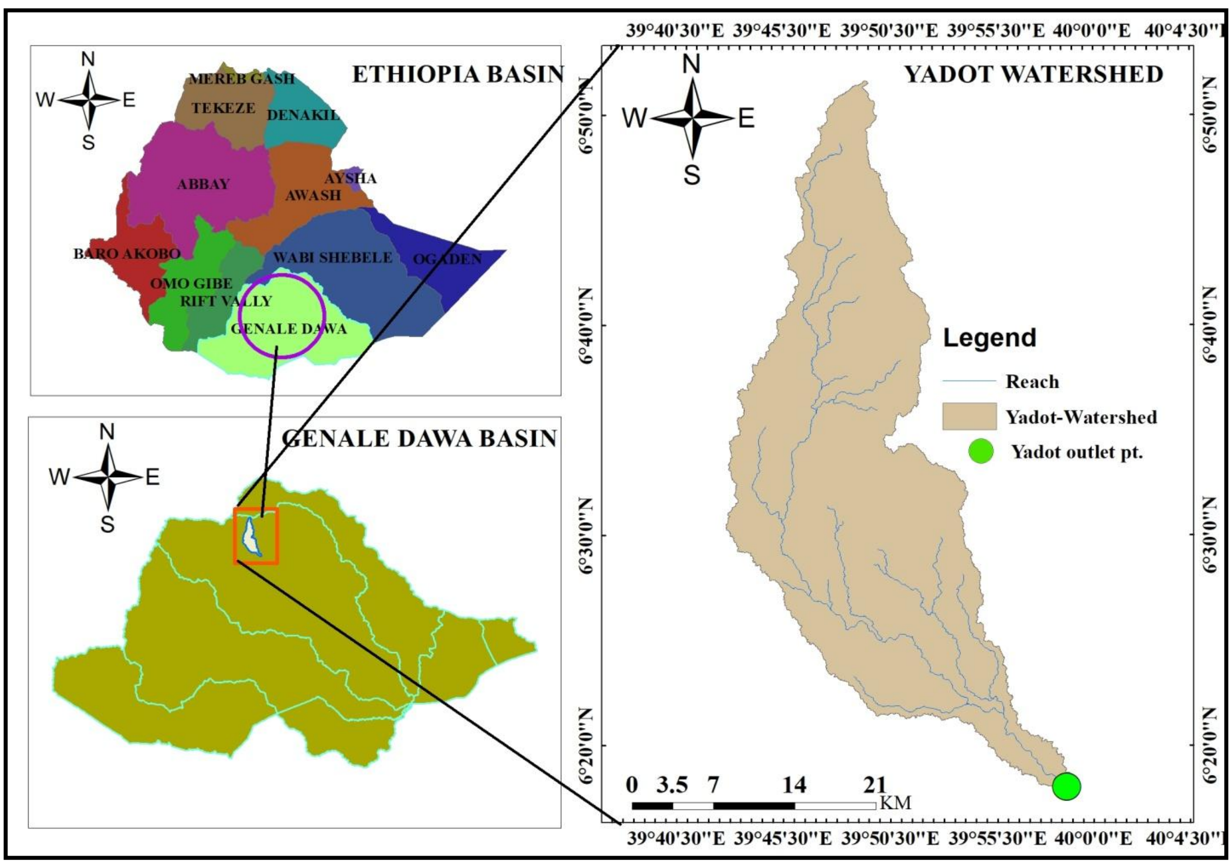

Figure 3.1: Location map of Yadot Watershed

3.1.2. Climate

Ethiopian climate is mainly controlled by the seasonal migration of the Intercontinental Convergence Zone (ITZ) which is conditioned by the convergence of trade winds of the northern and southern hemisphere and associated atmospheric circulation. It is also influenced by regionally and locally by the complex topography of the county. The inter-tropical convergence zone (ITCZ) is the major rain causing mechanism in Ethiopia. The movement of ITCZ in the northward direction brings moisture from the South Atlantic Ocean, which results in the high rainfall in the study area. The traditional climate classification of the country is based on altitude and temperature Wurch (cold climate at more than 3000 m altitude), Dega (temperate like climate-highland with 2500-3000 m altitude), Woina-Dega (warm 1500-2500 m altitude), Kola (hot and arid type, less than 1500 m in altitude), and Bereha (hot and hyper-arid type) climate (NMSA, 2001). According to this classification, the study area falls in Wurch, Dega, Woina Dega and Kola climate zone. Distributions of basin precipitation and temperature are strongly related to the altitude with increasing precipitation and temperature decreasing with altitude. Altitude, topography and vegetation influence climate greatly, resulting in micro climate in specific localities and macro climate in larger areas.

A. Rainfall

The southern regions of Ethiopia experience two distinct wet seasons, which occur as the ITCZ passes through this to its southern position. The entire Genale river sub-basin falls under the “bi-modal” rainfall regime with two wet seasons. The major rainfall occurs from March to May with peak flow in May and again there is rainfall from September to November with peak rain fall in October. The mean annual rainfall (1985-2015) of the study area as shown in (Figure 3.2) varies from around 975 mm Rira up to 1059 mm for Delo Mena and mean annual areal rainfall of the watershed is 1029 mm (Figure 3.3).

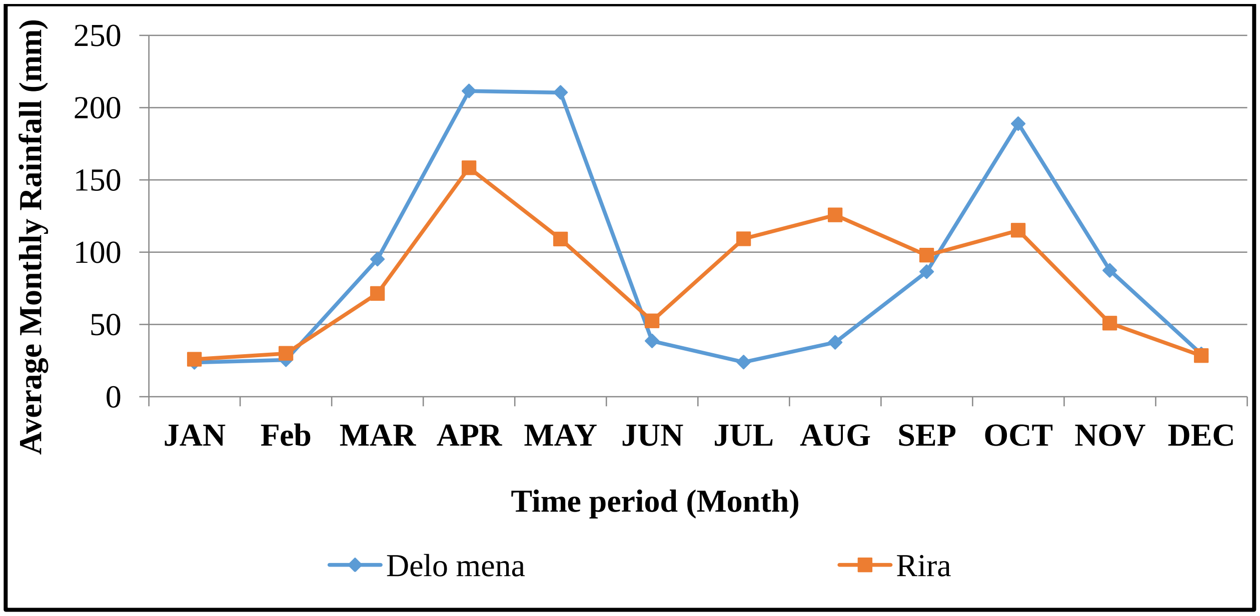

Figure 3.2: Mean Monthly Rainfall Distributions of the Stations (1985-2015)

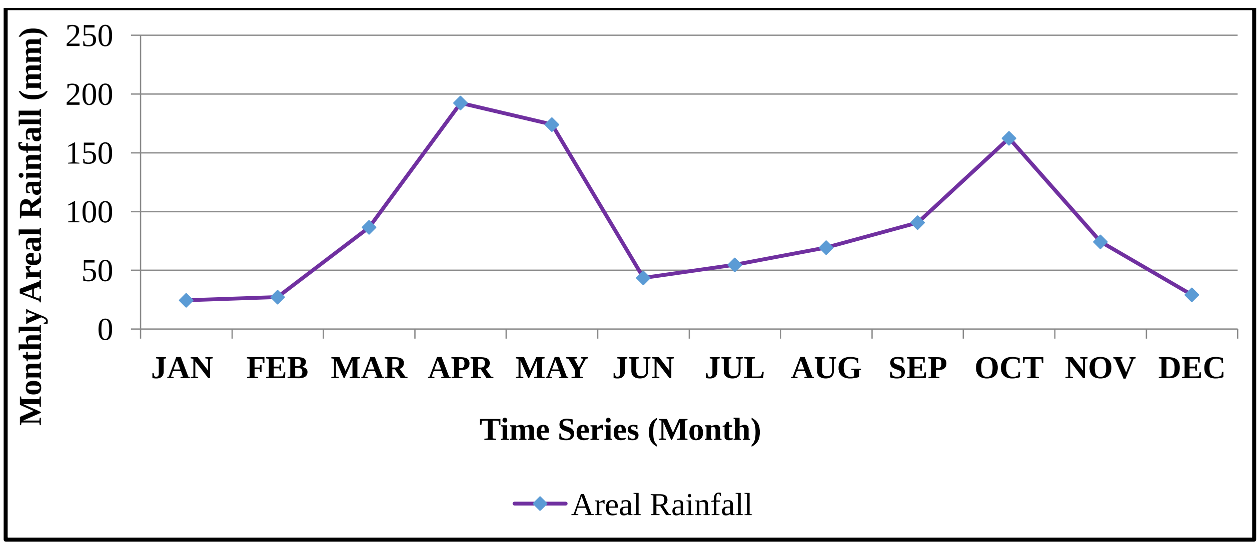

Figure 3.3**:** Mean areal rainfalls of the watershed from (1985-2015)

A. Temperature

It is widely agreed that in the region distribution of temperature is strongly reliant on elevation. Previous studies on Genale Dawa River Basin show that the predicted rise of temperature with a decreasing elevation was closer to 0.64ºC per 100 m elevation (Tsegazeab, 2014). Latitude is a secondary factor influencing mean monthly temperature. The Mean annual maximum temperature at the study varying from 21.6^{0}C at Rira to 28.72^{0}C in Delo Mena and mean annual minimum temperature in the sub basin varies from 9.78^{0}C to 15.62^{0}C at Rira and Delo mean, respectively. The mean annual temperature varies from 12.7^{0}C to 25.16^{0}C in the study period (Figure 3.4).

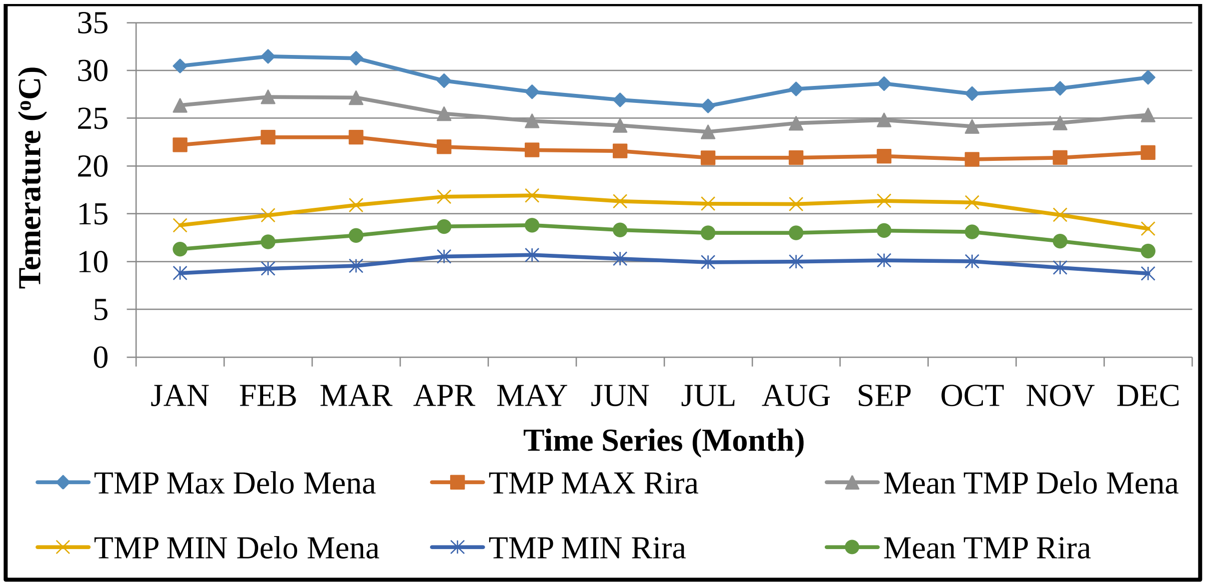

Figure 3.4: Average Monthly Max, Min and Mean Temp in the period of (1985-2015)

3.1.3. Land Use Land Cover

The main land use land covers of the watershed are agricultural lands, grass/range land, forest land, scrub/bush land, wood land and settlement. Out of the total watershed areas 735.6 km^2 (about 60.45%) is covered with dominant forest land and 14.21 % cover with agriculture based on land use land cover map 2015 (Table 4.4) and Figure (4.1).

3.1.4. Soil

Soil data is a significant component for land use land cover change impact on hydrological components of watershed management. According to Food and Agricultural Organization – Harmonized World Soil Database (FAO-HWSD) soil classification, the soil mapping units have been identified in the study area at a scale of 1:1250, 000. The soil type identified in the study area encompasses eight soil types’ and the dominant soil type were pellic vertisols and chromic vertisols covers about 37.84% and 26.42% of the watershed total area, respectively (Appendices Table 2).

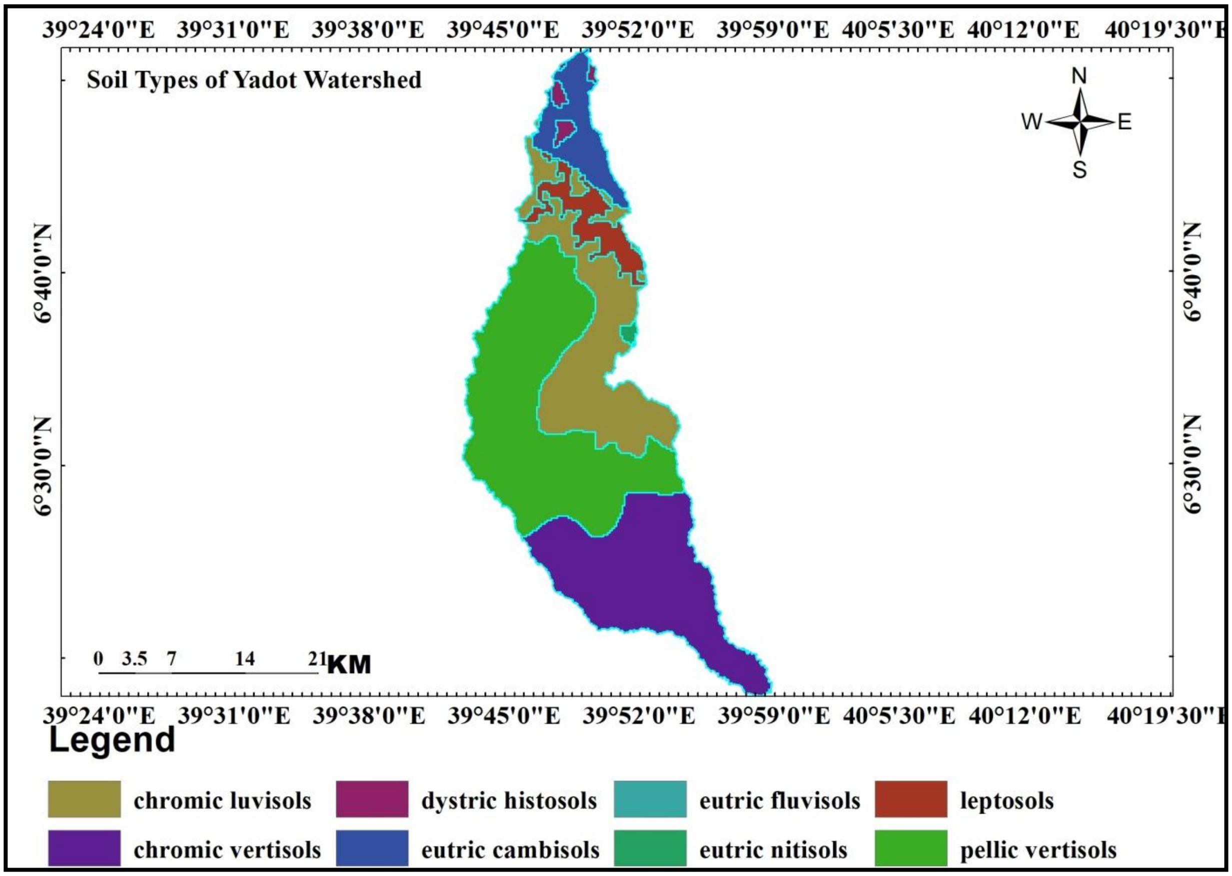

Figure 3. 5: Soil map of the study watershed

3.2. Data Collection Methods and Procedures

3.2.1. Data Collection

3.2.1.1. Digital Elevation Model

Digital Elevation Model (DEM) of 12.5m x 12.5m resolution was processed for the extraction of flow direction, flow accumulation, stream network generation and delineation of the watershed and sub-basins. The topographic parameters of the study watershed, such as terrain slope, channel slope or reach length was also derived from the DEM.

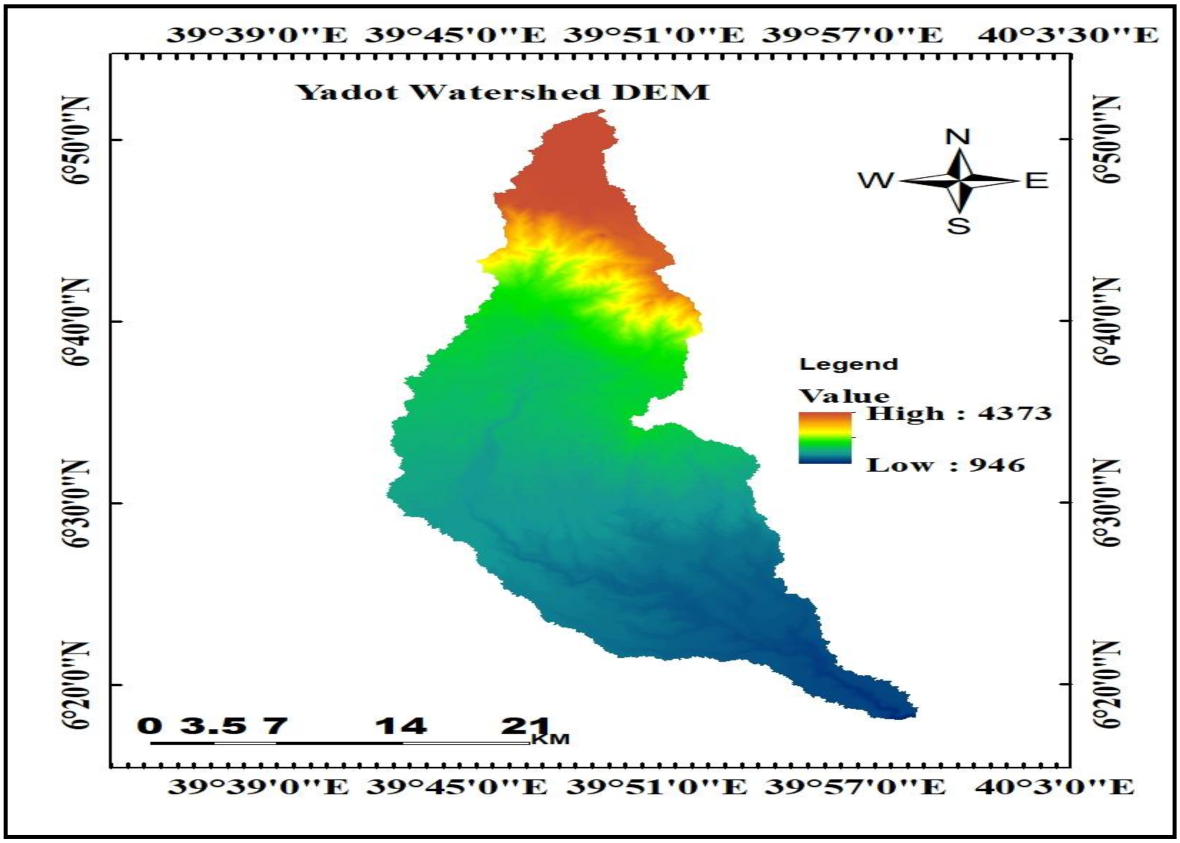

Figure 3.6: Digital Elevation Model of Yadot watershed

3.2.1.2. Land Use Land Cover Data

Land use land cover is one of the main input data of the SWAT model to analyze the impacts on stream flow of the watershed and describe the Hydrological Response Units (HRUs) of the watersheds. The historical LULC images were obtained from Landsat images and classified using supervised classification in Earth Resource Data Analysis System (ERDAS) imagine model. Therefore, the classified 1985, 2000 and 2015 and the predicted future LULC 2035 and 2055 maps was based on the classified historical satellite images using IDRISI Selva v.17 model in the study watershed. The SWAT model has predefined four letter codes for each land use category. These codes were used to link or associate the land use map of the study area to SWAT land use databases. Hence, while preparing the lookup-table, the land use types were made compatible with the input needs of the model.

3.2.1.3. Soil Map Data

Soil properties are one of the major inputs data required by SWAT2012 model of the watershed. The soil map of the study area obtained from Food and Agricultural Organization – Harmonized World Soil Database (FAO-HWSD) and cross checked with HWSD Viewer soil map. According to this soil database there are 8 soil types in the study watershed. To integrate the soil map with SWAT model, a user soil database which contains textural and chemical properties of soils was prepared for each soil layers and added to the SWAT user soil databases using the data management append tool in ArcSWAT10.4.1.

3.2.1.4. Hydro – Meteorological Data

Weather data required for SWAT input includes daily data of precipitation, maximum and minimum temperature, relative humidity, wind speed and solar radiation. For this study only two station within and around Yadot watershed are Delo Mena and Rira station considered due to total absence recorded data in other station and absence of the influence remaining station in Thiessen Polygons. The climate data used for this study cover 31 years from January 1985 to December 2015. Rainfall and temperature data are available in all the stations whereas sunshine hours, wind speed and relative humidity data were not available for Rira stations. The Delo Mena station was used as weather generator station so as to generate weather variables for missing records assigned with no data code value (-99) in SWAT database. The climate data for study periods was finally prepared in text file format and imported to the SWAT model database.

The stream flow data of the Yadot watershed is needed for the calibration and validation of the model. The daily stream flow data (1985-2008) at near Delo Mena station collected from the Minister of Energy and Water Resources of Ethiopia for the Yadot watershed. The missing flow data were filled by linear regression from the nearby river gauged station.

3.2.1.5. Checking Hydro-Meteorological Data quality

A. Filling of missing Precipitation data

Hydro-meteorological data missing is a common challenge to perform hydrological analysis and modeling to use long time series data and filling the missing data is very crucial. Failure of any rain gauge or absence of observer from a station causes a short break in the record of rainfall at a given station. Methods used to fill missing data such as: arithmetic mean method, normal ratio method and inverse distance weighing method. Arithmetic mean method can be used to fill in missing data when normal annual precipitation is within 10% of the gauge/station for which data are being reconstructed. The normal ratio method is used when the normal annual precipitation at any of the index station differs from that of the precipitation station by more than 10%. The Arithmetic mean method is given as (equation number 8).

$$Px = \frac{\sum_{i=1}^{n}}{n} Pi \text{--} 8$$

Where: - *Px* is the missing precipitation value for station *i (i=1, 2, 3...n)*, and *P1, P2… Pn* are precipitation values at the adjacent stations for the same period and *n* is the number of nearby stations. The normal ratio method is as given (equation number 9).

$$Px = \frac{1}{n}\sum_{i=1}^{n}\frac{Pi}{Ni}Nx ------------------------------ 9$$

where *PX* is the missing precipitation value for station *X* for a certain period of time, *Pi* is precipitation values at adjacent stations for the same period, *NX* is the long-term, annual average precipitation values at station *X; Ni* is the long-term precipitation for neighboring stations and *n* is the number of adjacent stations.

B. Checking the Consistency of Data

Checking for inconsistency of the record is done by the double-mass curve technique (Subramanya, 2013) for this study. The principle of double mass analysis is to plot cumulative values of the station under investigation against cumulative values of another station, or cumulated values of the average of other stations, over the same period of time. Double mass curve is a graphical method for identifying and adjusting inconsistency in a station record by comparing its time trend with those of adjacent stations. The problem occurs when the watershed rainfall data at the rain gauge station is inconsistent over a period and adjustment of the measured data is necessary to provide a consistent record. If significant change in the regime of the curve is observed, it should be corrected by using (equation number 10).

$$Pcx = \frac{Px * Mc}{Ma} \text{--} 10$$

Where: **Pcx** is corrected precipitation at any time period, **Px** is original recorded precipitation at time period, **Mc** is corrected slope of the double mass curve and **Ma** is original of the slope of double mass curve.

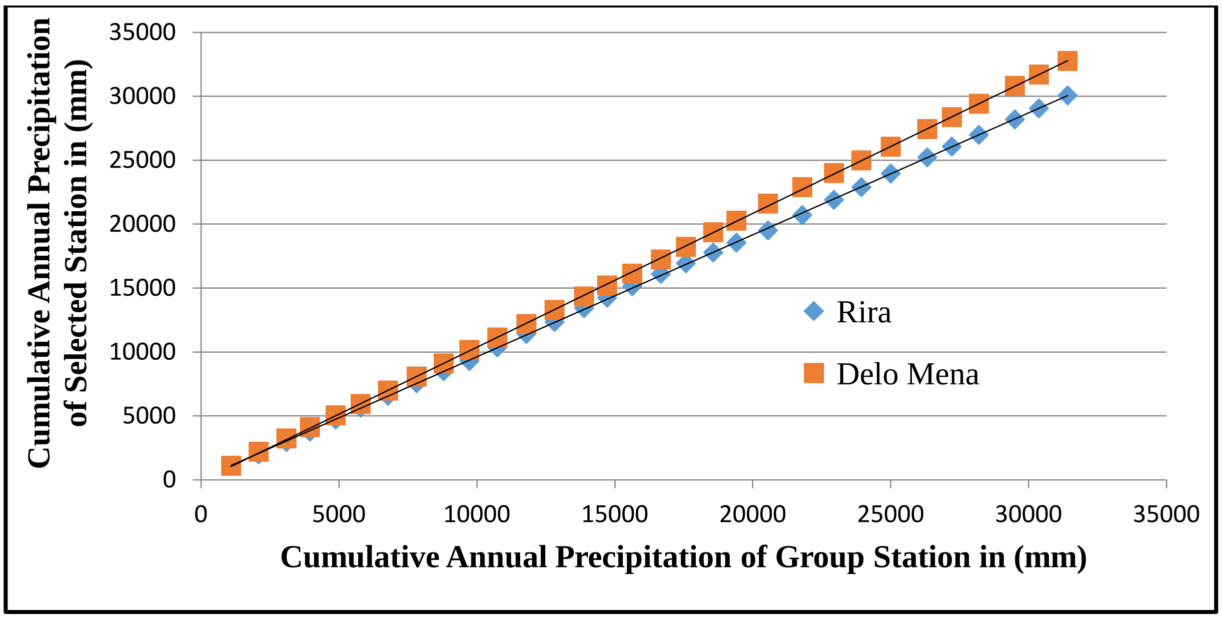

Figure 3.7: Double Mass Curves for the Stations

C. Climate Data Homogeneity Test

The total annual rainfall data of all stations those selected in and around the sub basin was homogenous as verification by the study analysis (Figure 3.8) and (Table 3.4).

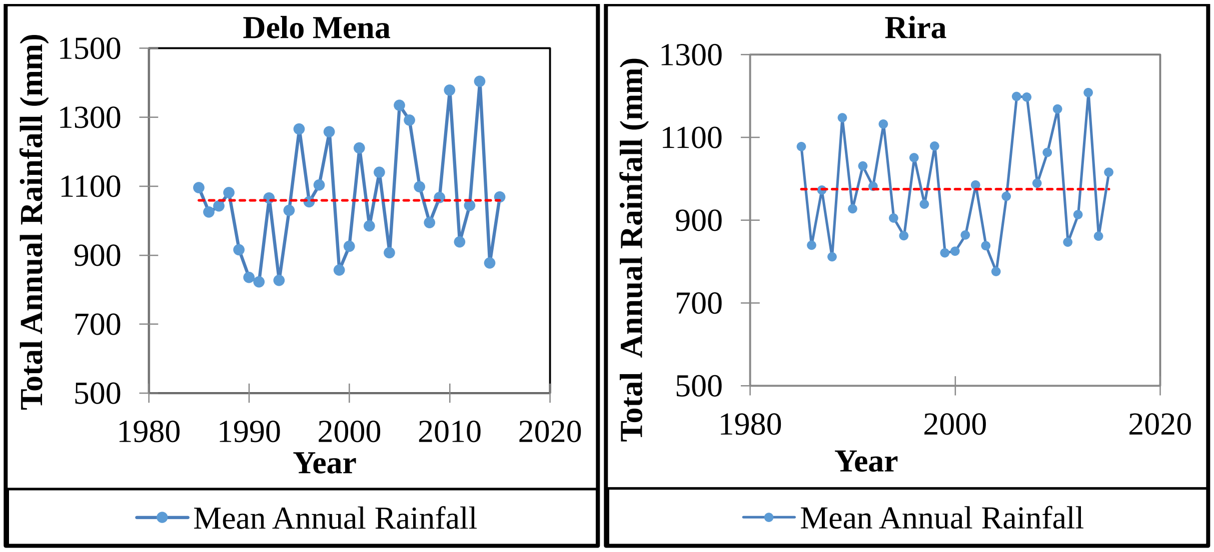

Figure 3.8**:** Homogeneity tests of annual rainfall data of individual rain gauge stations

Table 3.1: Summary of Homogeneity test climate data with 5% ($\alpha = 0.05$) significance level

No	Station	Minimum	Maximum	Mean	Std. deviation
1	Delo Mena	822.54	1404.18	1059.42	163.11
2	Rira	730.10	1268.66	975.30	147.53

The annual stream flow (m^3/year) of Yadot River near Delo Mena gauging station was checked for homogeneity test for the period of 1985 – 2008 as shown in (Figure 3.9) below.

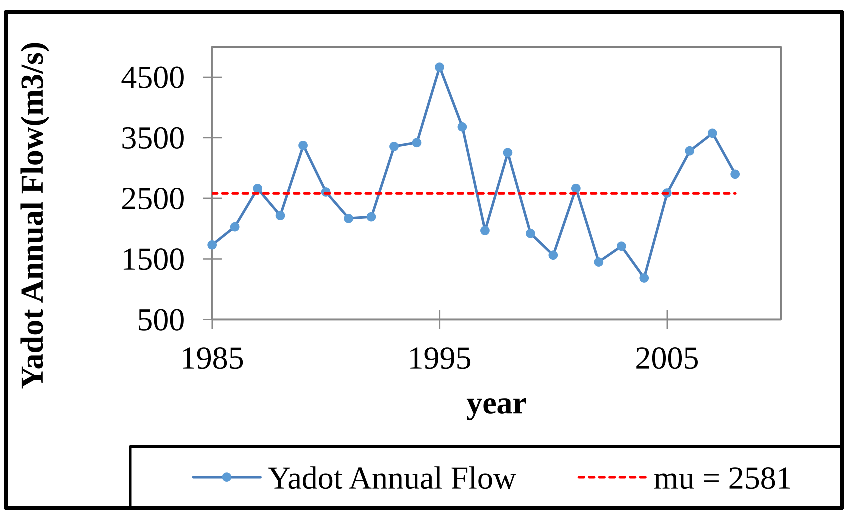

Figure 3.9: Pettitt's Homogeneity test of Annual Stream flow

3.2.2. Land Use Land Cover Change Detection

3.2.2.1. Image Processing and Date of Acquisition

In the study of the impacts of land use land cover and climate change on stream flow of the watershed, remote sensing images are required and can be processed by computers to produce land use land cover map. Data from remote sensing sensors sometime came with sort of errors. Errors may not be used for mapping without correction. Different data pre-processing techniques were used such as; image enhancement, geometric and radiometric correction were implement to prepare land use map. Land sat 5 TM, Landsat7 ETM+ and Land Sat8 OLI/TIRS were selected for the period of 1985, 2000 and 2015 respectively (Table 3.2). Each land sat was geo-referenced to WGS_84 datum and Universal Traverse Mercator (UTM) Zone 37N. To avoid a seasonal variation in vegetation pattern and distribution throughout the study year, the selection of dates of the acquired data were made as much as possible in the same annual season of the acquired years. In order to view and discriminate the surface features clearly, all the input satellite images were composed using the true (RGB) colour composition and false colour composition to identify images provide complete coverage of Yadot sub basin

Table 3.2**:** Land sat images used for LULC change analyses and their characteristics

Sensor	Path/Row	Date of acquisition	Resolution	Season
Land sat 5 TM	167/055	14/01/1985	30x30m	Dry
	167/056	14/01/1985	30x30m	Dry
Land sat 7 ETM+	167/055	18/01/2000	30x30m	Dry
	167/056	18/01/2000	30x30m	Dry
Land sat 8 OLI	167/055	03/03/2015	30x30m	Dry
	167/056	03/03/2015	30x30m	Dry

3.2.2.2. Image Classification

Image classification is a process of assigning pixels to predefined land use land cover classes or done in order to assign different spectral signatures from the LANDSAT datasets to different LULC. The main objective of image classification is to place all pixels in an image into LULC classes in order to draw out useful thematic information.

In remote sensing, there are various image classification methods. There appropriateness depends on the purpose of land use land cover maps produced for and the analyst's knowledge of using the algorithms. However, in most cases the researchers categorized them into three major categories: supervised, unsupervised and hybrid. For this research, supervised classification approach was adopted so as to have acceptable classification accuracy. In this system the user should have a good knowledge about the land cover to be studied. In supervised image classification system, the user relies on her/his prior knowledge and skills and can select a group of pixels belongs to a particular land use land cover.

The supervised classification was applied after defined area of interest (AOI) which is called training sample. The training site were selected in agreement with the Land sat Image and connects with Google Earth, then the samples for each land cover type were merge together. Using Google Earth historical Image, topographic map and original mosaic image as a reference compared with the corresponding classification. In supervised classification, defining of training sites, extraction of signature editor and classification of image was performed using Maximum Likelihood classifier. Accordingly, six categories of LULC were identified based on the nature and similarity of the use and cover types. This classification is in agreement with (Desalegn *et al.* 2014; and Adane and Getachew, (2017) in Bale eco-region.

Agriculture: - This land use encompasses areas that allocated for crop production of both annuals and perennials,

Grass/Range land: - Either communal or private grazing lands that are used for livestock grazing. The land is basically covered by small grasses, grass like plants and herbaceous species. It also includes area covered with range or grass used for grazing, as well as little grassland with some bare lands or includes other small sized plant species

Forest: - Land area covered with a high density of trees or dense trees and nearly closed canopies which include evergreen forest and plantation forests.

Scrub/Bush land: - Land area covered by Asta scrubland, Erica bushes, alpine vegetation and small white leaves found at top of Sanette Platue and habitats of Ethiopian Wolf.

Wood Land: - Land not classified as forest, spanning more than 0.5 hectares include deciduous forest and mixed forest land.

Settlement: - Land feature where there is a permanent populated urban settlement, densely concentrated rural settlement and other facilities.

3.2.2.3. Accuracy Assessment

Accuracy assessment is the comparison of a produced classification with what actually exists on mapped image for the same location to evaluate how well the classification results. It is performed by comparing a map created by using remote sensing analysis to a reference map based on different information sources such as Google Earth and original mosaic images.

The classification accuracy assessment is based on the samples collected from the image, the generating of enhanced images and the computation of the probability in which this pixel belong to this class. Total test samples of 150, 180 and 228 for the image 1985, 2000 and 2015 were randomly selected from the original mosaic images for the validation of 1985 and 2000 and Google earth images for 2015 with ERDAS IMAGINE 2015, respectively. Evaluation of the accuracy of a classified image can be done using an error matrix sometimes called confusion matrix. An error matrix is a square array of rows and columns and presents the relationship between the classes in the classified and reference data. The columns normally represent the reference data, while the rows indicate the classification generated from classified image. Error of omission refers to pixels in the reference map that were identified as something other than their "accepted" value. Whereas error of commission, on the other hand refers to pixels that were incorrectly classified as a class in a row.

Overall accuracy, user's accuracy and producer's accuracy were derived to test the classification. The overall accuracy provides accuracy of the whole image classification (number of correctly classified pixels divided by the total number of pixels in the error matrix). Most of the classification accuracy measurements are derived from an error matrix. Based on this, user's accuracy refers to the probability that a given pixel can be found in the ground as it is in the classified image, whereas producer's accuracy refers to the percentage of a given class that is correctly identified on the map (Sahalu, 2014).

3.2.3. Land Use Land Cover Change Detection Analysis

Land use land cover change detection is the process to determine a change in the classified class of satellite images by looking at different periods of studies. Change detection entails findings the type, amount and location of land use changes. In this study five time periods LULC change detection has been made i.e. for 1985, 2000 and 2015 for historical and 2035 and 2055 for future period. These time periods were chosen based on the resettlement program, the availability of quality satellite image and other data like weather and hydrological data in the study area. The LULC change detection was performed using post classification cross-tabulation approach in ArcGIS software. The classified images were compared in the three time periods and change statistics was computed by comparing the values of area of one LULC data set with the corresponding value of the next data set for each period (using equation 4). The annual rate of change of each land use land cover was calculated using the following formula (number 5).

The comparison of the LULC statistics assisted in identifying the percentage change, trend and annual rate of change between 1985 and 2015. In achieving this, the first task was to develop a table showing the area in hectares and the percentage change for each past LULC 1985, 2000 and 2015 and for future LULC 2035 and 2055 measured against each LULC type.

$$\text{Percentage Change} = \frac{\text{Final Year Area} - \text{Initial Year Area}}{\text{Initial Year Area}} \ldots\ldots\ldots\ldots\ldots\ldots\ldots\ldots\ldots\ldots 4$$

$$\text{Annual Rate of Change} = \frac{\text{Final Year Area} - \text{Initial Year Area}}{\text{Number of Year Between two image}} \ldots\ldots\ldots\ldots\ldots\ldots\ldots\ldots 5$$

3.2.4. Land Use Land Cover Prediction and Model Validation

3.2.4.1. Land Use Land Cover prediction

Land Use Land Cover change predictions for 2035 and 2055 periods were employed using the CA-Markov model, which is available in IDRISI; Geospatial software for monitoring and modeling the Earth system; version 17.0. The Cellular Automata (CA) and Markov Chain models are considered to be advantageous for modeling land use changes (Mishra and Rai, 2016; Parsa *et al*., 2016). CA-Markov, when compared with other dynamic models has advantages such as the ability of individuals to boost information that has under the regular principles, regulates their evaluation, and analysis of the spatial (space) characteristics, used to easily predict land use in the future (Gambo *et al*., 2018). CA-Markov predicts both the trend and the spatial structure of different LULC categories (Wang et al., 2012; Li et al., 2015) based on the basis observed LULC image, transition probability matrix and suitability images as a group file (Clark labs, 2012; Eastman, 2012). The minimum level for accuracy assessment in identification of LULC categories in remote sensing data should be at least 85%. Afterwards, the data is exported into an ASCII text file to enable for further analysis in ArcGIS version 10.4.1 .This study employed the 2015 classified map as a basis LULC image, and the 2000 and 2015 maps for assembly transition probability matrix (with the proportion errors of 0.15). The land use maps of 2000 and 2015 were taken as a baseline map and CA-Markov in IDRISI software was used to predict future land use maps of LULC 2035 and LULC 2055.

3.2.4.2. Validating LULC Prediction Model

The CA-Markov chain is a stochastic procedures model that pronounces the possibility of change from one land use land cover class into another land use land cover class using a transition probability matrix. In this study, IDRISI Selva v.17 is used to predict the future LULC of study area on CA-Markov model. CA-Markov will use the 1985 and 2000 maps to produce a simulated 2015 map, which is important to validate with actual LULC of 2015 map through KIA (Kappa Agreement of Index) approach (Mishra and Rai, 2016; Parsa *et al*., 2016). Any model prediction requires model calibration and validation. Then, the simulated LULC map of 2015 was compared with the observed 2015 LULC map using the Kappa index:

$$\mathbf{K}appa = \frac{\mathrm{P}o-\mathrm{P}c}{1-\mathrm{P}c} \text{---}6$$

In the above equation, Po is the proportion of correctly simulated cells; Pc is the expected proportion correction by chance between the observed and simulated map. If Kappa ≤ 0.5 shows rare agreement, 0.5 ≤ Kappa ≤ 0.75 shows a medium level of agreement, 0.75 ≤ Kappa ≤ 1 shows a high level of agreement and Kappa = 1 for perfect agreement (Pontius and Malanson, 2005).

3.2.5. Near-term and Mid-term Climate Projection

3.2.5.1. GCMs and RCMs used for this study

In this study, the dynamically downscaled RCM product of daily precipitation, maximum and minimum temperatures outputs from the fifth phase of the Coupled Model Inter comparison Project (CMIP5) over the CORDEX-Africa domain at spatial grid resolution of 0.44^{o} (~50 Km) were used. The CORDEX-Africa program provided climate data that were simulated by three GCMs (HadGM2-ES, MPIESM-LR and ICHEC-EC) and dynamically downscaled by three RCMs, which are Regional Climate Limited-area modeling (CCLM), Rossby Center regional atmospheric model (RCA4) and KNMI Regional Atmospheric Climate Model, version 22 (RAMO22T), respectively for each GCM (Table 3.3). The selected RCMs run on SWAT with two RCP scenarios of the high emission scenario of RCP8.5 and mid emission of RCP4.5. All Regional Climate Models have simulated seasonal mean annual cycles of precipitation and temperature with a significant bias shown on individual models. However, the use of ensemble mean over the individual RCMs helps to minimize the highest and lowest projections and enables to minimize the uncertainties by working with the average of the RCMs. The reference to this study was (Wakjira *et al*., 2019) in their study of evaluation of the CORDEX regional climate models performance in simulating climate conditions of two watersheds in Upper Blue Nile Basin.

For this study, climate model selection was based on the previous study on Africa by other researchers and literature (Lennard *et al.*, 2018: Samuel *et al*., 2019) and Hussen *et al*., 2013) over East Africa. Hussen *et al.,* (2013) conducted Assessment of the Performance of 10 CORDEX Regional Climate Models in Simulating East African Rainfall and reported; apart from REMO and CCLM most of the model showed bias under wet and dry season. Samuel *et al*., (2019) on comparison of 30 GCM models outputs reported that CanESM2 and HadGEM2-ES performed best in terms of the correlation coefficient between gauged and simulated rainfall amounts. Therefore, for the climate scenarios, the daily inputs of precipitation and temperature (maximum and minimum) were obtained from downscaled projections for two representative concentration pathways of RCP4.5 and RCP8.5. The future scenario was made up to 2080 years for near and midterm in this study and the impact was analyzed per 30 years.

The RCMs climate data obtained from CORDEX-RCM is in a NetCDF format with a rotated pole of (longitude and latitude) then extracted on ArcGIS10.4.1. The unit of precipitation and temperature were kg/m^2/s and Kelvin, respectively and there is a need for correcting the rotated pole and units before using the data in any impact analysis. Therefore, to obtain precipitation in mm/day the given data was multiplied by 86400 (24 * 60* 60) and to obtain temperature in Celsius by subtract 273.15 from downscaled data using the above conversion factors.

Table 3.3: Summaries of GCM and RCM climate model used in the study

GCM Model	Full Name GCM	Model	Full Name of RCM	Spatial Resolution	Climate Center
HadGEM2-ES	Hadley Global Environment Model 2-Earth System	CCLM	Regional Climate Limited-Area Modeling	0.44^0	Met Office Hadley Center
MPI-ESM-LR	Coupled Model Version 5, Medium Resolution	RCA4	Rossby Center Regional Atmospheric Model	0.44^0	Max Planck Institute for Meteorology (MPI-M)
EC-EARTH	Irish Center for High-End Computing Earth Consortium	RACMO22T	KNMI Regional Atmospheric Climate Model, version 2.2	0.44^0	EC-EARTH Consortium

3.2.5.2. Bias Correction of Future Climate Data

Bias correction is widely used in climate impact aims to adjust selected statistics of a climate model simulation to better match between observed meteorological data. Statistical bias corrections often need to be performed to better match the model output to the observations (piani *et al.*, 2010). Bias correction is usually needed as climate models often provide biased representations of observed time series data due to systematic model errors caused by imperfect conceptualization, discretization and spatial averaging within grid cells.

Power transformation: - uses the exponential form p^b that is used to adjust the statistical variance standard deviation and coefficient of variation as well as the mean of precipitation time series. In this nonlinear correction each daily precipitation amount P is transformed to a corrected P^* using (equation number 7).

$$P* = aP^b ----------------------------------7$$

Where: P^* is the bias corrected daily precipitation; P is the uncorrected daily precipitation; and a and b are the transformation coefficients. The determination of the b parameter is done iteratively so that, for areal of each grid box in each month, the coefficient of variation of the corrected RCM daily precipitation time series matches that of the observed precipitation time series. Then a is the coefficient that is determined from the mean of observed precipitation data and the mean of P^b. Finally, monthly constants a and b are applied to each uncorrected daily observations corresponding to that month in order to generate the corrected daily time series

Variance Scaling: - to correct temperature time series, as temperature is known to be approximately normally distributed (Yang et al, 2015). The VARI method was developed to correct both the mean and variance of normally distributed variables such as temperature (Teutschbein and Seibert, 2012). Temperature is normally corrected using the VARI method (equation number 8).

$$Tc = [T - \mu(T)]x\frac{\sigma(To)}{\sigma(T)} + \mu(To) ----------------------------8$$

Where

T*c:* the corrected daily temperature; T: the uncorrected daily temperature from RCM model; σ(To) is the standard deviation of the observed temperature; σ(T) is the standard deviation of the uncorrected temperature; μ(T) is the simulated mean temperature and μ(To) is the observed mean temperature.

3.2.6. Impact of Climate and LULC Change on Stream flow

3.2.6.1. Climate Change Impact Simulation Using SWAT Model

The projected precipitation, temperature, baseline and future land use land cover maps were used as input to the calibrated and validated SWAT model by keeping constant wind speed, solar radiation and relative humidity throughout the future simulation period to determine stream flow in the future time period. The baseline period consists of the years 1985–2015 and future simulation include two future period (2021-2050) and (2051 -2080) for near and midterm. Three simulation scenarios were developed for the independent and combined effects of the Land Use Land Cover Change and climate change. The first scenario (S1) considers Only Land Use Land Cover Change effects on stream flow using land use maps of 1985, 2000, 2015, 2035 and 2055 with baseline climate data from 1985 – 2015 for stream flow simulation. The second scenarios (S2) considers only a climate change effects on stream flow using single baseline land use map of 2015 with three future climate scenario data of 1985–2015, 2021–2050 and 2051–2080 for stream flow simulation. The third scenario (S3) considers combined effect of climate and Land Use Land Cover change on stream flow using land use maps of 2015 as baseline period, LULC map of 2035 for near-term, while LULC map of 2055 for the midterm simulation with baseline and future climate data of 1985–2015, 2021–2050 and 2051–2080, respectively.

3.2.6.2. Description of SWAT Model

Hydrological models have been developed for different reasons and different forms. It is mathematical descriptions of the different components of the hydrologic cycle. However, hydrological models are generally developed to meet the primary objectives of enabling better understanding of the hydrologic processes and for hydrologic prediction in a watershed.

The reasons, for selecting SWAT model for this study are:-

- It has been applied in studies related to land use land cover and climate changes in different parts of the world including Ethiopia and proved for sufficiency of performance.
- The model can simulates the required hydrological process in the study watershed
- Less demanding of the input data is Advantageous.

- It is readily and freely available.

The Soil and Water Assessment Tool (SWAT) is an open-source-code, semi-distributed model with a large and growing number of model applications in a variety of studies ranging from watershed to continental scales (Arnold *et al.*, 2012, Neitsch et al., 2011). It evaluates the impact of LULC and climate change on water resources in a basin with varying soil, land use and management practices over a period of time (Arnold *et al.*, 2012). SWAT model has the ability to simulate and predict the long-term changes of various hydrological elements under different land use types, soil types and management practices on the large scale complex basin. SWAT hydrological models has been successfully used in the studies of the impact of land use land cover and climate change on water resources in a basin with varying soil, land use and management practices over a set period of time (Arnold *et al.*, 2012). It is evident that the SWAT model has yielded high accuracy for short/long-term simulations of yearly and monthly mean streamflow (Zuo et al., 2016; Anand et al., 2018).

In SWAT, the watershed is divided into multiple sub-basins, which are further subdivided into hydrological response units (HRUs) consisting of homogeneous land use management, slope and soil characteristics (Arnold et al., 1998: Arnold et al., 2012). HRUs are the smallest units of the watershed in which relevant hydrologic components such as evapo-transpiration, surface run-off and peak rate of run-off, groundwater flow and sediment yield can be estimated. Water balance is the driving force behind all the processes in the SWAT calculated using (equation 9).

$$\boldsymbol{SW_t = SW_0 + \Sigma_{n=1}^{t}(R_{day} - Q_{surf} - E_a - W_{seep} - Q_{gw})} \ldots\ldots\ldots\ldots\ldots\ldots\ldots\ldots\ldots\ldots\ldots\ldots \quad \mathbf{9}$$

Whereas, SW_t is the final soil water content in [mmH_2O], SW_0 is the initial soil water content on day i [mm], t is the time [days], R_{day} is amount precipitation on specific days i [mmH_2O], Q_{surf} is the amount of surface runoff on specific day i [mmH_2O], E_a is amount evapo-transpiration on a day i [mmH_2O], W_{seep} is the amount of water entering the vadose zone from soil profile on day i [mmH_2O] and Q_{gw} is amount of return flow on a day i [mmH_2O].

3.2.6.3. Data Input for SWAT Model

For this study, Digital Elevation Model (DEM) of 12.5m by 12.5m was downloaded from https://vertex.daac.asf.alaska.edu/ to delineate the watershed of the study area. DEM was used in the SWAT model along with soil and land use land cover data to delineate the watershed and to further divide the watershed into sub watersheds and hydrologic response units (HRUs). The soil map of the study area was obtained from Ministry of Water, Irrigation and Energy of Ethiopia. Remote sensing satellite data used for this study were obtained from the United States Geological Survey (USGS) Earth Resources Observation and Science (EROS) data center (https://earthexplorer.usgs.gov/) website in GEOTIFF file format. Satellite data include Land sat 5 TM, Land sat 7 ETM+, and Land sat 8 OLI images for the year 1985, 2000 and 2015. Earth Resource Data Analysis System (ERDAS) imagine version 15 and ArcGIS10.4.1 software packages were utilized for the classification of LULC changes.

The climate model data were obtained from outputs of high resolution regional climate models of CORDEX RCM dynamically downscaled by the regional climate model are (CCLM4-8-17, RACMO22T and RCA4) https://climate4impact.eu/impactportal/data/esgfsearch.jsp.

Daily climate variables include daily precipitation [mm], maximum and minimum temperature [ºC], solar radiation [MJ/m2/day], wind speed [m/s] and relative humidity [-]) were obtained from National Meteorological Service Agency of Ethiopia (NMSA), while Observed Daily stream flow data of Yadot River at Delo Mena gauging Station were obtained from Ministry of Water, Irrigation and Electricity (MoWIE) .

3.2.7. SWAT Model Setup

3.2.7.1. Watershed Delineation

The watershed and sub watershed delineation was performed using 12.5m resolution DEM data using Arc SWAT model watershed delineator tools. First, the SWAT project set up was creating necessary folders and databases to store all the data. The watershed delineation process consists of five major steps, DEM setup, stream definition, outlet and inlet definition, watershed outlets selection and definition and calculation of sub basin parameters. Once, the DEM setup was completed and the location of outlet was specified on the DEM, the model automatically calculates the flow direction and flow accumulation. Finally stream networks, sub watersheds and topographic parameters were calculated using the respective tools.

The stream definition and the size of sub basins were determined by selecting the threshold area or minimum drainage area required to form the origin of the streams to be two thousands (2000 hectares) in order to decrease sub basin number. The Yadot watershed was delineated into 23 sub basins having an estimated total area of 735.6km^2.

3.2.7.2. Hydrological Response Unit (HRU)

After watershed delineation, land use, soil and slope characterization for watershed was performed using commands from the HRU analysis menu on the Arc SWAT Toolbar. The HRU analysis tool in Arc SWAT helps to load land use, soil layers and slope map to the project. The HRUs represent areas with homogeneous land use/cover, management, and soil characteristics. After HRUs created promptly two common options were provided in the model to define the HRUs. The first was by assigning a single HRU and the other was with multiple HRUs option.

In this study, therefore, the multiple HRUs option was employed aiming at obtaining reliable results of simulation. The SWAT user's manual suggests that a 20 % land use threshold, 10 % soil threshold and 20 % slope threshold are adequate for most modeling application. However, (Setegn et al, 2008), suggested that HRU definition with multiple options that account for 10% land use, 20% soil and 10% slope threshold combination gives a better estimation of runoff and sediment components. Therefore, for this study, HRU definition with multiple options that accounts for 10% land use, 20% soil and 10% slope threshold combination was used to eliminate minor land use and land covers in sub basin, minor soil within a land use and land cover area and minor slope classes within a soil on specific land use and land cover area. Due to this the Yadot Watershed was divided into 185 HRUs, each has a unique land use and soil combinations.

3.2.7.3. Sensitivity Analysis

Sensitivity analysis is the process of determining the rate of change in model output with respect to changes in model parameters (Arnold *et al.*, 2012). Sensitivity analysis provides for better understanding of the behavior of the system being modeled, such as model parameters and applicability, thus it increases the confidence level of the model and its predictions. Therefore, prior to calibration and validation process, sensitivity analysis was carried out to reduce the number of parameters that needs optimization. In this study semi-automated Sequential Uncertainty Fitting (SUFI 2) was used to identify the sensitive parameters. Global analysis requires large number of simulations (Arnold et al, 2012) which can also be a problem. However, in this research the number of simulations used for calibration was 1000, which is large enough to get accurate results for global sensitivity analysis. The average monthly stream flow data of 15 years from 1988 to 2002 of the watershed gauging station were used to compute the sensitivity of the stream flow parameters.

The aim of sensitivity analysis is to estimate the rate of change in the output of a model with respect to changes in watersheds that result in a clear difference in hydrologic sensitivity. In the sensitivity analysis process, by using SWAT-CUP, first create the new folders and copy the SWAT simulation results to perform the sensitivity analysis and the location of the sub basin where observed data was compared against simulated output then, chosen parameters were entered for the sensitivity analysis with the default lower and upper parameter bounds.

3.2.7.4. Model Calibration

Calibration is a major aspect of hydrological modeling which intended to fit the simulated outputs of the model to the recorded stream flow data of the watershed by adjusting the model parameters, thereby reducing the prediction uncertainty. Parameters for modification are selected from those identified by sensitivity analysis. Additional parameters other than those identified during sensitivity analysis are used primarily for calibration due to the hydrological processes naturally occurring in the watershed.

Therefore combination of both manual and automatic or numerical parameter optimization method was used in this particular study. First the parameters were calibrated manually for the period of fifteen year (1988 – 2002) and warm-up period of three year (1985-1987) until the model simulation results acceptable as per the model performance measures. Next, the final parameter values that would be manually calibrated were used as the initial values for the auto calibration procedure. The graphical and statistical approaches were also be used to evaluate the SWAT model performance a number of times until the acceptable values were obtained for surface runoff independently.

3.2.7.5. Model Validation

Validation is the comparison of the model outputs with independent data set without making any adjustment. The purpose of model validation is to check whether the model can predict flow for another range of period. In order to utilize any predictive watershed model for estimating the effectiveness of future potential management practices the model must be first calibrated to measured data and should then be tested (without further parameter adjustment) against an independent set of measured data. The model was validated using stream flow from 2003 to 2008 at the location of study area for six year.

3.2.7.6. Model Performances Evaluation

The goodness of fit was evaluated with Nash-Sutcliffe efficiency (NSE), coefficient of determination (R^2), root mean square error standard deviation ratio (RSR), and percentage bias (PBIAS) were used for model evaluation for quantification of accuracy in watershed modeling.

Coefficient of Determination (R2), a measure of consistency of simulated and observed data, was also considered in evaluating the model. The closer the value of R^2 to one implies a perfect agreement between the simulated and observed flow (Singh *et al.*, 2005).

$$R2 = \frac{\sum(Xi-Xav)*\sum(Yi-Yav)}{\sum\sqrt{(Xi-Yav)2}\sum\sqrt{(Yi-Yav)2} }\text{---14}$$

Where Xi = measured value (m^3/s); Xav = average measured value (m^3/s); Yi = simulated value (m^3/s) and Yav is average simulated value (m^3/s)

The Nash-Sutcliffe efficiency coefficient (Nash and Sutcliffe, 1970) is used to assess the predictive power of the hydrological models. The Nash-Sutcliffe simulation efficiency indicates how well the plot of observed and simulated value fits. When the value of NSE is 1, the simulated value is the same as observed (perfect). When the value is between 0 and 1, it indicates the deviations between observed and simulated data. An efficiency of lower than zero indicates that the mean value of the observed time series would have been a better predictor than the model (Krause et al., 2005). The Nash-Sutcliffe efficiency (NS) is calculated by using equation 15:

$$\text{ENS} = 1 - \frac{\sum(\text{Xi}-\text{Yi})2}{\sum(\text{Xi}-\text{Xav})2} \dots\dots\dots\dots\dots\dots\dots\dots\dots\dots\dots\dots\dots\dots \ldots 15$$

Where Xi is measured value; Yi is simulated value and Xav is average observed value.

Table 3.4: Performance ratings of recommended statistics for monthly stream flow

Performance rating	R^2	**NSE**	**PBIAS (%)**	**RSR**
Very good	$0.86 < R^2 \leq 1$	$0.75 < NSE \leq 1$	$PBIAS < 10$	$0.0 <= RSR <= 0.5$
Good	$0.75 < R^2 \leq 0.86$	$0.65 < NSE \leq 0.75$	$10 \leq PBIAS < 15$	$0.5 < RSR <= 0.6$
Satisfactory	$0.65 < R^2 \leq 0.75$	$0.5 < NSE \leq 0.65$	$15 \leq PBIAS < 25$	$0.6 < RSR <= 0.7$
Un satisfactory	$R^2 \leq 0.65$	$NSE \leq 0.5$	$PBIAS \geq 25$	$RSR >= 0.7$

4. RESULTS AND DISCUSSION

4.1. Land Use Land Cover Classification Accuracy Assessment

The accuracy assessment is used to determine the degree certainty classified image. The results from accuracy assessment showed an overall accuracy obtained from the random sampling process for the image of 1985, 2000 and 2015 were 87.33%, 91.67% and 92.25%, respectively. The overall accuracy of LULC maps of 2015 show higher than 1985 and 2000 this may be due to higher spatial resolution of satellite images and clear visibility on Google earth. Therefore, the validation data set indicate excellent agreement of the classified image with ground truths as shown on (Table 4.1, 4.2 and 4.3).

Table 4.1: Confusion Matrix for LULC Classification 1985

	REFERENCE DATA							
LULC	AG	GL	FR	SB	WL	ST	Total	UA
AG	22	1	0	1	0	0	24	**91.67%**
GL	2	22	0	0	1	0	25	**88%**
FR	0	0	35	1	3	0	39	**89.75%**
SB	0	4	0	20	1	0	25	**80%**
WL	0	0	4	1	26	0	31	**83.87%**
ST	0	0	0	0	0	6	6	**100%**
Total	24	27	39	23	31	6	150	
PA	**91.67%**	**81.5%**	**89.75%**	**86.96%**	**83.87%**	**100%**		K= 0.843

Overall Classification Accuracy = 87.33%

Note: Agriculture = AG, Grass/Range Land = GL, Forest = FR, Scrub/Bush Land = SB,

Wood Land = WL, Settlement = ST, Producer Accuracy = PA, Users Accuracy = UA

The error matrix for 1985 reveals that settlement was most often accurately classified in that year of imagery followed by agriculture land, forest, wood lands, grass/range land and scrub/bush land (Table 4.1). Some areas covered by Grass/range, scrub/bush and forest land were sometimes mistaken for wood land in 1985. User accuracy for each classes range from 91.67% for agriculture land to 100% for settlement.

Tables 4.2: Confusion Matrix for LU/LC Classification of 2000

	REFERENCE DATA							
LULC	AG	GL	FR	SB	WL	ST	Total	UA
AG	28	2	0	0	0	1	32	**90%**
GL	1	19	0	0	1	0	21	**90%**
FR	0	0	50	0	3	0	53	**94.3%**
SB	0	2	1	25	0	0	28	**89.3%**
WL	0	0	2	1	33	0	36	**91.7%**
ST	1	0	0	0	0	10	11	**90%**
Total	30	23	53	26	37	11	180	
PA	**93.33%**	**82.6%**	**94.3%**	**96.1%**	**89.2%**	**90%**		K = 0.896

Overall Classification Accuracy = 91.67%

Table 4.3: Confusion Matrix for LU/LC Classification of 2015

	REFERENCE DATA							
LULC	AG	GL	FR	SB	WL	ST	Total	UA
AG	32	2	0	0	3	0	38	**84.2%**
GL	0	22	0	0	3	0	25	**88%**
FR	0	0	83	1	0	0	84	**98.8%**
SB	0	1	0	31	1	0	33	**93.94%**
WL	0	2	3	0	25	0	30	**83.33%**
ST	1	0	0	0	0	18	19	**94.74%**
Total	33	27	86	32	32	18	228	
PA	**97%**	**81.48%**	**96.51%**	**96.88%**	**78.13%**	**100%**		K = 0.904

Overall Classification Accuracy = 92.25%

The LULC map 2000 classification error matrix indicates that Forest was correctly classified, followed by wood land, Agriculture, Grass/range land, settlement and scrub/bush land as shown on (Table 4.2). In the 2000 classification, agriculture and scrub/bush land was commonly mistaken for grass/range land whereas grass/range and forest land mistaken for wood land. User accuracy for each classes range from 89.3% for scrub/bush land to 94.33% for forest land.

The 2015 classification error matrix reveals that forest was accurately classified, followed by settlement, scrub/bush, grass/range, agriculture land and wood land as shown (Table 4.3). In the 2015 classification agriculture, grass/range and scrub/bush land was commonly mistaken for wood land similarly agriculture, scrub/bush and wood land mistaken for grass/range land. The reason why forest land accurately classified is that because the forest land are well known and easily classified. The User's accuracy reflects the reliability of the classification and the more relevant measure of the classification's actual utility in the field.

4.2. Land Use Land Cover Change Analysis

The major land use land cover types shown on the maps of 1985, 2000, and 2015 include agriculture land, grass/range land, Scrub/Bush land, settlement, forest and wood land presented in (Table 4.4). Forest land comprised largest share of total area about 65.50% followed by wood land 13.29% based on 1985 LULC map which indicates that much of the area was covered by green vegetation. The 1985 historical reference LULC map show that 7.54%, 7.45%, 6.11% and 0.12%, of grass/range land, scrub/bush, agriculture and settlement land area, respectively. The analysis has shown that the agricultural land was increased from 6.11% to 14.21%, while settlement land increased from 0.12% to 0.73% between 1985 and 2015, respectively. The annual rate of agricultural land change showed 235.55ha/year, 161.94ha/year and 192.33 ha/year increment from 1985 to 2000, 2000 to 2015 and 1985 to 2015, respectively. Settlement revealed annual rate of increment by 15.43ha/year, 14.54ha/year and 14.50ha/year for the period 1985 to 2000, 2000 to 2015 and 1985 to 2015, respectively. Grass/range land area cover was increased from 7.54% to 7.7% between 1985 and 2000, while declined to 7.3%, from 2000 to 2015 of the total area of watershed. In the first scenarios the land under grass/range land increased by (2.15%), while in the second scenarios decreased by 5.25% and third scenarios grass/range land decline by 3.21%, respectively.

Table 4.4**:** The area coverage of LULC, percent, and rate of changes in the Ydaot watershed between 1985, 2000 and 2015

	Area (ha)			**Percentage change (%)**			**Rate of change (ha/year)**		
LULC	1985	2000	2015	1985 -2000	2000-2015	1985-2015	1985 -2000	2000-2015	1985-2015
Agriculture	4491.01 (6.11*)	8024.2(10.91*)	10453.4(14.21*)	78.67	30.27	132.76	235.55	161.94	192.33
Forest	48180.4(65.5*)	46415.1(63.1*)	45200.1(60.45*)	-3.66	-2.62	-6.19	-117.68	-81.00	-96.14
Grass/Range	5544.65(7.54*)	5663.72(7.7*)	5366.55(7.3*)	2.15	-5.25	-3.21	7.94	-19.81	-5.75
Scrub/bush	5476.35(7.45*)	5401.33(7.34*)	5253.04(7.14*)	-1.37	-2.75	-4.08	-5	-9.89	-7.20
Settlement	87.83(0.12*)	319.23(0.43*)	537.41(0.73*)	263.47	68.34	511.88	15.43	14.54	14.50
Wood land	9773.05(13.29*)	7729.63(10.51*)	6742.77(9.17*)	-20.91	-12.77	-31.01	-136.23	-65.79	-97.75

*The number in parenthesis/bracket indicate percentage LULC

Key: - First scenarios (S1) (1985 to2000), Second scenarios (S2) (2000 to2015) and Third scenarios (S3) (1985 to 2015)

The annual rate of grass/range land change showed 7.94ha/year increments from 1985 to 2000, while declining by 19.81ha/year and 5.75ha/year between 2000 to 2015 and 1985 to 2015 period, respectively. Forest, woodland and scrub/bush land shows a declining trend for entire study periods from 1985 to 2015 with the magnitude of 6.19%, 31.01% and 4.08%. In the first scenarios the land under forest decreased by 3.66%, wood land by 20.91% and the land under scrub/bush land declined by 1.37%, respectively. The result for the second scenarios indicate that land under forest, wood land and scrub/bush land continued to decrease by 2.62%, 12.77% and 2.75%, respectively. The annual rate of decline of forest, wood land and scrub/bush land was 117.68ha/year, 136.23ha/year and 5ha/year in the first scenarios, while for the second scenarios declined by 81ha/year, 65.79ha/year and 9.89ha/year, respectively (Table 4.4). The classified images were obtained after pre-processing and supervised classifications as shown below on figures 4.1.

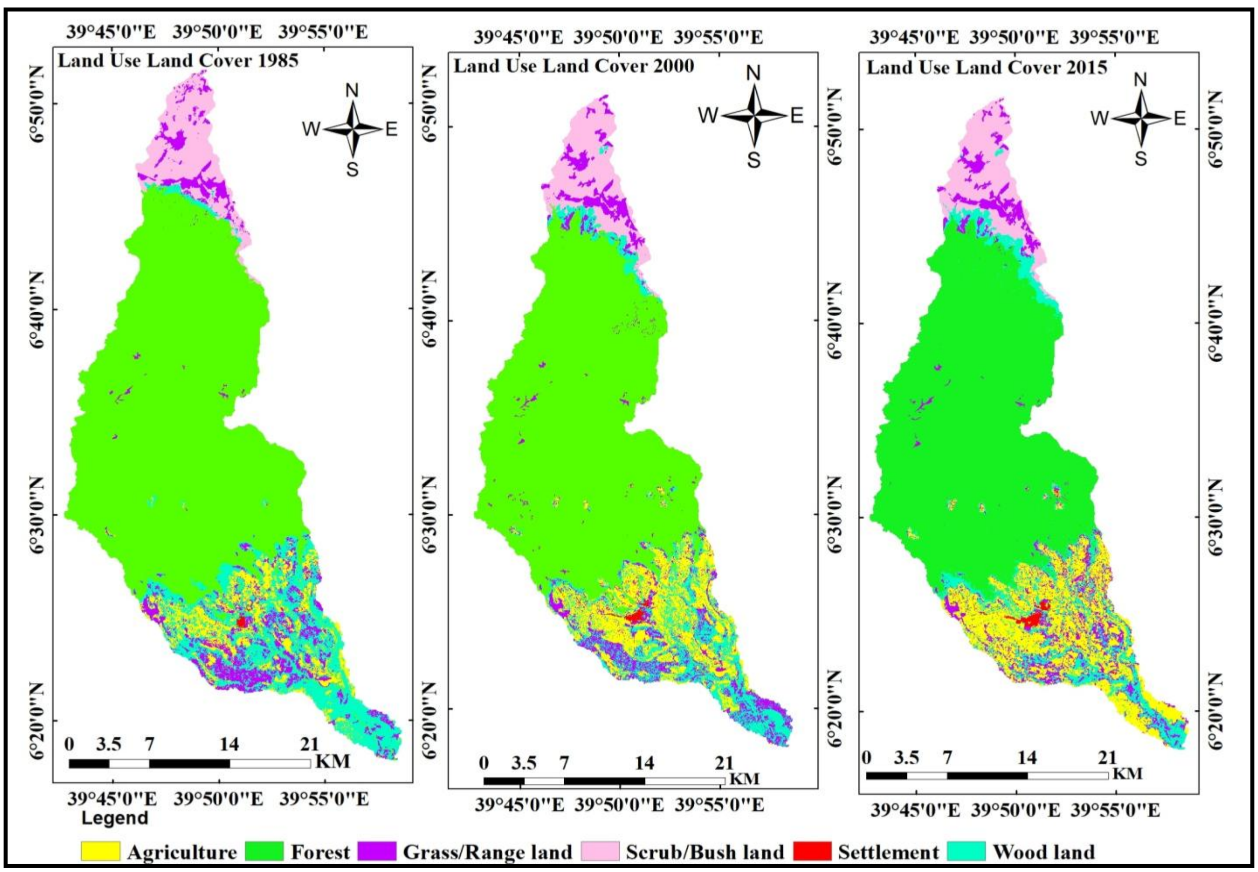

Figure 4.1: LULC Map of Yadot Watershed in the period 1985, 2000, and 2015

The increase of grass/range land may due to shifting cultivation practices contributed for conversion of other LULC to grass/rangelands. On the other hand fallowing is one way of farmland management practices in the study area, implying that the fallow farmlands used as a grazing land for cattle. The increasing trend of agriculture and settlement is due to the expansion of human needs and population growth. Generally, the result indicates that forest land, wood land, scrub/bush land and grass/range land decreased, while agricultural land and cultivated settlement increased. This may be due to the incasing of population growth rate and the need to secure more farm land. The findings of the study are consistent with other studies conducted in Ethiopia such as. Similarly (Dires and Temesgen, 2020) reported that agricultural land and settlement areas increased from 1984 to 2018 in the Lake Tana Basin. This result was lies with (Tatek and Danial, 2019) revealed a significant increasing trend of agriculture and settlement areas by 12 and 270%, respectively. In contrast, grasslands, forest lands and shrub-bush lands showed a declining trend of about 40, 21 and 12%, respectively in the Muga watershed. Similarly (Mesfin, 2018) reported that increasing settlement and agriculture in shaya watershed between1987 and 2015. Study (woldeamlak and Solomon, 2013) reported expansion of open grassland, agriculture and settlements in a tropical highland watershed, Ethiopia as a result of human activities such as the reduction of natural vegetation cover.

4.3. LULC Change Transition Probability Matrix between 1985 to 2015

Conversion between 1985 and 2000

The amount of LULC in hectare converted to other or gained from other type are important aspect of change detection. Agriculture gained about 3290.62ha, 1157.22ha, 121.26ha, 10.01ha and 2.49ha of land from wood land, grass/range land, forest, scrub/bush and settlement land, respectively. Conversely about 515.76ha, 395.31ha, 98.03ha, and 39.31ha of agricultural land lost to wood land, grass/range land, settlement and forest, respectively. The change detection indicted that the shifting of (524.56ha) forest land, (566.46ha) scrub/bush land, (1597.82ha) wood land, (2.86ha) settlement and (395.31ha) agricultural land had significantly changed to grass/range land. Moreover, the area of wood land (82.39ha), (0.06ha) scrub/bush land, (98.03ha) agriculture and (56.28ha) grazing land had changed slightly into a settlement. Gains and losses in forest, scrub/bush land and wood land were also taken place during these periods (Table 4.5).

Table 4.5: Transition Area Matrix (ha) between 1985-2000 and 200-2015 period in Yadot watershed.

		Land Use Land Cover 2000						
	Land use class	Agriculture	Forest	Grass/Range	Scrub/Bush	Settlement	Wood	Total
LULC1985	Agriculture	3442.61	39.31	395.31	0.00	98.03	515.76	4491.01
	Forest	121.26	46103.29	524.56	230.79	0.00	1200.46	48180.37
	Grass/Range	1157.22	23.94	2576.72	358.39	56.28	1372.10	5544.65
	Scrub/Bush	10.01	3.74	566.46	4692.66	0.06	203.42	5476.35
	Settlement	2.49	0.00	2.86	0.00	82.48	0.00	87.83
	Wood Land	3290.62	244.84	1597.82	119.49	82.39	4437.88	9773.05
	Total	8024.20	46415.13	5663.72	5401.33	319.23	7729.63	73553.25

		Land Use Land Cover 2015						
		Agriculture	Forest	Grass/Range	Scrub/Bush	Settlement	Wood	Total
LULC2000	Agriculture	5885.81	0.54	961.88	0.00	126.57	1049.40	8024.20
	Forest	148.04	45006.10	52.59	20.59	4.36	1183.45	46415.13
	Grass/Range	1683.82	145.61	2786.33	177.65	71.98	798.33	5663.72
	Scrub/Bush	75.02	0.00	176.13	5005.51	0.09	144.58	5401.33
	Settlement	40.67	0.00	6.06	0.00	267.01	5.50	319.23
	Wood Land	2620.00	47.86	1383.57	49.29	67.39	3561.51	7729.63
	Total	10453.35	45200.12	5366.55	5253.04	537.41	6742.77	73553.24

Conversion between 2000 and 2015

The conversions of LU/LC from one class to another class were revealed in all study periods. Between 2000 and 2015 period, 2620 ha, 1683.82 ha, 148.04 ha, 75.02ha and 40.67 ha of wood lands, grass/range lands, forest, scrub/bush land and settlement were converted to agriculture land, respectively. Similarly, 1049.40ha, 961.88ha, 126.57ha and 0.54ha agriculture land were lost to other LULC categories. In these periods, a significant area of wood land was converted from forest (1183.45 ha), agriculture 1049.40ha, settlement (5.50), scrub/bush land (144.58ha) and grass/range land (798.33 ha). In reverse, there was also a considerable conversion of wood land to other categories. During this period, some areas of settlement were also converted from farmland (126.57 ha), forestland (4.36 ha), wood land (67.39ha), scrub/bush land (0.09ha) and grassland (71.98 ha). Although, about 5.50 ha, 40.67 ha, and 6.06 ha of the settlement were also converted to wood land, agriculture and grass/range land, respectively. Gains and losses in forest, scrub/bush land and grass/range land were taken place in this study periods. A significant amount of gains and losses in the grass/range land has occurred in these periods. The gain of LULC for each class was determined from the result of persistence and the total column value, whereas the loss is from total row and the persistence (figure 4.2).

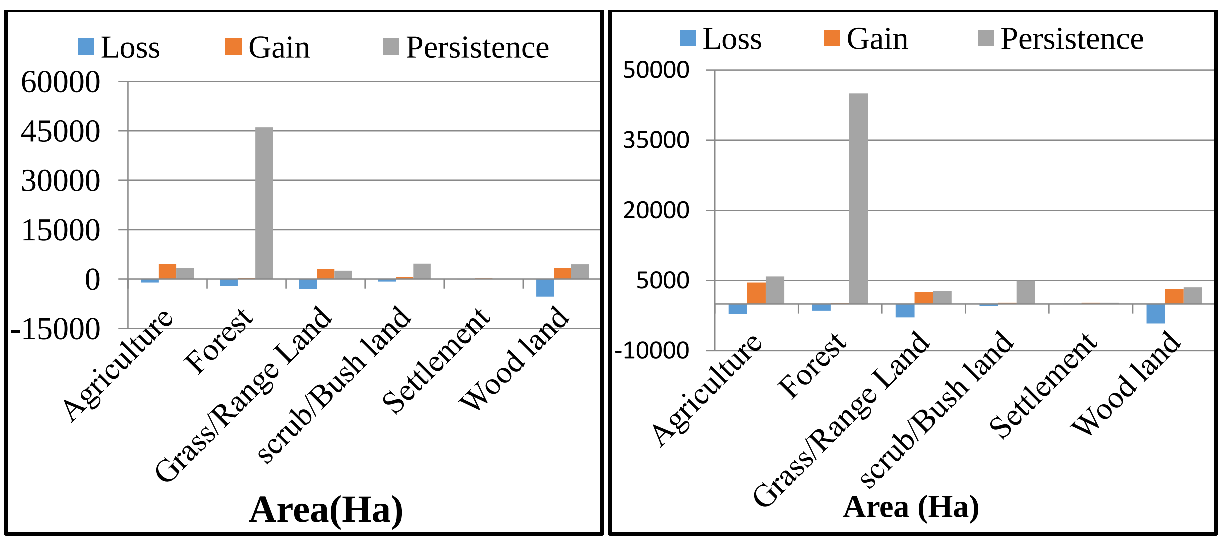

Figure 4.2: Gain, Loss and Persistence area of LULC class in (1985 -2000) and (2000-2015)

The gains and losses of the land use and land cover during the study period were derived from the cross tabulation of 1985, 2000 and 2015.

4.4.Future Land Use Land Cover Change prediction

4.4.1. Validation of CA-Markov Model

In order to validate the LULC prediction given by the CA-Markov model, the simulated land use areas were used to compare the actual and simulated land use areas. Then, the observed LULC 2015 was cross-compared with the simulated LULC 2015 to evaluate the performance of the model using the kappa index. The result on (Table 4.6) indicates agricultural, grass/range land and settlement have best agreement (Figure 4.3).

Table 4.6: Comparison of actual and projected LULC 2015

	Simulated		Classified	
LULC Types	Area (ha)	Percent (%)	Area (ha)	Percent (%)
Agriculture	10324.8	14.04	10453.4	14.21
Grass/Range Land	5175.2	7.04	5366.55	7.7
Forest	43,760.61	59.49	45200.1	60.45
Scrub/Bush Land	5902.1	8.02	5253.04	7.14
Wood Land	7865	10.69	6742.77	9.17
Settlement	526.3	0.72	537.41	0.73
Total	**73,553.31**	**100**	**73,553.31**	**100**

The simulated LULC map shows that forest land coverage areas are underestimated, while wood land and Scrub/Bush Land are overestimated. The values of k-index greater than 80% show good agreement between the projected and actual LULC map.

Table 4.7: The k-index values of the simulated LULC map of 2015

Index	Value
K no	0.891
K locations	0.9016
K location Strata	0.9016
K standard	0.84

All indices are greater than 80%, showing a good overall agreement and projection ability of the model. Therefore, CA-Markov model is strong to simulate the future for accurate prediction of future LULCs

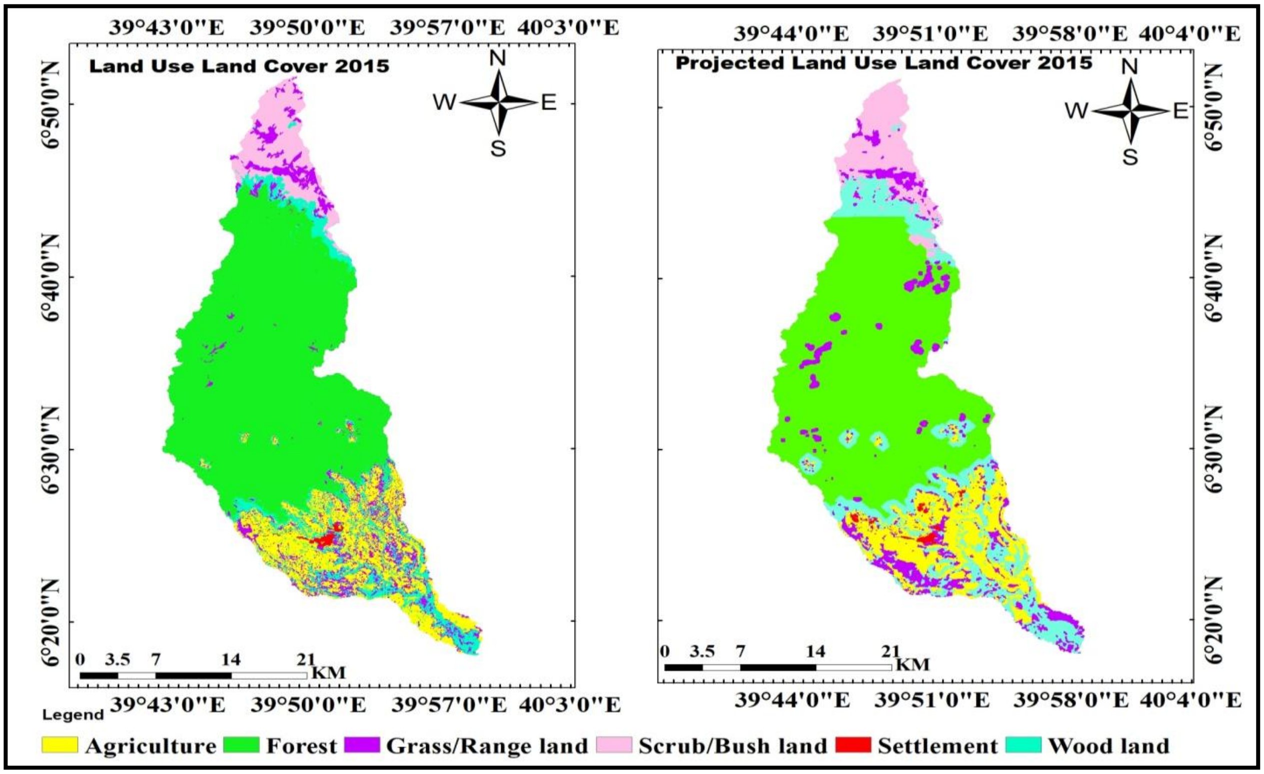

Figure 4.3: Simulated and observed LULC Map of 2015

4.4.2. Predicted future Land Use Land Cover

The future prediction of LULC 2035 and 2055 were executed using the 2015 land use map as a base map. The predicted LULC result of 2035 reflects that agricultural, settlement, grass/range land and wood land are increasing, while forest and scrub/bush land are decreasing. The LULC between the two future periods 2035 and 2055 indicate agricultural land and settlement predicted identical increasing trend, while forest, scrub/bush land, wood land and grass/range land showed a decreasing trend as shown on (Figure 4.4).

The predicted LULC result of 2035 and 2055 indicate agricultural and settlement showed identical increasing trend from 2015 to 2055 by 44.02% and 69.20% respectively. The annual rate of agricultural and settlement increment from 2015 to 2035 showed 89.34 ha/year and 11.66 ha/year, while from 2035 to 2055 increased by 140.74 ha/year and 6.94ha/year, respectively. Generally agricultural and settlement lands observed through the period 2015 to 2055 increased by 115.04 ha/year and 9.30ha/year, respectively.

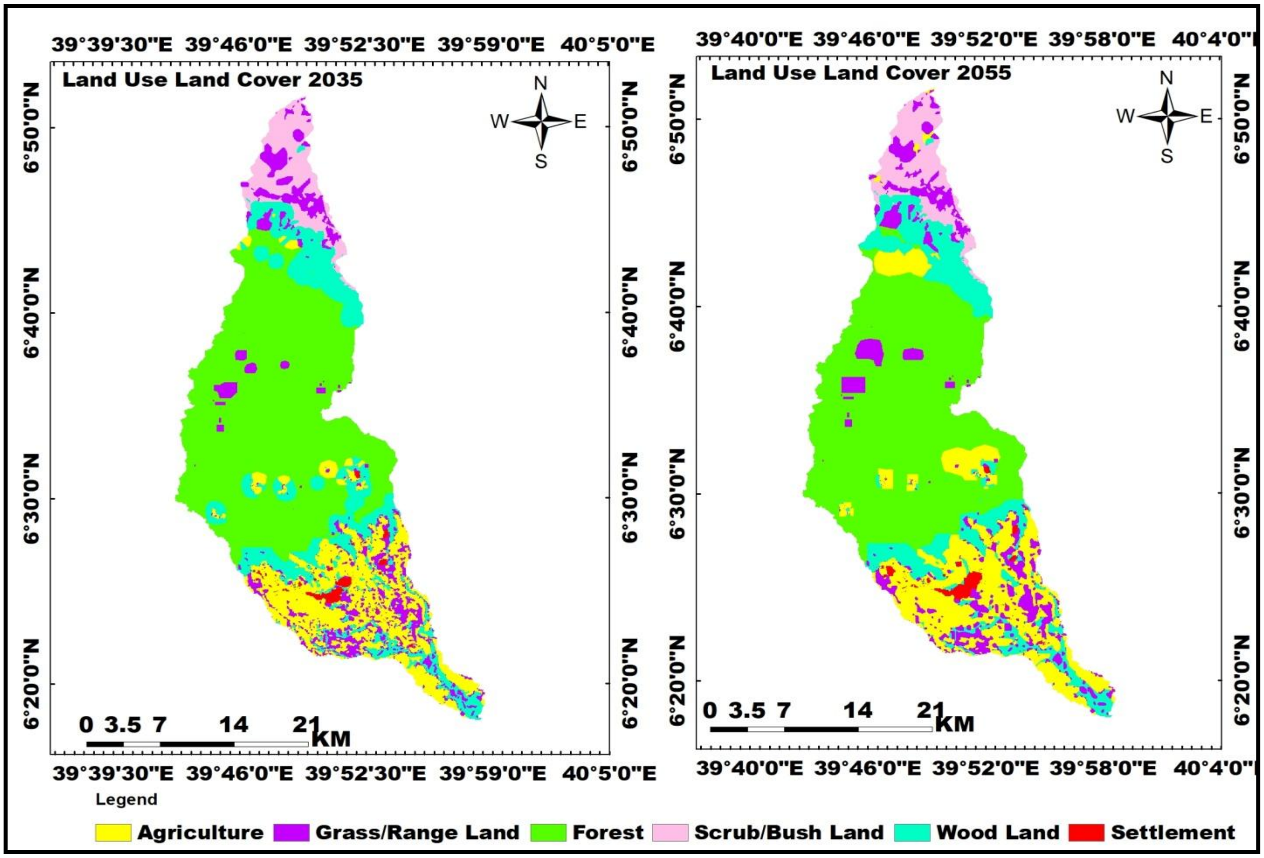

Figure 4.4: Predicted LULC Map of the year 2035 and 2055

Based on the LULC prediction result grass/range lands were increased by 32.38% between 2015 and 2035 at the expense of other LU/LC categories mainly woodland, scrub/bush land and agricultural lands as shown on (Table 4.8). Shifting cultivation practices contributed for conversion of woodlands to rangelands in the lowland parts of the watershed creating huge openings in woodland after cultivation is abandoned or due to continuous increase of future conservation works. The grass/range land cover slightly declined by 1.53% from 2035 to 2055 but greatly increased by 30.35% from 2015 to 2055. The LULC result in this study agrees with other previous studies in Ethiopia. For example (Bireda, 2015) reported that expansion of grassland between 1973 and 2015, almost 80% of was obtained from cultivated lands in Fagita Lekoma Woreda, Awi Zone, North Western Ethiopia.

Table 4.8: The area coverage of LULC, percent, and rate of changes in the Ydaot watershed between 2015, 2035 and 2055

	Area (ha)			Percentage change (%)			Rate of change (ha/year)		
LULC	2015	2035	2055	2015 -2035	2035-2055	2015-2055	2015 -2035	2035-2055	2015-2055
Agriculture	10453.4(14.21*)	12240.1(16.64*)	15054.9(20.47*)	17.09	23	44.02	89.34	140.74	115.04
Forest	45200.1(60.45*)	36945.1(50.23*)	35467.6(45.22*)	-18.26	-4	-21.53	-412.75	-73.88	-243.31
Grass/Range	5366.55(7.3*)	7104.26(9.66*)	6995.56(9.51*)	32.38	-1.53	30.35	86.89	-5.44	40.73
Scrub/bush	5253.04(7.14*)	4690.07(6.38*)	4671.12)6.35)	-10.72	-0.4	-11.08	-28.15	-0.95	-14.55
Settlement	537.41(0.73*)	770.55(1.05*)	909.27(1.24*)	43.38	18	69.2	11.66	6.94	9.30
Wood land	6742.77(9.17*)	11803.1(16.05*)	10454.9(14.21*)	75.05	-11.42	55.05	253.02	-67.41	92.80

*The number in parenthesis/bracket indicate percentage LULC

Key: - First scenarios (**S1**) (2015 to 2035), Second scenarios **(S2**) (2035 to 2055) and Third scenarios (**S3**) (2015 to 2055)

Similarly (Afera, 2018) also reported expansion of grassland at the expense of built up area and water body of Woreta Zuria, Ethiopia Watershed between 1997 and 2017.

The forest and scrub/bush land cover showed continuously declining trend from 2015 to 2055 by 21.53% and 11.08% with annual rate of decline by 243.31ha/year and 14.55 ha/year, respectively. Wood land showed increasing trend from 2015 to 2035 by 75.05% but slightly declined by 11.42% from 2035 to 2055. The annual rate of wood land increment showed 253.02 ha/year from 2015 to 2035, while declined with annual rate of 67.41ha/year for the period 2035 to 2055, respectively. In general increment of wood land from 2015 to 2035 may be due to the planned afforestation and green legacy strategies of government are the possible reason. (Semegnew *et al*., 2021) summaries forestland was declined to 77.8% in 2017, whereas farmland, settlement, and grassland increased by 17.4%, 3.4%, and 1.4%, respectively from 2002 to 2017. Similarly (Adane and Getachew, 2017) reported that overall increasing grass/range land from2006 to 2026 in Bale eco-region. Therefore Prediction of LULC using time serious data is important for the future management plan of LULC. Hence, a rational land use plan should be proposed in order to sustain livelihoods of local communities.

4.5. LULC Transition Probability Matrix between 2015 to 2055

Conversions between 2015 and 2035

In these periods, 1001.34 ha, 1086.84ha, 552.32 ha, ha, 50.84 ha and 0.23 ha of agricultural land will be converted from forest land, wood land, grass/range land, settlement and scrub/bush land, respectively. About 159.19 ha, 66.60 ha, 64.08 ha and 0.11 ha of settlement will be also reverted from agriculture, wood land, grass/range land and forest land, respectively. Although agricultural and settlement land will be converted from other land uses, there will be also a significant loss of agricultural and settlement land to other land uses (Table 4.9). Between these periods, there will be a huge loss of forest, wood land, grass/range land, scrub/bush land to other land uses. For example about, 6499.04ha, 1001.34 ha, 755.21ha and 0.11ha of forest land will be converted to wood land, agriculture, grass/range land and settlement, respectively. About 1086.84ha, 757.59ha, 64.08ha, 1.54ha and 0.21ha of wood land will be also converted to agriculture, grass/range land, settlement, scrub/bush land and forest land, respectively. The grass/range land converted to agricultural land, wood land, settlement, scrub/bush land and forest land will be 552.32 ha, 173.16 ha, 66.60 ha, 6.49ha and 0.49 ha, respectively.

In contrast, wood land grass/range land, forest land and scrub/bush land will be also gain from 6970.64 ha, 2536.77ha, 8.02ha and 0.71ha other categories (Table 4.8). In the watershed, the downstream and partly at the upstream areas, which were previously covered by forests, scrub/bush land and range lands, have been converted to agricultural land and settlement.

Conversion between 2035 and 2055

The significant increase of agricultural land and settlement with the sharp decline of forest land, wood land and scrub/bush land in the watershed were the major transformations observed. For example, 1476.73ha, 760.80ha, 218.09ha, 55.44ha and 1390.60ha of agriculture land will be reverted from forest, grass/range land, scrub/range land, settlement and wood land, respectively. Conversely about 338.33ha grass/range land, 594.57ha wood land, 90.52ha settlement, 63.44ha forest and 0.02ha scrub/bush land were lost from agricultural land, respectively.

The conversions of wood land (64.90ha), agriculture land (90.52ha), scrub/bush land (0.09ha) and grass/range land (43.76ha) was the major contributing land use for the settlement. Conversely about 55.44ha agriculture and 5.11ha grass/range land were lost from settlement, respectively. An estimated 1390.60ha, 1508.95 ha, 226.27ha, 57.99ha and 64.90 ha of wood land were also converted to agriculture, forest, grass/range land, scrub/bush land and settlement, respectively. The forest land which is the highest class has 33849.98ha with the probability of remaining as forest land in 2035–2055. In reverse, there was also a considerable gain and los of scrub/bush land to other categories. The major reason for the expansion of grassland was low productivity of agriculture lands and migration of people in search food for their cattle in the forest and wood land (Table 4.9). In 2035–2055 the two highest class loss was the change of wood land to forest land by 1508.95ha and forest land to agriculture by 1476.73ha. The minimum loss of LULC category was observed from settlement to agriculture 55.44ha and grass/range land 5.11ha.

Table 4.9: Transition Area Matrix (ha) between 2015 - 2035 and 2035 - 2055 period in Yadot Watershed

		Land Use Land Cover 2035						
LULC class		Agriculture	Forest	Grass/Range	Scrub/Bush	Settlement	Wood	Total
Land Use Land Cover 2015	Agriculture	9548.52	0.00	561.53	0.00	159.19	184.12	10453.35
	Forest	1001.34	36944.43	755.21	0.00	0.11	6499.04	45200.13
	Grass/Range Land	552.32	0.49	4567.49	6.49	66.60	173.16	5366.55
	Scrub/Bush Land	0.23	0.00	457.97	4682.04	0.00	112.79	5253.04
	Settlement	50.84	0.00	4.48	0.00	480.57	1.52	537.41
	Wood Land	1086.84	0.21	757.59	1.54	64.08	4832.50	6742.77
	Total	12240.10	36945.14	7104.26	4690.07	770.55	11803.1	73553.25
		Land Use Land Cover 2055						
		Agriculture	Forest	Grass/Range	Scrub/Bush	Settlement	Wood	Total
Land Use Land Cove 2035	Agriculture	11153.21	63.44	338.33	0.02	90.52	594.57	12240.10
	Forest	1476.73	33849.98	583.58	0.00	0.00	1034.85	36945.14
	Grass/Range Land	760.80	45.18	5814.91	170.58	43.76	269.02	7104.26
	Scrub/Bush Land	218.09	0.00	27.34	4442.53	0.09	2.02	4690.07
	Settlement	55.44	0.00	5.11	0.00	710.00	0.00	770.55
	Wood Land	1390.60	1508.95	226.27	57.99	64.90	8554.43	11803.14
	Total	15054.87	35467.55	6995.56	4671.12	909.27	10454.9	73553.26

Note: The shade numbers indicate the unchanged LULC proportions

Generally, the patterns of LULC change showed that the agricultural land gained the most area compared to the other LULC types.

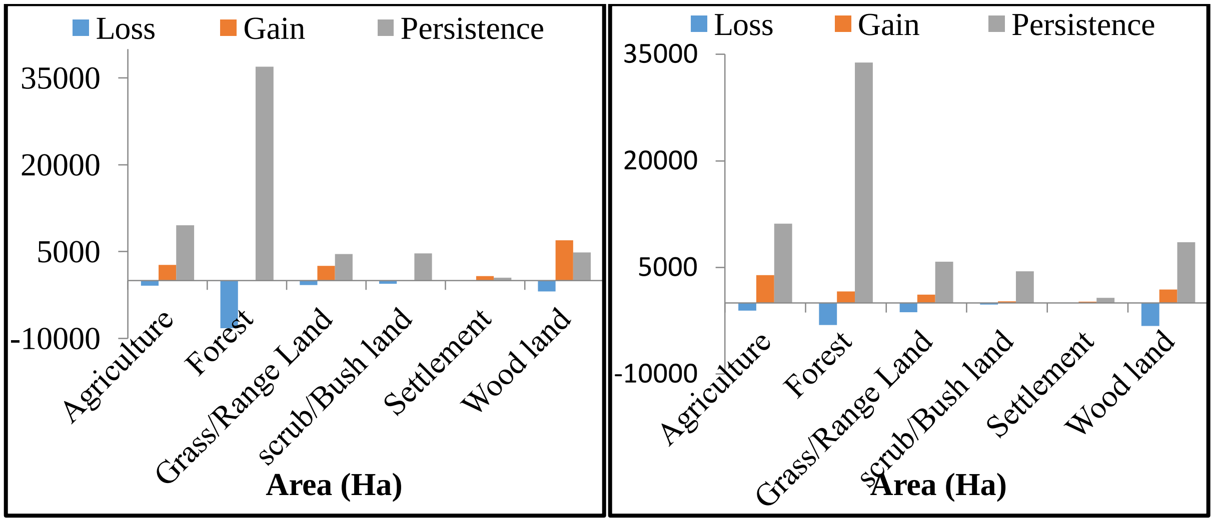

Figure 4.5: Gain, Loss and Persistence area of LULC class in (2015 -2035) and (2035-2055)

The significant increase of agricultural land and settlement, with the sharp decline of forest land, scrub/bush land, wood land and grass/range land experienced reduction in coverage throughout the study periods, the greatest reduction rate was observed in forest land. In general the study show that agriculture and settlement area increase was consistent with (Megersa et al., 2021) reported the future projection of agricultural land increased from 61.19% in 2019 to 72.98% in 2035 and 73.24% in 2050, whereas forest cover will further degrade from 16.94% in 2019 to 8.07% in 2050. Similarly the predicted result of the year 2019 to 2050 showed an increase of urban land from 1.2% in 2019 to 3.8% in 2050. (Birhan et al., 2021) prediction of the LULC change using the CA-Markov chain model indicates that cropland, tree cover, and built-up areas are likely to increase by 2020s, 2050s, and 2080s in the Lake Tana Basin, upper Blue Nile River Basin. (Wakjira et al., 2020) reported that agricultural land and urban and built-up continuously increase while forest land decrease throughout the study period 1987 to 2055 respectively. Therefore, to mitigate the rapid rates of LULC conversions at watershed, the application of integrated watershed management strategies, managing the rapid population growth, afforestation of degraded or deforested areas, and reducing the dependency of locals on forest products is critically important.

4.6.Future Climate Projection

4.6.1. Precipitation Projection under RCP4.5 and RCP 8.5 scenarios

A. Projected Rainfall under RCP4.5

The seasonal rainfall distribution under RCP4.5 and RCP8.5 scenarios were similar to the baseline period. However, the mean annual rainfalls under RCP4.5 and RCP8.5 scenarios slightly increased than the baseline period except in the near-term under RCP 8.5 of the watershed. The mean annual rainfall is projected to increase by 1.38 mm and 13.26 mm for the near and midterm period compared to baseline under RCP4.5 scenarios, respectively. The projections of mean annual rainfall showed a slight increasing trend for near and midterm according to scenario RCP4.5. For Scenario RCP8.5 the projected mean annual rainfall is higher compared to scenario RCP4.5. This increase is mainly due to the projected increases in wet season rainfall, partially offset by projected decreases in dry season rainfall (Figure 4.6).

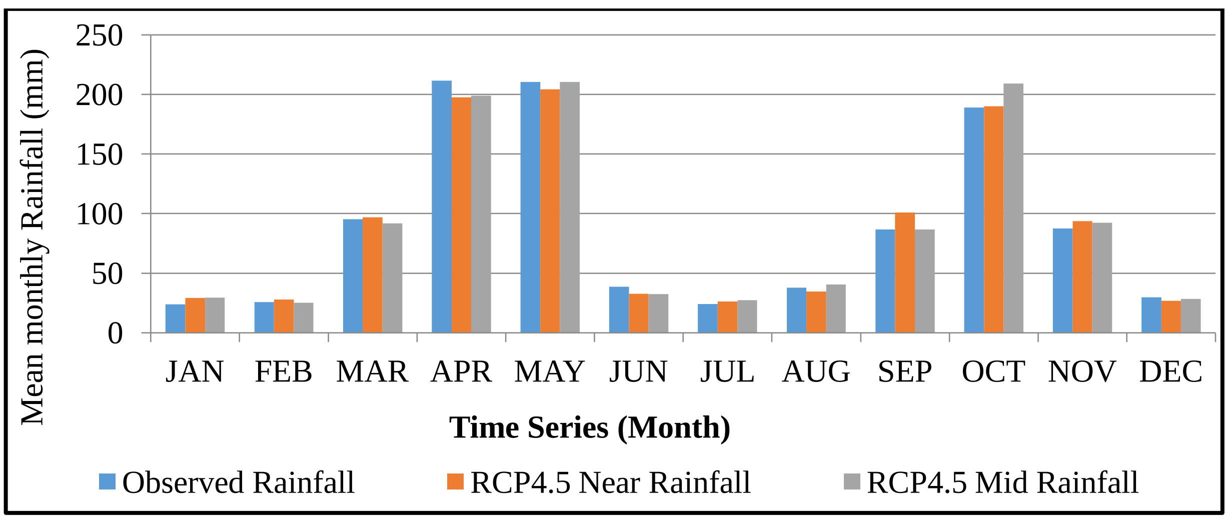

Figure 4.6: Mean monthly precipitation under RCP4.5 for near and mid future compared to baseline period.

The seasonal classifications were made based on the rainfall patterns of the study area into, Dry season (January, February, June, July and December) and Wet season (March, April, May, August, September, October and November), therefore, it is applicable only in south eastern (bimodal type of rainfall) of Ethiopia. Seasonal rainfall in wet season showed maximum increase of 12.28 mm in midterm under RCP 4.5 scenarios.

The projected mean monthly rainfall showed inconsistent directions and magnitude of change under RCP4.5 and RCP8.5 scenarios. The mean monthly rainfall may increase during dry season (January, February and July) with maximum increase in January (22.2%), while decreased (June and December) with maximum decrease in June (15.43%) in the near-term. Similarly in the midterm mean monthly rainfall increased in dry season (January and July) with maximum increase in January (23.28%), while decrease (February, June and December) with maximum decrease in June (15.87%), respectively under RCP4.5 scenarios from baseline period. The mean monthly rainfall in the study watershed is projected to increase in the wet season (March, September, October and November) with maximum increase in September (16.67%), while decrease (April, May and August) with maximum decrease in August (8.38%) in the near-term under RCP4.5 scenarios. The midterm mean monthly rainfall increased during wet season (August, September, October and November) with maximum increase in October (10.74%), while decreased (March April and May) with maximum decrease in April (12.64%), respectively under RCP 4.5 scenarios as shown on (Figure 4.7).

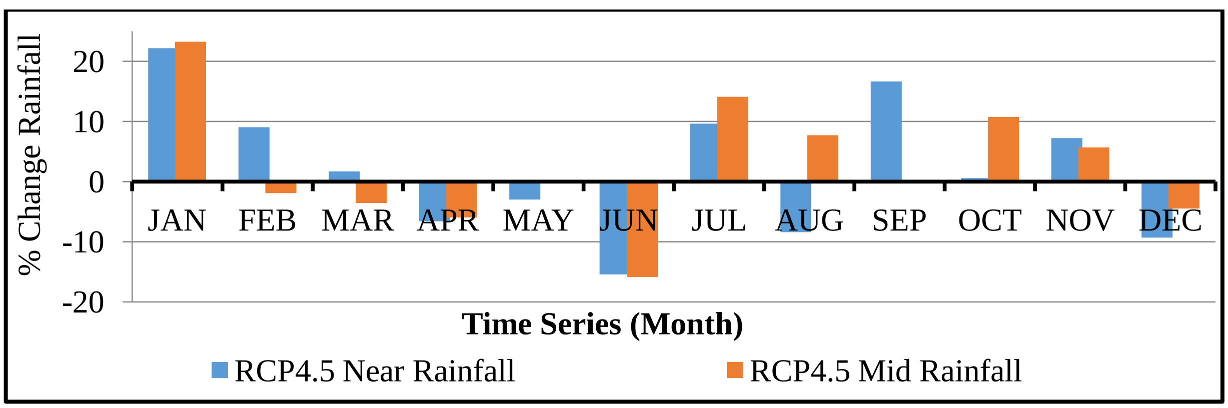

Figure 4.7: Percentage changes of monthly rainfall for near-term and midterm under RCP 4.5 scenarios from baseline period

B. Projected Precipitation Under RCP8.5

The projected change in precipitation varies with mean annual and seasonal under RCP8.5 scenarios. The mean annual rainfall projection show slight decreasing trend by 4.85 mm in the near-term, while increased by 17.56 mm in the midterm under RCP8.5 scenarios from the baseline period. Similar to temperature, rainfall simulations under RCP8.5 is substantially greater than under RCP4.5 in the watershed even if rainfall decrease in the near-term.

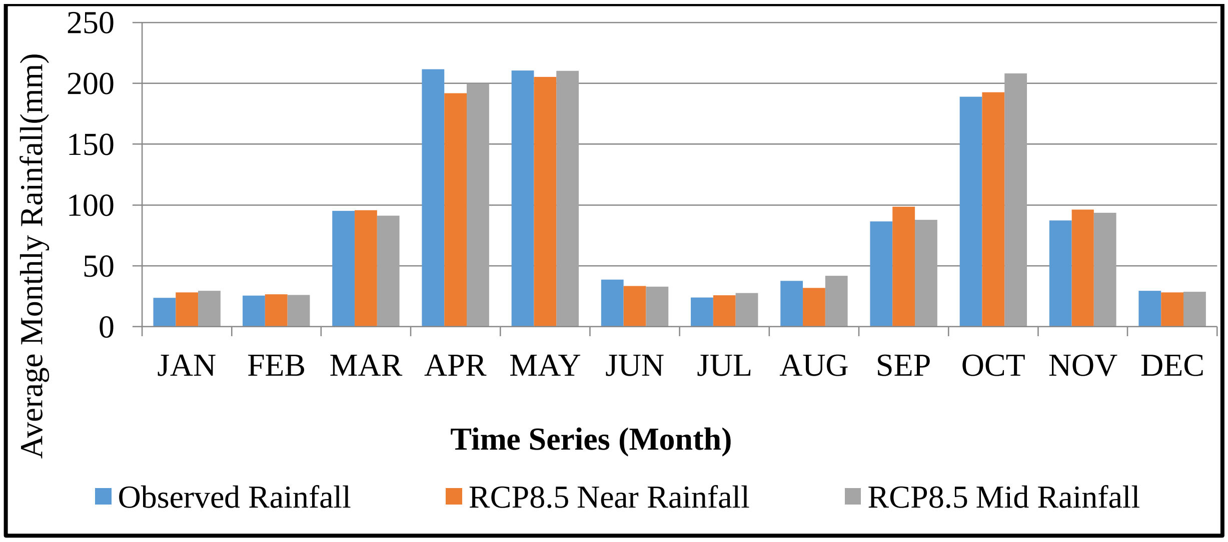

Figure 4.8: Mean monthly precipitation under RCP8.5 for near and mid future compared to baseline period

Under RCP8.5 the mean seasonal rainfall is projected to increase in dry and wet season. For the RCP8.5 of the midterm rainfall expected to increase with maximum of 14.60 mm in the wet season, while decreased by 5.69 mm in near-term of dry season from the baseline (Figure 4.8). The mean monthly change in rainfall is not systematic i.e. rainfall increases in some months and decreases in other months. The seasonal rainfall is projected to increase during dry season in January, February and July with maximum increase in January by 18.79% and 23.55% for near and midterm under RCP8.5 scenarios respectively. The projected rainfall expected to decrease in June and December with maximum decrease in June by 13.52% and 14.62%, respectively for both near-term and midterm under RCP8.5 scenarios from baseline. Similarly mean monthly rainfall increased in wet season for the month of (March, September, October and November) with maximum increase in September by 14.03%, while decreased for the month of (April, May and August) with maximum decrease in August by 15.14% in the near-term under RCP8.5 scenarios from baseline, respectively.

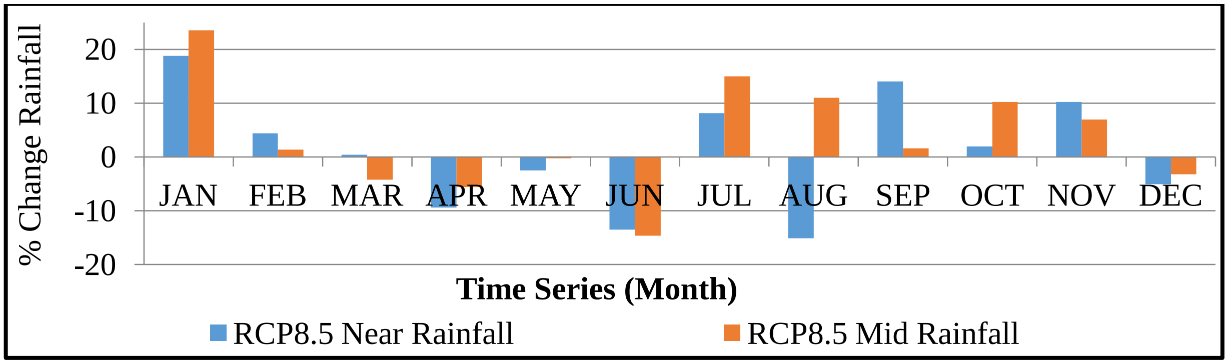

Figure 4.9: Percentage changes of monthly rainfall for near-term and midterm under RCP 8.5 scenarios from baseline period

For the midterm mean monthly rainfall expected to increase in wet season (September, August, October and November) with maximum increase in October by 19.28%, while decrease in March, April and May with maximum decrease in April by 5.57% under RCP8.5 scenarios from the baseline period respectively. In general future projection of precipitation show increasing trend annually from the baseline period under RCP4.5 and RCP8.5 scenarios. On Figure 4.9 above upward sign indicates an increase from the baseline period, while a downward signs indicates decrease from the baseline period. There are different studies that shows increase rainfall in the future in agreement with these results include: (Tesfaye *et al*, 2019) study in Awata River watershed, Genale Dawa basin indicates that precipitation does not show systematic increase or decrease. But overall mean annual precipitation shows an increasing trend for both RCP4.5 and RCP8.5 scenario with the percent of increment up to 26.8% and 35.1% at near (2020) and mid-term (2050) respectively. The study by (Megersa *et al*., 2021) also confirmed an increasing trend in annual precipitation by +26.3 and +31.85% for RCP4.5 and RCP8.5 climate scenarios, respectively, at the end of twenty-first century in the Upper Wabe Bridge Watershed in Wabe Shebele River Basin. (Mesgana *et el*., 2017) conclude that the mean annual precipitation is projected to increase by about 6% (9%) in 2050s (2080s) in Awash, Baro, Genale and Tekeze rivers of four major river basins in Ethiopian. (Birhan *et al*, 2021) precipitation would increase by up to 25% in the Lake Tana Basin, of the upper Blue Nile River Basin

4.6.2. Temperature Projection under RCP4.5 and RCP 8.5 Scenarios

A. Projected Temperature Under RCP4.5

The dynamically downscaled mean annual maximum and minimum temperature showed increasing trend in the near and midterm under RCP4.5 and RCP8.5 scenarios. Compared to the baseline period, seasonal (dry and wet) changes of maximum and minimum temperatures are predicted to increase in the watershed under RCP4.5 and RCP8.5 scenarios. Therefore baseline and projected minimum and maximum temperatures under both scenarios flows a similar seasonal trend. The mean annual maximum temperature is projected to increase from 0.65^{0}C to 1.05^{0}C under RCP4.5 scenarios in the near-term and midterm, respectively. Similarly the mean annual minimum temperature is expected to increase from 0.48^{0}C to 0.85^{0}C in the near and midterm from baseline period under RCP4.5 scenarios.

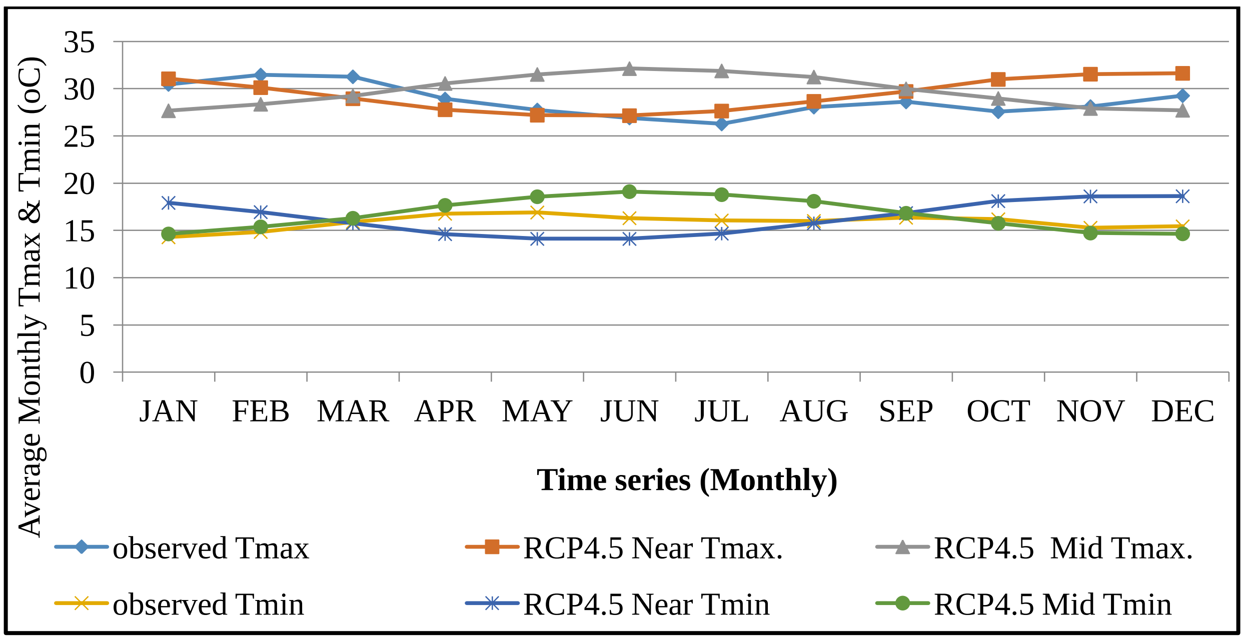

Figure 4.10: Mean monthly maximum and minimum temperatures of near and mid future period with respect to baseline period under RCP 4.5 scenarios

The simulation result showed a consistent increasing trend of mean annual for both minimum and maximum temperature in the near and midterm with a higher rate of increase towards the end of the century. It also noted that the rate of change of maximum temperature is higher than the rate of change of minimum temperature. As shown in (Figure 4.10) above. The mean wet season increase in maximum temperature shows a variation with a range from 0.65^0C to 1.31^0C, whereas the mean dry season increase in maximum temperature shows a variation with a range from 0.65^0C to 0.68^0C in the near-term and midterm under RCP4.5 scenarios, respectively. However, mean wet season increase in minimum temperature shows a slight variation with a range from 0.06^0C to 0.65^0C, whereas the mean dry season increase in minimum shows a large variation with a range from 1.07^0C to 1.13^0C in the near-term and midterm under RCP4.5 scenarios respectively. The simulated maximum temperature is higher in wet season of the midterm, while highest increase in minimum temperature is projected to occur in dry season of the midterm in the watershed. Even though the mean annual maximum and minimum temperature has show increasing trends in all future under RCP4.5 scenarios. The mean monthly simulated maximum and minimum temperature shows an inconsistent directions and magnitude change in all months from the near to midterm of future periods under RCP4.5 scenarios as shown below on (Figure 4.11).

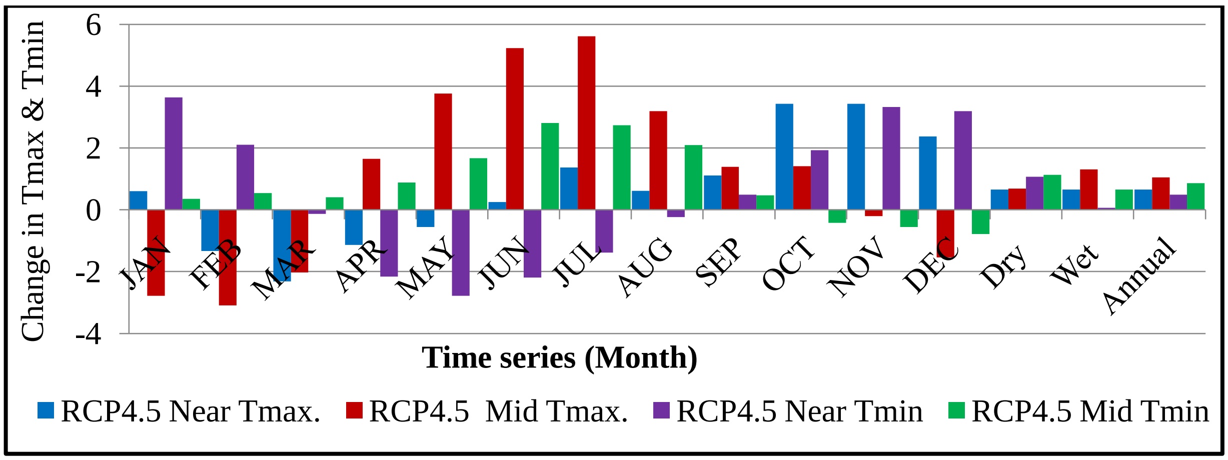

Figure 4.11: Mean monthly and seasonal changes in maximum and minimum temperature (°C) for near and midterm from baseline period under RCP 4.5 scenarios.

The mean monthly maximum temperature increased under RCP4.5 from 0.25^0C to 3.43^0C with the maximum increase in November, while decreased from 0.55^0C to 2.32^0C with the maximum decrease in March in the near-term compared to baseline period, respectively. Minimum temperature increased under RCP4.5 from 0.49^0C to 3.64^0C with the maximum increase in January, while decrease from 0.13^{0}C to 2.78^{0}C with the maximum decrease in May in the near-term from baseline period, respectively. The mean monthly maximum temperature may increase under RCP4.5 scenarios range from 1.39^{0}C to 5.61^{0}C with the maximum increase in July, while decrease from 0.2^{0}C to 3.10^{0}C with the maximum decrease in February midterm compared to baseline period respectively. Minimum temperature expected to increase under RCP4.5 from 0.35^{0}C to 2.81^{0}C with the maximum increase in June, while decrease from 0.42^{0}C to 0.78^{0}C with the maximum decrease in December in the midterm compared to baseline period respectively.

B. Projected Temperature Under RCP8.5

Mean annual maximum temperature is projected to increase from 0.71^{0}C to 2^{0}C, while minimum temperature is expected to increase from 0.56^{0}C to 1.8^{0}C under RCP8.5 scenarios in the near and midterm, respectively from baseline period. Compared to the baseline period, the mean seasonal maximum temperature in dry season increased from 0.61^{0}C to 1.9^{0}C, while the minimum temperature increased from 1.14^{0}C to 2.01^{0}C under RCP8.5 for near and midterm, respectively as shown on (Figure 4.12).

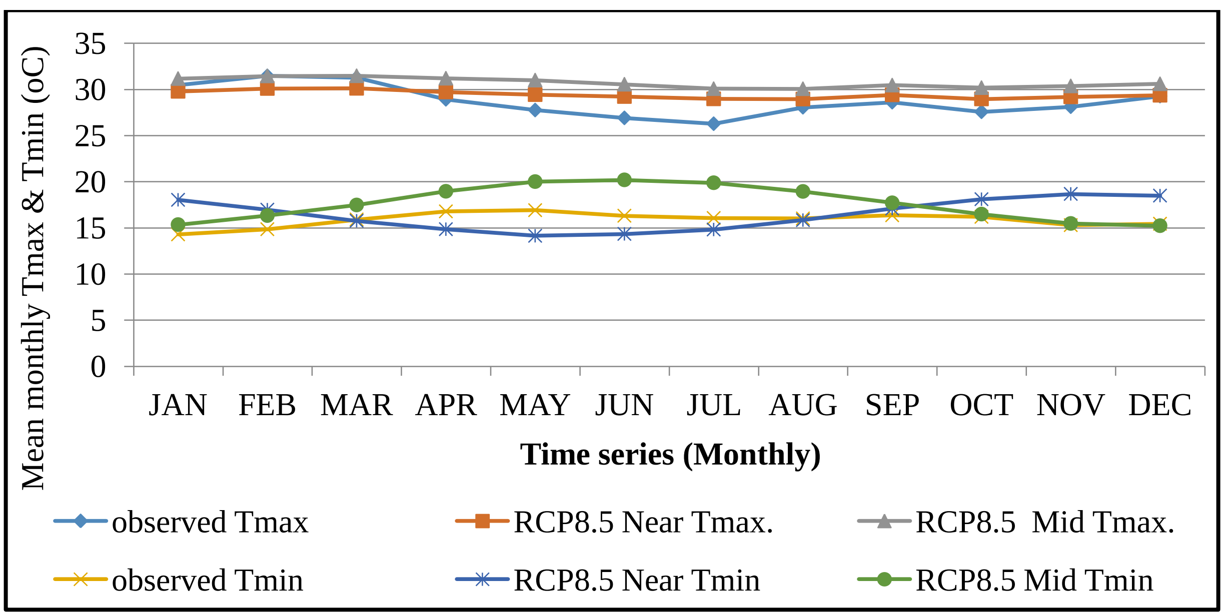

Figure 4.12: Mean monthly maximum and minimum Temperature of near-term and midterm with respect to baseline period under RCP8.5 scenarios

Similarly the projected mean seasonal maximum temperature show an increasing trend in wet seasons from 0.78^{0}C to 2.07^{0}C, while the minimum temperature increased from 0.14^{0}C to 1.66^{0}C under RCP8.5 in the near-term and midterm, respectively relative to the baseline period. The increase of maximum temperature is higher in wet season of midterm compared to dry season, while the increasing of minimum temperature is larger in dry season of midterm under RCP 8.5 scenarios.

The projected mean monthly maximum temperature has larger magnitude of increment under RCP8.5 scenarios range from 0.09^{0}C to 2.69^{0}C with the maximum increase in the month of July, while the maximum temperature decreasing from 0.67^{0}C to 1.36^{0}C with the maximum decrease in February for the near-term. On the other hand, the minimum temperature increased under RCP8.5 ranges from 0.72^{0}C to 3.74^{0}C with the maximum increase in January, while decrease from 0.14^{0}C to 2.77^{0}C with the maximum decrease in May for the near-term, respectively from baseline period. The mean monthly maximum temperature may increase under RCP8.5 from 0^{0}C to 3.79^{0}C with the maximum increase in July for the midterm compared to baseline period, respectively as shown on (Figure 4.13).

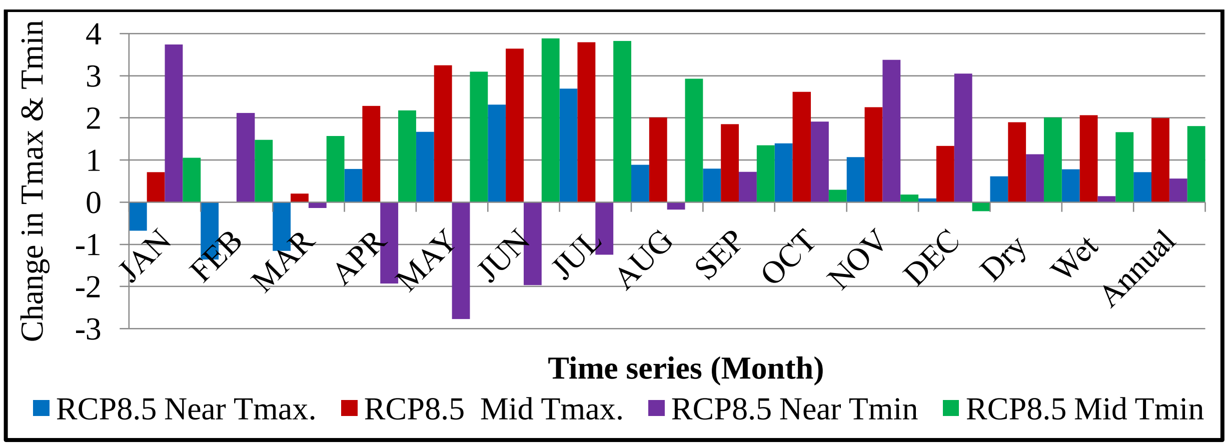

Figure 4.13: mean monthly and seasonal changes in maximum and minimum temperature (°C) for near and midterm from baseline period under RCP 8.5 scenarios.

Minimum temperature may increase under RCP8.5 from 0.18^{0}C to 3.89^{0}C with the maximum increase in June, while minimum temperature decrease only for January by 0.21^{0}C under RCP8.5 in the midterm, respectively from to baseline period. The increase in mean annual maximum and minimum temperature under RCP8.5 is larger than that under RCP4.5 scenario because RCP 8.5 scenario represents a high emission scenario which produces more CO_2 concentration than the RCP 4.5 scenario which represents a medium emission scenario (Ba et al., 2018). These results are in agreement with results from previous studies in the Genale dawa basin (Tufa and Sarma, 2021; Lemesa, 2017) and Tesfaye et al., 2019) in Awata River watershed, Genale Dawa basin. Also similar study by (Wakjira et al., 2020) and (Megersa et al., 2021) in the Finchaa catchment and Upper Wabe Bridge Watershed in Wabe Shebele River Basin show a consistent increasing trend of maximum and minimum temperature for all time horizons with a higher rate of increase towards the end of the century.

4.7.Calibration and Validation of SWAT Model

4.7.1. Sensitivity Analysis

Sensitivity analysis was performed on SWAT flow parameters at monthly time step to identify most sensitive parameters using a global sensitivity analysis of SWAT-CUP at Delo Mena gauging station. All flow parameters were considered to identify which parameters were more sensitive in Yadot watershed. For this analysis, 21 flow parameters which may affect stream flow were considered and only 10 parameters were identified to have significant influence in controlling the stream flow in the watershed (Table 4.10). Maximum canopy storage (CANMX), SCS runoff curve number (CN2), saturated hydraulic conductivity (SOL_K) and Soil evaporation compensation factor (ESCO) were found to be the most sensitive parameters for the stream flow predications. A Study by (Tufa and Sarma, 2021) identified (CN2) and (SOL_K) most sensitive parameters for runoff estimation in Genale watershed also (Samuel, 2016) identified (CN2) and (CANMX) to be highly sensitive parameters at upper Awash Basin.

Table 4.10: Sensitive Flow Parameters, their rank and fitted value

Parameter Name	Sensitivity Rank	t-Stat	P-Value	Min Value	Max Value	Fitted Value
2:V__CANMX.hru	1	-28.82	0.00	0.00	20.50	2.70
1:R__CN2.mgt	2	-23.56	0.00	-0.18	1.70	-0.12
3:R__SOL_K (..).sol	3	12.54	0.00	-0.09	0.21	0.20
4:V__ESCO.hru	4	7.44	0.00	0.89	0.98	0.98
8:V__CH_K2.rte	5	3.92	0.00	30.18	85.08	75.61
6:R__SOL_AWC (..).sol	6	3.57	0.00	-0.10	0.23	-0.01
10:V__GW_DELAY.gw	7	-1.69	0.09	52.19	67.10	61.84
9:V__GWQMN.gw	8	0.43	0.67	3379.73	3682.36	3423.16
7:V__ALPHA_BF.gw	9	-0.29	0.77	0.65	0.86	0.81
5:V__RCHRG_DP.gw	10	-0.01	0.99	0.78	0.89	0.88

Note: A, indicates add the fitted value to the existing value, V implies replace the existing value with the fitted value; R indicates multiply the existing value with (1+ the fitted value).

4.7.2. Calibration of SWAT Model

The result of calibration for monthly flow shows that there is a good agreement between the measured and simulated average monthly flows with Nash-Sutcliffe simulation efficiency (NSE) of 0.73 and coefficient of determination (R2) of 0.80 as shown below on (Table 4.12) and (Figure 4.14). Similarly, (Dagnenet *et al.*, 2018) found the correlation coefficient (R2=0.80) and the Nash – Sutcliffe simulation efficiency (NSE =0.70) which was a very good agreement between observed and simulated for upper Blue Nile River basin during the calibration period. Thus, SWAT model can be considered reliable model in simulating stream flow in Ethiopia condition in different watersheds after calibration.

The measured and simulated average monthly flow for the study area in the calibration period was obtained to be 9.31m^3/s and 9.41m^3/s, respectively. This show that average monthly simulated stream flow is slightly higher than the observed stream flow measured during stream flow calibration. The model has slightly overestimated stream flow during calibration.

The linear regression of the scattering plot of observed stream flow and simulated stream flow for calibration is show on (Figure 4.15).

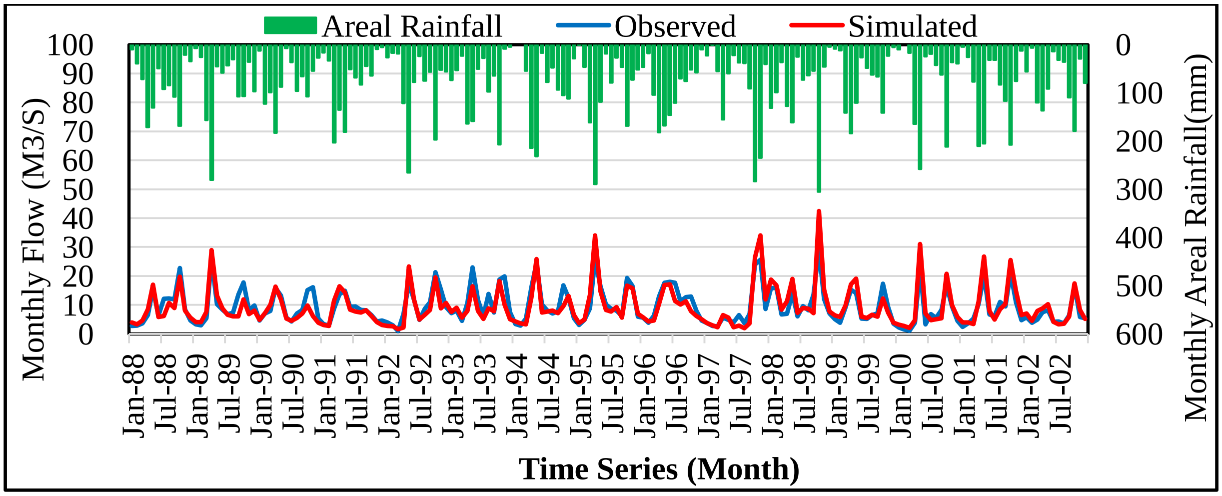

Figure 4.14: Calibration result for average monthly stream flow (1988-2002)

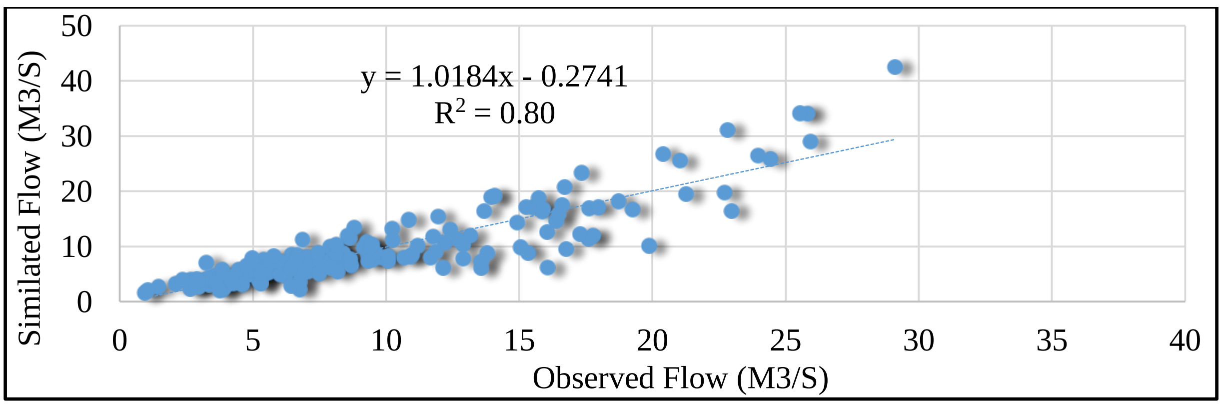

Figure 4.15: Scatter plots of observed and simulated stream flow for Calibration (1988-2002).

4.7.3. Validation of Model

Validation proves the performance of the model for simulated flows in periods different than the calibration period without any further adjustment in the calibrated parameters. The validation was performed for six years, period from 2003 to 2008 shown on (Figure 4.16). The result of coefficient of determination and Nash-Sutcliff efficiency indicates acceptable accuracy for the model to predict the watershed response. Based on the model performance determination coefficient (R2 = 0.83) and Nash-Sutcliff's simulation efficiency (ENS = 0.77) assures that the model shows a good performance during validation so as to able to simulate the stream flow in the study area (Table 4.11). (Wakjira *et al*., 2020) indicated that the model performance show a good correlation and agreement between the monthly measured data and simulated (ENS=0.76 and R2=0.81) flow in Finchaa Watershed for validation period as shown on The linear regression of the scattering plot of observed stream flow and validation stream flow is show on (Figure 4.17).

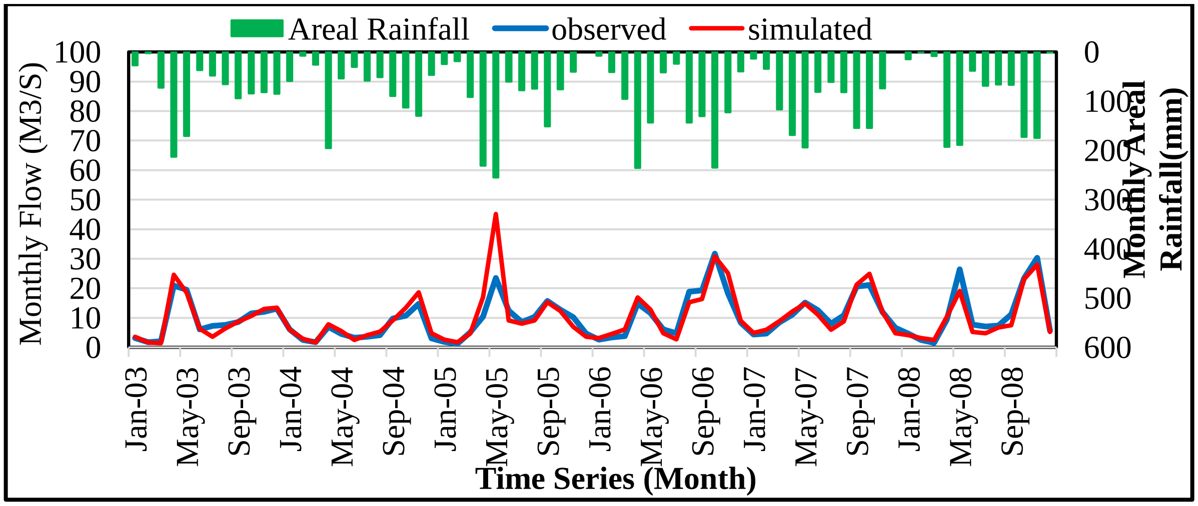

Figure 4.16: Validation result for average monthly stream flow (2003-2008)

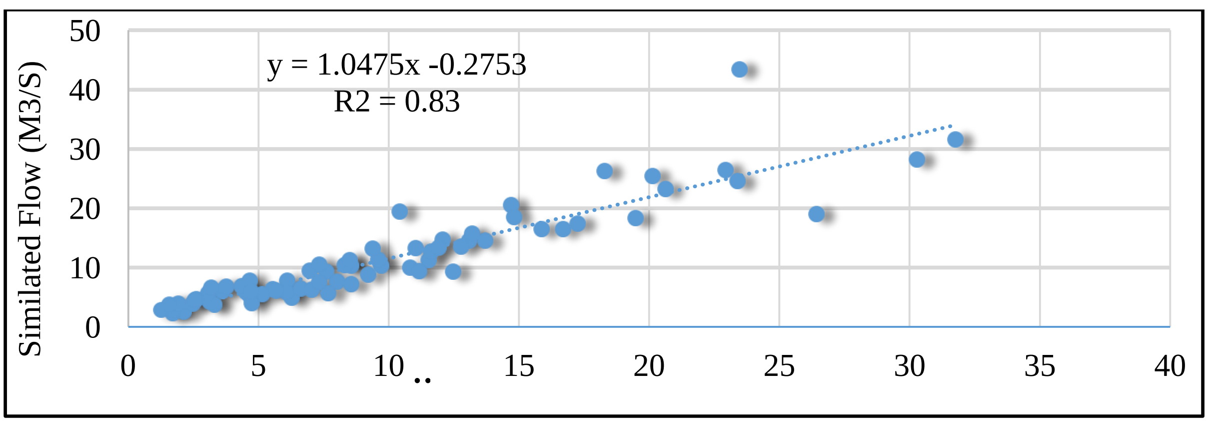

Figure 4.17: Scatter plot of observed and simulated stream flow for Validation (2003-2008)

Table 4.11: Model Performance Evaluation Statistics for calibration and validation

Periods	Model Performance Evaluation Criteria					
	R^2	NSE	% PBIAS	RSR	P-factors	R- factors
Calibration (1988 -2002)	0.80	0.73	16.1	0.52	0.76	0.81
Validation (2003 – 2008)	0.83	0.77	11.2	0.48	0.82	0.79

4.8. Independent and Combined effect of Climate and LULCC on Stream Flow

4.8.1. Past Land Use Land Cover Change Impact on Stream flow

One of the most important parts of the study was to assess the impact of past LULC change on stream flow of the Yadot watershed as summarized in (Table 4.12). The assessment of stream flow was done in terms of annual, seasonal and monthly basis at outlet of the watershed.

Table 4.12: Mean Annual and Seasonal changes of stream flow results for past LULC change.

Years of study	**Past LULC changes**			**Change detection m^3/s**			**(%) change of flow**		
	1985	2000	2015	**S1**	**S2**	**S3**	**S1**	**S2**	**S3**
Annual	573.9	576.5	581.14	2.6	4.64	7.24	0.45	0.80	1.26
Wet season	576.5	581.14	576.5	4.47	6.41	10.88	1.10	1.56	2.68
Dry season	410.57	416.98	410.57	-1.87	-1.78	-3.65	-1.11	-1.07	-2.22

Note: S1 Scenarios (1985 to 2000), **S2** Scenarios (2000 to 2015) **S3** Scenarios (1985 to 2015)

The simulated mean annual stream flows exhibited a higher increase in the second scenarios 4.64m^3/s (0.80%) than the first scenarios 2.6m^3/s (0.45%). Unfortunately, the stream flow will be lower in the first scenarios compared to the second scenarios due to the gradual increase of grass/range land starting from the year 1985 to 2000. The continued increase of agricultural and settlement lands and extraction of forest cover and wood land will further increase the mean annual flow with magnitude of 7.24m^3/s (1.26%) throughout study period from 1985 to 2015.

Seasonal change of stream flows was assessed for the wet (March, April, May, August, September, October and November) and dry (January, February, June, July and December) season. As indicated in (Table 4.12) above, the mean wet season flow was increased by 4.47m^3/s (1.1%) and 6.41m^3/s (1.56%) for the first and second scenarios, respectively. This is due to rainfall satisfies soil moisture deficit more quickly in the agriculture and settlement than forest thereby generating more flow in agricultural and settlement. Conversely, the reduction of vegetation cover and the increase of agriculture and settlement were reduced the dry season flow by 1.87m^3/s (1.11%) and 1.78m^3/s (1.07%) for the first and second scenarios, respectively.

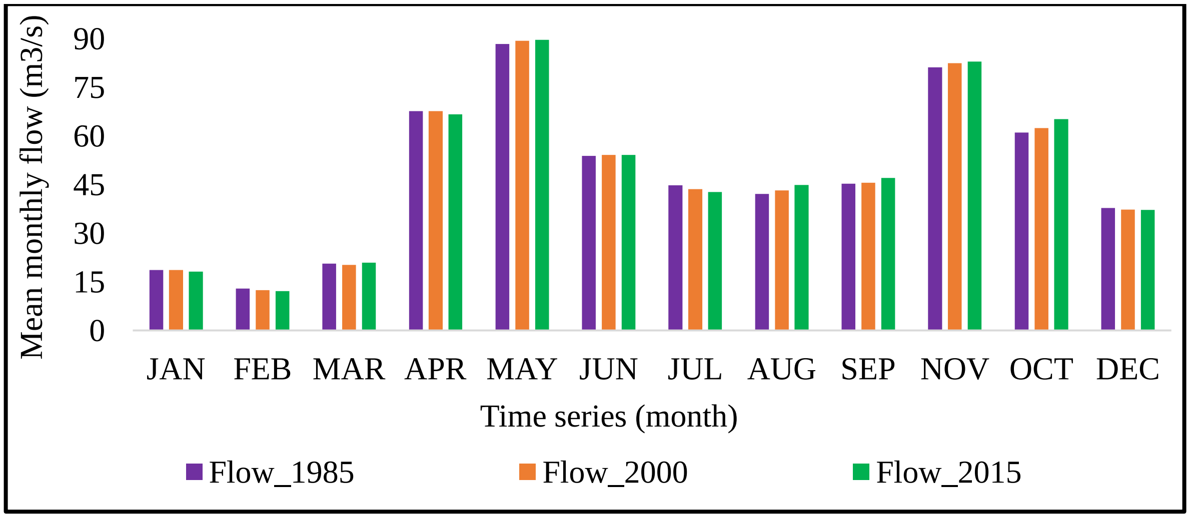

Figure 4.18: Mean monthly stream flow results for the past three land use land cover

Mean monthly stream flow depicted a higher increase in 2015 LULC as compared to 2000 and 1985. This was attributed due to increment of agricultural and settlement and reduction of forest, scrub/bush land, grass/range land and wood land cover of the watershed. As result of expansions in agricultural land rainfall infiltrate in to the soil decrease and the soil moisture shortage more rapidly satisfied under agricultural land than forest thereby producing more runoff in agricultural land and so, more flow was created in 2000 LULC than 1985 LULC.

Generally, during the study period from 1985 to 2015 mean monthly stream flows increased by 10.88m^3/s for the wet season as a result of agricultural and settlement land expansion by 132.76% and 511.88% and decreases of other LULC separately. These result in agreement with several studies. For instance (Temesgan *et al*., 2018) interpreted that, annual stream flow increase by 300.6mm, 304.5mm and 307.3mm for 1985, 2000 and 2015 LU/LC respectively, associated with expansion of cultivated land and built-up area and the reduction of forest, shrub land and grassland in Andassa watershed, Blue Nile Basin, Ethiopia. The study (Moges *et al*., 2019) showed the increase in stream flows can be directly attributed to the expansion of cultivated lands at a cost of the forested vegetation. (Mesfin, 2018) reported expansion of settlement and agriculture land as result mean monthly stream flow increased by 5.97m^3/s and

0.96m^3/s during wet season and dry season flow in shaya catchment Genale Dawa Basin. Generally (Asmamaw, 2013) reported an increase of cultivated land decline forest and shubland result increased the wet months flow, while the flow during the dry months decreased.

4.8.2. Future Land Use Land Cover Change Impact on Stream flow

The study in this section mainly focused on analyzing the impact of LULC change on Yadot watershed stream flow response to future LULC change. The simulated stream flows due to the future LULC change were compared with past LULC change to estimate the effects of LULC change on the stream flow.

Table 4.13: Mean Annual and Seasonal change of stream flow results for future LULC change.

	Future LULC changes			**Change detection m^3/s**			**% change of flow**		
Years of study	**2015**	**2035**	**2055**	**S1**	**S2**	**S3**	**S1**	**S2**	**S3**
Annual	581.14	584.88	588.07	3.74	3.19	6.93	0.64	0.55	1.19
Wet season	416.98	423.1	429.08	6.12	5.98	12.1	1.47	1.41	2.90
Dry season	164.15	161.79	158.99	-2.36	-2.8	-5.16	-1.44	-1.73	-3.14

Note: **S1** scenarios (2035 -2015), **S2** scenarios (2055 -2035) and **S3** scenarios (2015-2055)

Stream flows showed a slight increase in the first scenarios by 3.74m^3/s (0.64%) than the second scenarios 3.19m^3/s (0.55%). Generally stream flows has increased throughout the future study period with a magnitude of 6.93m^3/s (1.19%). Therefore continued increment of agricultural and settlement and extraction of vegetation cover lead to change the future LULC of the watershed is expected to further increase the mean annual stream flow.

The amount of mean monthly stream flow was decreased by 2.36m^3/s (1.44%) and 2.8m^3/s (1.73%) for the first and second scenarios, respectively during the dry season. However, during the wet season mean monthly stream flow was increased by 6.12m^3/s (1.47%) and 5.98m^3/s (1.41%) for the first and second scenarios, respectively as shown on (Table 4.13). In general the future LULC increased mean monthly stream flow by 12.1m^3/s (2.9%) for the period from 2015 to 2055 during the wet season mainly due to an increase of agricultural and settlement land by 44.02% and 69.20% which implies that agricultural and settlement land increased surface runoff. On the other hand, mean monthly stream flows has showed a decreasing trend for the whole study period during dry season with a magnitude of 5.16m^3/s (3.14%) which reflect that base flow has decreased with an intense agricultural and settlement expansion.

The stream flow was contributed more in wet months from surface runoff while in dry months; it was contributed from groundwater. During the study period wet season flow is less sensitive to LULC change than dry season flow due to ground water contribution during the dry season was reduced because of less infiltration that largely caused less vegetation cover. The rate of increment of stream flow was higher for the past LULC compared to future LULC mainly due to expansion of wood land and grass/range land couple with increasing of agriculture and settlement.

The result in this study agrees with other previous studies such as (Temesgan, 2018) revealed that annual and wet season flow, surface runoff and water yield increased while the dry season flow, groundwater flow, lateral flow and ET have reduced in the periods 1985-2015 due to LULC change in Upper Blue Nile Basin. The result also shows that for LULC 2030 and 2045 flow expected to increase annually and during wet season, surface runoff and water yield, while dry season flow, groundwater flow, lateral flow and ET reduce (Rajib and Merwade, 2017) results suggest an increase of 0.5% and 3.5% in the average annual streamflow at the basin outlet during 2081–2100 for future LULC, respectively. Conversion of cropland, forest, or grassland to perennial hay/pasture areas would lower surface runoff by 25%, whereas persistent forest cover in the northern region would cause up to 7% increase in evapotranspiration.

4.8.3. Impact of Climate Change on Stream flow

The impact of climate change was analyzed taking baseline simulated stream flow against two future flow in the near and midterm period. The simulated mean annual stream flow may increase by 7.63% and 5.76% from baseline flow in the near-term under RCP4.5 and RCP8.5

scenarios, respectively. For the midterm mean annual stream flow expected to increase by 8.25% and 6.07%, respectively, from the baseline flow under RCP4.5 and RCP8.5 scenarios.

Table 4.14: Mean annual and seasonal change of flow under RCP4.5 and RCP8.5 scenarios for climate change only from baseline period

	Simulated stream flow in (m^3/s)				**% change of stream flow**			
Scenarios	RCP4.5		RCP8.5		RCP4.5		RCP8.5	
	Near-term	**Midterm**	**Near-term**	**Midterm**	**Near-term**	**Midterm**	**Near-term**	**Midterm**
Annual	625.46	629.06	614.61	616.40	7.63	8.25	5.76	6.07
Wet season	452.34	456.03	442.97	447.07	8.48	9.36	6.23	7.21
Dry season	173.11	173.03	171.65	169.33	5.46	5.41	4.57	3.16

The seasonal variation of projected stream flow from the baseline period was computed for wet (March to May and August to November) and dry (January, February, June, July and December) season. Future change of stream flow for wet and dry season is important to understand hydrological impact of climate change. The wet season mean stream flow of the watershed expected to increase by 8.48% and 6.23% from the baseline flow in the near-term under RCP4.5 and RCP8.5 scenarios, respectively. For the midterm mean wet season stream flow may increase by 9.36% and 7.21% from the baseline stream flow under RCP4.5 and RCP8.5scenarios, respectively (Table 4.15). Dry season mean stream flows is projected to increase in the watershed by 5.46% and 4.57% from baseline flow in the near-term under RCP4.5 and RCP8.5scenarios, respectively. Similarly midterm the mean dry season stream flow expected to increase by 5.41% and 3.16% from the baseline stream flow under RCP4.5 and RCP8.5scenarios, respectively.

The mean monthly percentage change of stream flow in the near and midterm for RCP4.5 and RCP8.5 scenarios from the baseline stream flow are presented in (Figure 4.19). The mean monthly stream flow may expected to increase for all months except for the month of

February, July, August and September showed a decrease in the near and midterm under RCP4.5 and RCP8.5 scenarios from the baseline period, respectively.

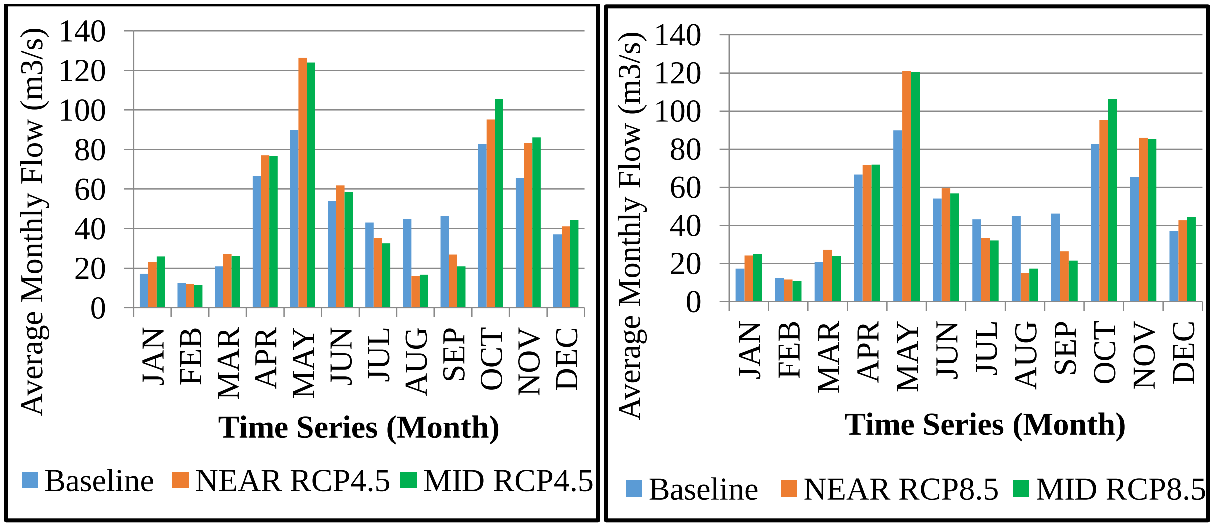

Figure 4.19: Mean monthly flow for near and midterm under RCP4.5 and RCP8.5 scenarios from the baseline period.

The maximum increase in mean monthly stream flown expected in May with 36.6m^3/s (40.75%) and 34.16m^3/s (38.02%) in the near and midterm, while highly decline in August by 28.8m^3/s (64.21%) and 28.16m^3/s (62.78%) for near and midterm under RCP4.5 from the baseline flow, respectively.

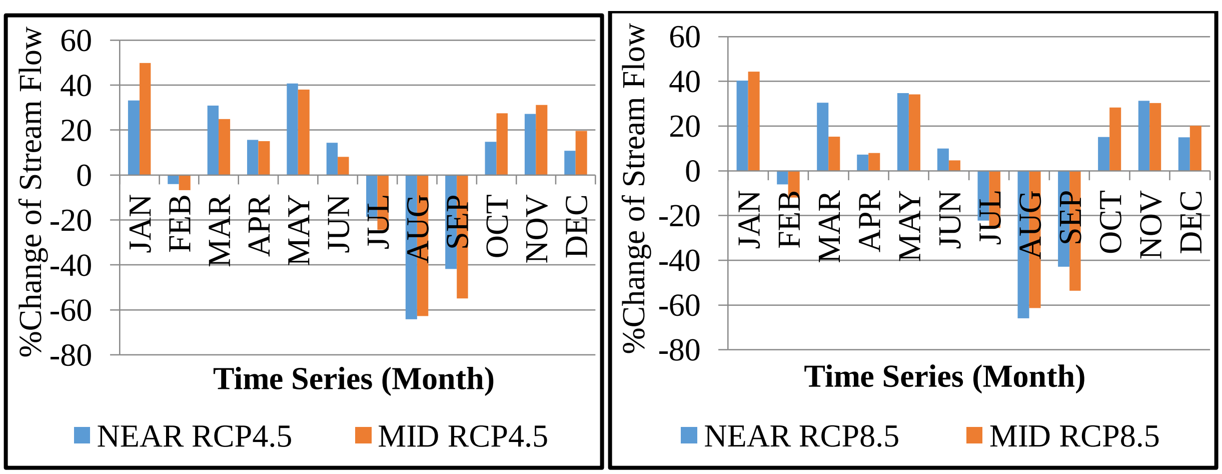

Figure 4.20: Percentage change of flow for near and midterm future under RCP4.5 and RCP8.5 scenarios compared to baseline period.

Mean monthly stream flow showed highest increase for the month of May by 31.16m3/s (34.68%) and 30.75m^3/s (34.22%), while maximum reduction occurred in August by 29.61m^3/s (66%) and 27.53m^3/s (61.38%) from the baseline flow in the near and midterm under RCP8.5 scenarios, respectively. The high flow months in the baseline period such as August and September will be highly impacted in the near and midterm for both RCP 4.5 and RCP 8.5 scenarios as shown on (Figure 4.20). In general overall trend shows that the annually, seasonal and monthly change of stream flow expected to increase in all future of Yadot watershed under RCP4.5 and RCP8.5 scenarios.

The projected increase in stream flow into the watershed is in agreement with studies (Tufa and Sarma, 2021) reported that mean annual stream flow consistently increased with the predicted changes in rainfall and temperature patterns in the future period 2022–2080 under the RCP 4.5 and RCP 8.5 emission scenarios of Genale watershed. (Tesfaye *et al*, 2019) summaries increase in average total annual, seasonal and monthly flow volume is observed for the period (2018 to 2077) corresponding to increase in mean annual, seasonal and monthly precipitation during future scenario of Awata river watershed, Genale Dawa Basin. Similarly (Anwar *et al*., 2016) conclude that Stream flow projections for future time periods showed that mean annual stream flow increase by 7.1, 9.7, and 10.1 % at 2020s, 2050s, and 2080s, respectively, from the baseline period for A2 scenario, whereas for B2 scenario, it will be expected to increase by 6.8, 7.9, and 6.4 % for 2020s, 2040s, and 2080s, respectively in the Upper Gilgel Abay Watershed, Blue Nile basin. Therefore, the fluctuation mean stream flow for annual, wet and dry month will result from climate change in the Bale highlands not only affects the livelihood of people in the Bale zone but also all inhabitants at the downstream areas whose life depends on the flow of yadot River.

4.8.4. Combined Impact of Climate and LULC Change on Stream flow

To determine the combined impacts of climate and LULC change on steam flow, four simulations were carried out by using a combination of two futures LULC (2035 for near term and 2055 for midterm) with two RCP4.5 and RCP8.5 scenarios. The combined impacts climate and future land use land cover change on stream flow in the study area were simulated using the calibrated SWAT model the results of which are presented on (Table 4.15).

The simulated mean annual stream flow showed increasing trend under both climate scenarios in the future projection periods. The simulated mean annual stream flow showed an increasing by 8.13% and 6.26% in the near-term from baseline period under RCP4.5 and RCP8.5 scenarios, respectively. Compared to RCP4.5 in the near-term RCP8.5 showed slight decline of mean annual stream flow mainly due to annual and seasonal decline of precipitation from baseline period with an increase in temperature over the watershed.

Table 4.15: Mean Annual and Seasonal change of flow under RCP4.5 and RCP8.5 scenarios for combined climate and LULC change from baseline period.

	Stream flow in (m^3/s)				**% change of stream flow**			
Scenarios	RCP4.5		RCP8.5		RCP4.5		RCP8.5	
	Near-term	**Midterm**	**Near-term**	**Midterm**	**Near-term**	**Midterm**	**Near-term**	**Midterm**
Annual	628.36	633.23	617.52	620.47	8.13	8.96	6.26	6.77
Wet season	453.34	451.98	443.92	443.07	8.72	8.39	6.46	6.25
Dry season	175.02	181.24	173.60	177.40	6.62	10.42	5.76	8.07

Note: Near-term (2021-2050) and midterm (2051 -2080)

In the midterm projected mean annual stream flow increased by 8.96% and 6.77% in the midterm under RCP4.5 and RCP8.5 scenarios from baseline flow, respectively (Table 4.16). The change in stream flow for impact of combined climate and LULC change is consistent with climate change alone. The highest the rainfall under RCP8.5 in the midterm the lower the simulated mean annual stream flow compared to RCP4.5 in the same time period mainly due to high temperature and increased evapo-transpiration in the midterm. If change in land use land cover, were held constant for both scenarios. There will be higher rates of evaporation in Ethiopia due to warming over the country. Such changes are expected to impact the economy of East African countries, including Ethiopia (Change 2014). Therefore stream flow was sensitive to change in the temperature than rainfall and LULC change for the midterm in the Yadot watershed.

The seasonal variation of stream flow for the projected climate parameter change from the baseline period was computed for wet and dry season (Table 4.15). The mean wet season stream flow may increase by 8.72% and 6.46%, while the dry season flow may increase by 6.62% and 5.76% from baseline period for near-term under RCP4.5 and RCP8.5 scenarios, respectively. For the midterm mean wet season flow will increase by 8.39% and 6.25%, while the dry season flow will be expected to increase by 8.07% and 10.42% from baseline period under RCP 4.5 and RCP 8.5 scenarios, respectively. The combination of LULC and climate change scenario will have an additive effect on stream flow simulation. Therefore, simulation results showed that if all other variables are held constant, an increase in river flow may be expected in the future as a consequence of climate and LULC change, while the impacts associated should be effectively planned for and mitigated. Therefore mean wet and dry season stream flow may increase for the coming century under both RCP from baseline period.

Mean monthly change of steam flow indicate there may be an increase for the months of (January, March, April, May, June, October, November and December), while decrease for the month of (February, July, August and September) under both RCP from baseline period for near and midterm, respectively as shown on (Figure 4.21).

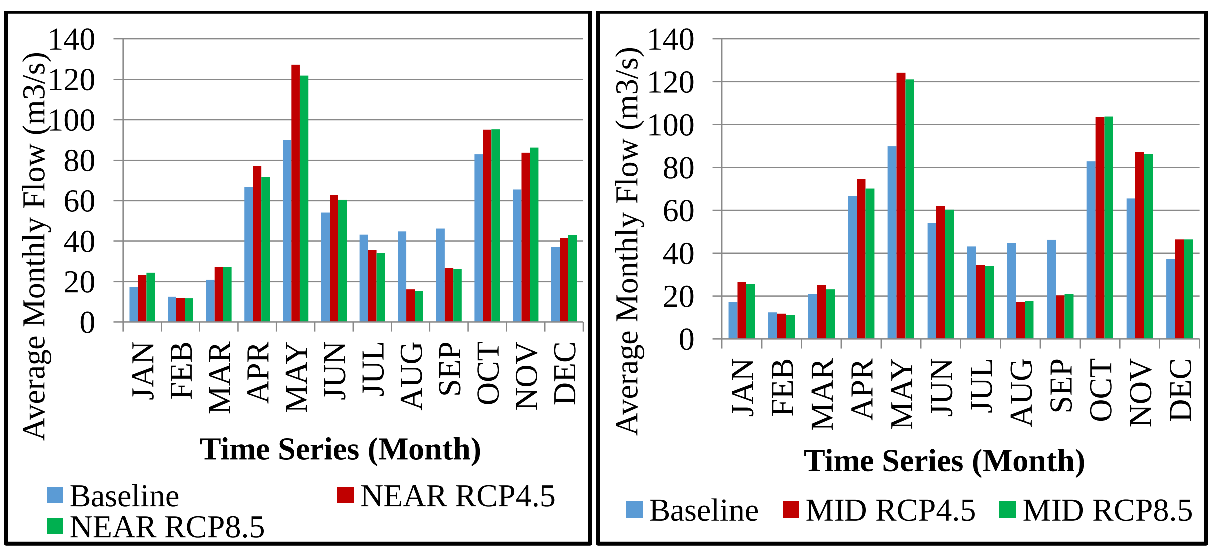

Figure 4.21: Mean monthly stream flow for near and midterm under RCP4.5 and RCP8.5 scenarios compared to baseline period.

The maximum mean monthly change of flow increment was observed in May by 35.39m^3/s (39.4%) and 31.77m^3/s(35.36%), while minimum mean monthly steam flow increment was in December and March by 5.87m^3/s (15.81%) and 2.3m^3/s (11%) for near-term under RCP4.5 and RCP8.5 from baseline period. Mean monthly change of flow showed maximum reduction in August by 28.66m^3/s (63.9%) and 27.12m^3/s (60.46%), whereas the minimum decline of flow in February by 1.53m^3/s (12.3%) and 2.3m^3/s (18.45%) for near-term from baseline period under RCP4.5 and RCP 8.5, respectively.

The largest percentage change of mean monthly flow increment observed in May by 34.39m^3/s (38.28%) and 31.27m^3/s (34.80%), while the future mean monthly change of flow showed smallest nominal increment in March by 4.19m^3/s (20.09%) and 2.3m^3/s (11.03%), from baseline period in the midterm under RCP4.5 and RCP8.5, respectively (Figure 4.22).

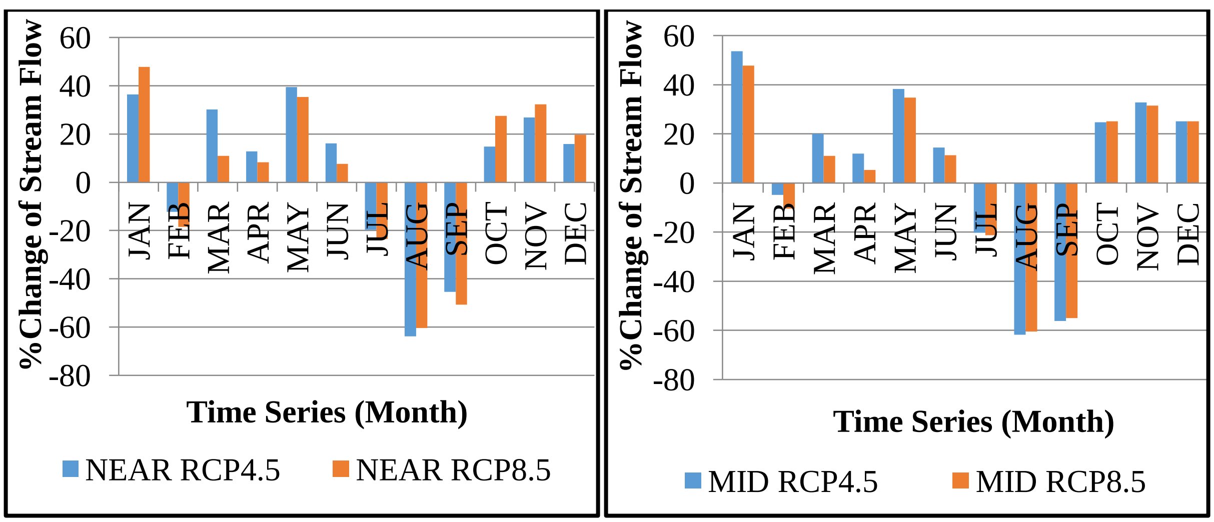

Figure 4.22: Percentage change of flow for near-term and midterm under RCP4.5 and RCP8.5 scenarios compared to baseline period.

The simulated mean monthly steam flow change showed significant decline in August by 27.7m^3/s (61.76%) 27.12m3/s (60.46%), whereas the minimum reduction in mean monthly flow occurred in February by 0.6m^3/s (4.82%) and 1.3m^3/s (10.42%) in the midterm from baseline period under RCP4.5 and RCP8.5, respectively. Comparing the impacts of climate change and LULC change on stream flow, it is clear that climate change impact was dominant and its impact increase stream flow compared to baseline period. Stream flow is more sensitive to climate change than to changes in LULC and thus the changes in stream flow under future conditions of climate and LULC change are remarkably consistent with those in which future climate changed and secondary role with change in LULC. Changes in future LULC produced small changes in stream flow and combined scenario predicted larger changes in stream flow than which considered under only LULC change and only climate change from baseline flow. Therefore results show that the combined climate and LULC change have a more noticeable effect on stream flow in comparison with the baseline period, the stream flow gradually increased in the future in general.

The results of this study is consistent with other regional and local climate change impact assessment studies by (Birhan *et al*., 2021) the increasing trend to of stream flows in relation to temperature and precipitation increase in the basin by the end of the 21st century in the Lake Tana Basin, upper Blue Nile River Basin. A similar study in Kesem sub-basin of the Awash River basin, showed an increase in mean annual stream flow by 14.5 and 19.1% for RCP 4.5 and by 4.7 and 6.9% for RCP 8.5 scenarios parallel to rainfall and temperature increases from the 2050s to 2080 period (Negash *et al*., 2020). (Dagnenet *et al*., 2018) reported that precipitation increase by up to 25% in the Upper Blue Nile River Basin which result in projected increase of stream flow and lateral flow by up to 12.85% (9.9%), 28.5% (20.03%) and 26.4% (29.12%) under LULC, climate and combined climate and LULC change scenarios, respectively. Study (Babur *et al*., 2016) report from Pakistan reported an increase in mean annual flow under RCP 4.5 and RCP 8.5 scenarios between the years 2011–2040, 2041–2070, and 2071–2100. Therefore, soil and water conservation activities should be adopted by the community as well as the water harvesting structure should be properly designed and applied to the watershed to compensate for this fluctuation of flow in the Yadot River. Also larger increment of stream flow from the baseline scenario may cause flooding to flood plain zones. It is crucial to consider and implement integrated water resources management to meet the alarmingly increasing water demand due to high population growth rate.

5. SUMMARY CONCLUSIONS AND RECOMMENDATION

5.1.Summary and Conclusions

Climate and land use land cover changes are the two inseparable linked global environmental challenges the world faces today (IPCC, 2019). In this study the potential impact of climate and land use land cover change on stream flow of Yadot watershed analyzed by considering past and future LULC change and climate change indicator parameters (precipitation and temperature) as an input of the SWAT model. CA-Markov model was used to predict future LULC change for 2035 and 2055 using IDRISI software. In order to detect and analyze changes in LULC for the study periods of 1985, 2000 and 2015 GIS and Remote Sensing techniques were applied to generate LULC maps through a maximum likelihood supervised image classification algorithm. Over the past three decades, the predominant patterns of LULC change were the transitional conversions among agricultural land, settlement, grass/range land, wood land, forest land and Scrub/bush land.

The dominant changes were decline of forest and scrub/bush land coverage and an increase of agriculture and Settlement with total human population increment. The LULC change results showed that throughout the study period, agricultural and settlement land significantly increased from 6.11% and 0.12% to 20.47% and 1.24%, respectively, while scrub/bush land and forest continuously decline from 65.5% and 7.45% to 45.22% and 6.35%, respectively. Conversely on average grass/range land and wood land shows decline in the past from 7.54% and 13.29% to 7.3% and 9.17% and expected to increase from 2015 to 235 to 9.66% and 16.05%, respectively, while it will decline to 9.51% and 14.21% from 2035 to 2055 in the total coverage of the watershed, respectively.

The ensemble mean of three RCMs output in the coordinated regional climate downscaling experiment (CORDEX)-RCM shows parallel daily precipitation and temperature increase in the two future periods under RCP 4.5 and RCP 8.5 but varies on monthly basis. Except in the near-term under RCP8.5 precipitation decrease compared to baseline and highest increment of precipitation observed in the midterm under RCP8.5 scenarios. Precipitation may increase in some months and decrease in other months for both RCP4.5 and RCP8.5 scenario in all future.

The mean annual maximum temperatures projected to increase by 0.65^0C and 1.05^0C, while the mean annual minimum temperature would increase by 0.48^0C and 0.85^0C under RCP4.5 scenario in the near and midterm, respectively, while mean annual maximum temperature simulated to increase by 0.71^0C and 2^0C, while mean annual minimum temperature was increase by $0.56^0C$and 1.8^0C under RCP 8.5 scenario in the near and midterm from baseline period, respectively. The overall study result shows the projected maximum and minimum temperature under RCP8.5 is warmer than RCP4.5. Compared with the historical period, the annual mean temperature would face a continuously increasing trend under both scenarios from baseline. In general annual precipitation and mean annual temperature would increase to varying degrees in the future.

The result of the dynamically downscaling Model outputs for future scenario on a monthly and seasonal basis indicates that precipitation does not show a systematic increase or decrease. However annual and seasonal flow shows an increasing trend under RCP4.5 and RCP8.5 scenarios compared to the baseline period. The mean annual stream flow projected to increase by 7.63% (8.13%) and 5.76% (6.26%) for near-term (2021-2050), whereas for the midterm (2051 – 2080) model shows an increase by 5.76% (6.26) and 6.07% (6.72%) at the outlet of the watershed for both climate only and combined climate and LULC change from baseline period for both RCP4.5 and RCP8.5 scenarios, respectively. Predicted seasonal flow shows an increase for dry and wet seasons compared to baseline period under RCP4.5 and RCP8.5 scenarios in all future. The dry season flow show a highest increasing trend for the midterm under both scenarios compared to wet season flow. Mean monthly change of stream flow clearly shows the season which may be impacted highly with climate change

Generally, the result of future stream flow projection suggests that the combined scenarios were slightly higher than the climate change alone. However, increase in future stream flow primarily driven by future climate change, whereas the changes in LULC play a secondary role, but highest the rainfall under RCP8.5 in the midterm the lower the simulated mean annual stream flow compared to RCP4.5 in the same time period mainly due to high temperature and increased evapo-transpiration in the midterm.

5.2. Recommendation

Depending on the results of the study the following recommendation:-

- The watershed water management system should be following the future trends of rainfall peaks as the temporal shift in peak rainfall showed a direct impact on the flow of Yadot river watershed Therefore, soil and water conservation activities should be adopted by the community as well as the water harvesting structure should be properly designed for the effective planning and management practices of soil and water resources applied to the watershed to compensate the fluctuation of flow in the Yadot River.
- Water play significant role for small & large scale irrigation, therefore mitigating adverse impacts of climate and LULC change is important. This study will then be meaningful to society and so that they can either be well adapted to the forthcoming climatic condition or mitigate the adverse impacts of changing climate and land use land cover change.
- For future, it is better to further analysis of other parameters in addition to climate and land use land cover change such as land use land cover change alone, population growth rate and water utilization efficiency to find out the characteristics' changes of on hydrology that might influenced by characteristics of these factors in Genale subbasin. It also important to study with the same title using more than three RCMs output.

6. REFERENCE

Abbas, N, S.A Wasimia and N Al-Ansari, 2016. Assessment of climate change impacts on water resources of Al-Adhaim, Iraq using SWAT model. Engineering, 8, pp.716-732.

Abdi Boru, Desalegn Chemeda and Ekasit Kositsakulchai, (2014). "“Modelling the effects of land use changes and management practices on Runoff and Sediment Yields in Fincha Watershed, Blue Nile.”." OIDA International Journal of Sustainable Development 07:11.

Abdulkareem, J.H., B. Pradhan, Sulaiman and N.R Jamil, 2018. Review of studies on hydrological modelling in Malaysia. Modeling Earth Systems and Environment, 4(4), pp.1577-1605.

Abebe Tariko, 2020. Modeling Impact of Land Use Dynamics on Hydrology and Sedimentation of Megech Dam Watershed, Ethiopia. The Scientific World Journal, 2020.

Aboelnour, M., M.W. Gitau and B.A Engel, 2019. Hydrologic response in an urban watershed as affected by climate and land-use change. Water, 11(8), p.1603.

Adane Mezgebu and Getachew Workineh, 2017. Changes and drivers of afro-alpine forest ecosystem: future trajectories and management strategies in Bale eco-region, Ethiopia. Ecological Processes, 6(1), pp.1-13.

Rajib. A, and Merwade.V, ,2017. Hydrologic response to future land use change in the Upper Mississippi River Basin by the end of 21st century. Hydrological Processes. 2017 Oct 15;31(21):3645-61.

Afera Halefom, Asirat Teshome, Ermais Sisay, D.Khare, Mihret Dananto, L. Singh and Dessalew Tadesse, 2018. Applications of Remote Sensing and GIS in Land Use/Land Cover Change Detection: A Case Study of Woreta Zuria Watershed, Ethiopia. Applied Research Journal of Geographic Information System, 1(1), pp.1-9.

Ahn, K.H. and V Merwade 2014. Quantifying the relative impact of climate and human activities on streamflow. Journal of Hydrology, 515, pp.257-266.

Aich, V., S Liersch, T.Vetter, S.Huang, J .Tecklenburg, P.Hoffmann, H.Koch, S. Fournet V Krysanova, E.N Müller and F.F Hattermann, 2014. Comparing impacts of climate change on streamflow in four large African river basins. Hydrology and Earth System Sciences, 18(4), pp.1305-1321.

Al-sharif, A., Pradhan, B. (2013). Monitoring and predicting land use change in Tripoli Metropolitan City using an integrated Markov chain and cellular automata models in GIS. Arab J Geosci. 7: 4291-4301.

Amare Sewnet, 2013). Retrospective Analysis of Land Cover and Use Dynamics in GilgelAbbay Watershed by Using GIS and Remote Sensing Techniques, Northwestern Ethiopia.International Journal of Geosciences, 4:1003-1008.

Amisigo, B.A., Logah, F.Y., Obuobie, E. and Kankam-Yeboah, K., 2018. Impacts of Climate Change on Stream Inflows into the Volta Lake. Ghana Journal of Science, 58, pp.23-3

Anand, J., Gosain, A. K., Khosa, R. 2018. Prediction of land use changes based on Land Change Modeler and attribution of changes in the water balance of Ganga basin to land use change using the SWAT model. Science of the Total Environment, 644, 503-519.

Andargachew melke and Fantahun Abegaz, 2017. Impact of climate change on hydrological responses of Gumara catchment, in the Lake Tana Basin-Upper Blue Nile Basin of Ethiopia. International Journal of Water Resources and Environmental Engineering, 9(1), pp.8-21.

Andualem, T., Belya, G. and Guadie, A. 2018. Land Use Change Detection Using Remote Sensing Technology. . J Earth Sci Clim Change 9, 488-496.

Anwar. A, Seifu.A, Essayas .K, Abeyou .W. Tewodros T. Shimelis .B and Assefa M, 2016. Climate change impact on stream flow in the upper Gilgel Abay Catchment, Blue Nile Basin, Ethiopia. In Landscape Dynamics, Soils and Hydrological Processes in Varied Climates (pp. 645-673). Springer, Cham.

Arnold, J.G., Moriasi, D.N., Gassman, P.W., Abbaspour, K.C., White, M.J., Srinivasan, R., Santhi, C., Harmel, R.D., Van Griensven, A., Van Liew, M.W. and Kannan, N., 2012. SWAT: Model use, calibration, and validation. Transactions of the ASABE, 55(4), pp.1491-1508.

Arsanjani, J. J., Helbich, M., Kainz, W., Boloorani, A. D. (2013): Integration of logistic regression, Markov chain and cellular automata models to simulate urban expansion. International Journal of Applied Earth Observation and Geoinformation 21: 265-275.

Asirat Teshome, 2018. Evaluating the Dynamics of Land Use/Land Cover Change Using GIS and Remote Sensing Data in Case of Yewoll Watershed, Blue Nile Basin, Ethiopia.

Asirat, Teshome, 2018. Evaluating the Dynamics of Land Use/Land Cover Change Using GIS and Remote Sensing Data in case of Yewoll Watershed, Blue Nile Basin, Ethiopia. . Applied Research Journalof Geographic Information System. , 1, 10-24.

Asmamaw Adamu, 2013. Assessing the impacts of land use and land cover change on hydrology of watershed: a case study on Gigel-Abbay Watershed, Lake Tana Basin, Ethiopia (Doctoral dissertation).

Azari, M., Moradi, H.R., Saghafian, B. and Faramarzi, M., 2016. Climate change impacts on streamflow and sediment yield in the North of Iran. Hydrological Sciences Journal, 61(1), pp.123-133.

Ba, W., Du, P., Liu, T., Bao, A., Luo, M., Hassan, M. and Qin, C., 2018. Simulating hydrological responses to climate change using dynamic and statistical downscaling methods: a case study in the Kaidu River Basin, Xinjiang, China. Journal of Arid Land, 10(6), pp.905-920.

Babur, M., Babel, M.S., Shrestha, S., Kawasaki, A. and Tripathi, N.K., 2016. The Impact of Climate Change on Reservoir Inflows Using Multi Climate-Model under RCPs' Including Extreme Events—A Case of Mangla Dam, Pakistan.

Belay Simane, Hunachew Beyene, Wakgari Deressa, Abera Kumie, Kiros Berhane and Jonathan Samet (2017). Review of Climate Change and Health in Ethiopia: Status and Gap Analysis. Ethiopia Journal of Health Development, 30(1), 1–23.

Belkele Megersa, Andre Markeman, Angassa and A.V. Zárate., 2014. The role of livestock diversification in ensuring household food security under a changing climate in Borana, Ethiopia. Food Security, 6(1), pp.15-28.

Binyam Alemu, Efrem Garedew, Zewdu Eshetu and Habtemariam Kassa, 2015. Land use and land cover changes and associated driving forces in north western lowlands of Ethiopia. Int Res J Agric Sci Soil Sci. 5: 28–44.

Bireda Alemayehu, 2015. GIS and remote sensing based land use/land cover change detection and prediction in Fagita Lekoma Woreda, Awi Zone, North Western Ethiopia. Addis Ababa, Ethiopia: Addis Ababa University.

Birhan Asmame and Assefa Abegaz, 2018. Land use/land cover changes and their environmental implications in the Gelana sub-watershed of Northern highlands of Ethiopia. Environmental Systems Research, 6(1), pp.1-12.

Birhan Getachew, B.R Manjunatha, and H.G Bhat, 2021. Modeling projected impacts of climate and land use/land cover changes on hydrological responses in the Lake Tana Basin, upper Blue Nile River Basin, Ethiopia. Journal of Hydrology, 595, p.125974.

Birhnu Liyew, Atsushi Tsunekawa Nigussie Haregeweyn, Derege Tsegaye, Enyew Adgo, Mitsuru Tsubo, Tsugiyiki Masunaga, Ayele Almaw, Dagenrnt Sultan Mesenbet Yibeltal, 2019. Exploring land use/land cover changes, drivers and their implications in contrasting agro-ecological environments of Ethiopia. Land Use Policy, 87, p.104052.

Bjørnæs, F., 2015. Som rekrutteringsrådgiver er det mitt største ansvar å komme bak Halo-effekten (Master's thesis, NTNU).

Chang, J., Ciais, P., Viovy, N., Vuichard, N., Sultan, B. and Soussana, J.F., 2015. The greenhouse gas balance of European grasslands. Global change biology, 21(10), pp.3748-3761.

Charles, J.P., Iwema, T., Epa, V.C., Takaki, K., Rynes, J. and Jindra, M., 2011. Ligand-binding properties of a juvenile hormone receptor, Methoprene-tolerant. Proceedings of the National Academy of Sciences, 108(52), pp.21128-21133.

Chen, J., Brissette, F.P., Leconte, R. and Caron, A., 2012. A versatile weather generator for daily precipitation and temperature. Transactions of the ASABE, 55(3), pp.895-906.

Clark Labs. (2012). Idrisi Selva help system. Clark University, USA.

Clerici, N., Cote-Navarro, F., Escobedo, F.J., Rubiano, K. and Villegas, J.C., 2019. Spatio-temporal and cumulative effects of land use-land cover and climate change on two ecosystem services in the Colombian Andes. Science of the Total Environment, 685, pp.1181-1192.

Dagnenet Fenta, Z. Duan, T. Rientjes, and Markus Disse., 2018. Analysis of combined and isolated effects of land-use and land-cover changes and climate change on the upper Blue Nile River basin's streamflow. Hydrology and earth system sciences, 22(12), pp.6187-6207.

Desalegn, T., Cruz, F., Kindu, M., Turrión, M.B. and Gonzalo, J., 2014. Land-use/land-cover (LULC) change and socioeconomic conditions of local community in the central highlands of Ethiopia. International Journal of Sustainable Development & World Ecology, 21(5), pp.406-413.

Devkota, L.P. and Gyawali, D.R., 2015. Impacts of climate change on hydrological regime and water resources management of the Koshi River Basin, Nepal. Journal of Hydrology: Regional Studies, 4, pp.502-515.

Di Gregorio, A., 2016. Land covers classification system: classification concepts. Software version 3.

Domínguez, M., Romera, R., Sánchez, E., Fita, L., Fernández, J., Jiménez-Guerrero, P., Montávez, J.P., Cabos, W.D., Liguori, G. and Gaertner, M.Á., 2013. Present-climate precipitation and temperature extremes over Spain from a set of high resolution RCMs. Climate research, 58(2), pp.149-164.

Eastman, J. (2012). IDRISI Selva manual, version 17. Clark University. p322.

Ebrahim Esa and Mohamed Assen, 2018. Land use/cover dynamics and its drivers in Gelda catchment, Lake Tana watershed, Ethiopia. Environmental Systems Research, 6(1), pp.1-13.

Emerta, B. and Aragie, A. (2013). Climate change, growth, and poverty in Ethiopia. TEXAS UNIV AT AUSTIN.

Ermias Teferi, Woldeamlak Bewket, S. Uhlenbrook, and J. Wenninger, 2013. Understanding recent land use and land cover dynamics in the source region of the Upper Blue Nile, Ethiopia: Spatially explicit statistical modeling of systematic transitions. Agriculture, ecosystems & environment, 165, pp.98-117.

Evans, J.P., 2011. Resilience, ecology and adaptation in the experimental city. Transactions of the institute of British Geographers, 36(2), pp.223-237.

Fasil, V.K. and Karmakar, S., 2012, July. Modeling and simulation based study for on-line detection of partial discharge of solid dielectric. In 2012 IEEE 10th International Conference on the Properties and Applications of Dielectric Materials (pp. 1-5). IEEE.

Gambo, J., Shafri, H.M., Shaharum, N.S.N., Abidin, F.A.Z. and Rahman, M.T.A., 2018. Monitoring and predicting land use-land cover (LULC) changes within and around Krau wildlife reserve (KWR) protected area in Malaysia using multi-temporal Landsat data. Geoplanning: Journal of Geomatics and Planning, 5(1), pp.17-34.

Gebre Hadgu, kindie Tesfaye and Girma Mamo Belay Kasa, 2013. Trend and variability of rainfall in Tigray, northern Ethiopia: analysis of meteorological data and farmers' perception. Academia Journal of Agricultural Research, 1(6), pp.088-100.

Gebre Hadgu, kindie Tesfaye and Girma Mamo, 2015. Analysis of climate change in Northern Ethiopia: implications for agricultural production. Theoretical and Applied Climatology, 121(3), pp.733-747.

Goitom Gebreluel, 2014. Ethiopia's Grand Renaissance Dam: ending Africa's oldest geopolitical rivalry?. The Washington Quarterly, 37(2), pp.25-37.

Gudeta W. Sileshi, 2016. The magnitude and spatial extent of influence of Faidherbia albida trees on soil properties and primary productivity in drylands. Journal of Arid Environments, 132, pp.1-14.

Guo, Y., Fang, G., Wen, X., Lei, X., Yuan, Y. and Fu, X., 2019. Hydrological responses and adaptive potential of cascaded reservoirs under climate change in Yuan River Basin. Hydrology Research, 50(1), pp.358-378.

Haile E Getachew and Assefa M Melesse, 2012. The impact of land use change on the hydrology of the Angereb Watershed, Ethiopia. International Journal of Water Sciences, 1(6).

Setegn, S.G., Srinivasan, R. and Dargahi, B., 2008. Hydrological modelling in the Lake Tana Basin, Ethiopia using SWAT model. *The Open Hydrology Journal*, *2*(1).

Halmy, M. W. A., Gessler, P. E., Hicke, J. A., Salem, B. B. (2015): Land use/land cover change detection and prediction in the north-western coastal desert of Egypt using Markov CA. – Applied Geography 63: 101-112.

Hartmann, D.L., Tank, A.M.K., Rusticucci, M., Alexander, L.V., Brönnimann, S., Charabi, Y.A.R., Dentener, F.J., Dlugokencky, E.J., Easterling, D.R., Kaplan, A. and Soden, B.J., 2013. Observations: atmosphere and surface. In Climate change 2013 the physical science basis: Working group I contribution to the fifth assessment report of the intergovernmental panel on climate change (pp. 159-254). Cambridge University.

Headey, D., Dereje, M. and Taffesse, A.S., 2014. Land constraints and agricultural intensification in Ethiopia: A village-level analysis of high-potential areas. Food Policy, 48, pp.129-141.

Hernández-Díaz, L., Laprise, R., Sushama, L., Martynov, A., Winger, K. and Dugas, B., 2013. Climate simulation over CORDEX Africa domain using the fifth-generation Canadian Regional Climate Model (CRCM5). Climate Dynamics, 40(5-6), pp.1415-1433.

Hussen Seid, P Omond, S. Jain, C. Lennard, B. Hewitson, L. Chang'a, J.L. Awange, Dosio, A., P. Ketiem, G. Nikulin, and H.J Panitz, 2013. Assessment of the performance of CORDEX regional climate models in simulating East African rainfall. Journal of Climate, 26(21), pp.8453-8475.

Hyandye, C.B., Worqul, A., Martz, L.W. and Muzuka, A.N., 2018. The impact of future climate and land use/cover change on water resources in the Ndembera watershed and their mitigation and adaptation strategies. Environmental Systems Research, 7(1), pp.1-24.

IPCC Climate Change, 2013. The physical science basis. Contribution of working group I to the fifth assessment report of the intergovernmental panel on climate change, pp.159-254.

IPCC. (2019). Climate Change and Land: IPCC Special Report on Climate Change, Desertification, Land Degradation, Sustainable Land Management, Food Security, and Greenhouse gas fluxes in Terrestrial Ecosystems. 1–1542.

IPCC-TGICA, A., 2007. General guidelines on the use of scenario data for climate impact and adaptation assessment (p. 66). version 2. Tech. rep.

Jones, C., Giorgi, F. and Asrar, G., 2011. The Coordinated Regional Downscaling Experiment: CORDEX–an international downscaling link to CMIP5. CLIVAR exchanges, 16(2), pp.34-40.

Kassie, B.T., Rötter, R.P., Hengsdijk, H., Asseng, S., Van Ittersum, M.K., Kahiluoto, H. and Van Keulen, H., 2014. Climate variability and change in the Central Rift Valley of Ethiopia: challenges for rainfed crop production. The Journal of Agricultural Science, 152(1), pp.58-74.

Kidane Welde, 2016. Identification and prioritization of subwatersheds for land and water management in Tekeze dam watershed, Northern Ethiopia. International Soil and Water Conservation Research, 4(1), pp.30-38.

Kinati Chimdessa, S. Quraishi, Asfaw Kebede Tena Alamirew, 2019. Effect of land use land cover and climate change on river flow and soil loss in Didessa River Basin, South West Blue Nile, Ethiopia. Hydrology, 6(1), p.2.

Koch, H., Biewald, A., Liersch, S., de Azevedo, J.R.G., da Silva, G.S., Kölling, K., Fischer, P., Koch, R. and Hattermann, F.F., 2015. Scenarios of climate and land-use change, water demand and water availability for the São Francisco River Basin. Brazilian Journal of Environmental Sciences (Online), (36), pp.96-114.

Koomen, E., Borsboom-van Beurden, J. (2011): Land-use modelling in planning practice. Springer, XVI-214.

Leal Filho, W., Azeiteiro, U.M. and Setti, A.F.F., 2021. Challenges in Sustainable Land Use Management. In Sustainability in Natural Resources Management and Land Planning (pp. 553-556). Springer, Cham.

Lemesa Muleta, 2017. Impact of climate change on water availability in Genale River Bub-basin, southeastern Ethiopia (Doctoral dissertation, Haramaya University).

Lennard, C.J., Nikulin, G., Dosio, A. and Moufouma-Okia, W., 2018. On the need for regional climate information over Africa under varying levels of global warming. Environmental Research Letters, 13(6), p.060401.

Li, J., Zhang, X.Y. and Yang, Y.Z., 2012. SWAT model of runoff study under different land use land cover scenarios in source region of the Yangtze River. Research of Soil and Water Conservation, 19(3), pp.119-124.

Li, J., Zheng, X., Zhang, C. and Chen, Y., 2018. Impact of land-use and land-cover change on meteorology in the Beijing–Tianjin–Hebei Region from 1990 to 2010. Sustainability, 10(1), p.176.

Li, S., Jin, B., Wei, X., Jiang, Y., Wang, J. (2015). Using CA-Markov model to model the spatiotemporal change of land use/cover in Fuxian Lake for decision support. International workshop on spatiotemporal computing, 13–15 July 2015, Fairfax, Virginia, Liersch, S., Tecklenburg, J., Rust, H., Dobler, A., Fischer, M., Kruschke, T., Koch, H. and Hattermann, F.F., 2018. Are we using the right fuel to drive hydrological models? A climate impact study in the Upper Blue Nile. Hydrology and Earth System Sciences, 22(4), pp.2163-2185.

Masui, T., Matsumoto, K., Hijioka, Y., Kinoshita, T., Nozawa, T., Ishiwatari, S., Kato, E., Shukla, P.R., Yamagata, Y. and Kainuma, M., 2011. An emission pathway for stabilization at 6 Wm− 2 radiative forcing. Climatic change, 109(1), pp.59-76.

Megersa Adugna Nura Boru and Abebe Debele, 2021. Modeling Climate Change Impact on the Streamflow in the Upper Wabe Bridge Watershed in Wabe Shebele River Basin, Ethiopia. International Journal of River Basin Management, (just-accepted), pp.1-46.

Megersa Kebede and A. Chakravarti, 2017. Sediment Yield Assessment and Mitigation Measures in Finchaa Watershed, Ethiopia. Int. J. Eng. Res. Technol, 6, pp.220-226.

Mesfin Reta, 2018. Impact of land use and land cover change on stream flow using mike she: case study of Shaya catchment, Ethiopia.

Mesgana Seyoum, Getu Fana, T.Y Gan, Semu Ayalew and H. Koivusalo, 2017. Potential impact of climate change on streamflow of major Ethiopian rivers. Climatic Change, 143(3), pp.371-383.

Minichil Jemberie, Tesfa Gebrie and Bogale Gebemariam, 2016. Evaluation of land use land cover change on stream flow: a case study of Dedissa sub basin, Abay basin, south western Ethiopia. Evaluation, 3(8).

Mishra, V. N., Rai, P. K. (2016): A remote sensing aided multi-layer perceptron Markov chain analysis for land use and land cover change prediction in Patna district (Bihar), India. – Arabian Journal of Geosciences 9 (4): 1-18.

Moges Kidane,Alemu Bezie, Nega Kesete and Tefere Tolessa, 2019. The impact of land use and land cover (LULC) dynamics on soil erosion and sediment yield in Ethiopia. *Heliyon*, *5*(12), p.e02981.

Moss, R.H., Edmonds, J.A., Hibbard, K.A., Manning, M.R., Rose, S.K., Van Vuuren, D.P., Carter, T.R., Emori, S., Kainuma, M., Kram, T. and Meehl, G.A., 2010. The next generation of scenarios for climate change research and assessment. Nature, 463(7282), pp.747-756.

Mwangi, W.W., Ho, K.W., Tey, B.T. and Chan, E.S., 2016. Effects of environmental factors on the physical stability of pickering-emulsions stabilized by chitosan particles. Food Hydrocolloids, 60, pp.543-550.

Natkhin, M., Dietrich, O., Schäfer, M.P. and Lischeid, G., 2015. The effects of climate and changing land use on the discharge regime of a small catchment in Tanzania. Regional Environmental Change, 15(7), pp.1269-1280.

Negash Tessema Asfaw Kebede Dame Yadeta, 2020. Modelling the effects of climate change on streamflow using climate and hydrological models: the case of the Kesem sub-basin of the Awash River basin, Ethiopia. International Journal of River Basin Management, pp.1-12.

Ngaina, J., Muthama, N., Mukhala, E. and Maingi, N., 2015. Variability and trends in past, current and future climate in East Africa.

Nikulin, G., Jones, C., Giorgi, F., Asrar, G., Büchner, M., Cerezo-Mota, R., Christensen, O.B., Déqué, M., Fernandez, J., Hänsler, A. and van Meijgaard, E., 2012. Precipitation climatology in an ensemble of CORDEX-Africa regional climate simulations. Journal of Climate, 25(18), pp.6057-6078.

Nikulin, G., Lennard, C., Dosio, A., Kjellström, E., Chen, Y., Hänsler, A., Kupiainen, M., Laprise, R., Mariotti, L., Maule, C.F. and van Meijgaard, E., 2018. The effects of 1.5 and 2 degrees of global warming on Africa in the CORDEX ensemble. Environmental Research Letters, 13(6), p.065003.

Ning, T., Li, Z. and Liu, W., 2016. Separating the impacts of climate change and land surface alteration on runoff reduction in the Jing River catchment of China. Catena, 147, pp.80-86

Obahoundje, S., Ofosu, E.A., Akpoti, K. and Kabo-bah, A.T., 2017. Land use and land cover changes under climate uncertainty: modelling the impacts on hydropower production in Western Africa. Hydrology, 4(1), p.2.

Osima, S., Indasi, V.S., Zaroug, M., Hussen Seid., Gudoshava, M., Misiani, H.O., Nimusiima, A., Anyah, R.O., Otieno, G., Ogwang, B.A. and Jain, S., 2018. Projected climate over the Greater Horn of Africa under 1.5 C and 2 C global warming. Environmental Research Letters, 13(6), p.065004.

Parsa, V. A., Yavari, A., Nejadi, A. (2016): Spatio-temporal analysis of land use/land cover pattern changes in Arasbaran Biosphere Reserve: Iran. – Modeling Earth Systems and Environment 2 (4): 178.

Neitsch, S.L., Arnold, J.G., Kiniry, J.R. and Williams, J.R., 2011. *Soil and water assessment tool theoretical documentation version 2009*. Texas Water Resources Institute.

Pinto, I., Lennard, C., Tadross, M., Hewitson, B., Dosio, A., Nikulin, G., Panitz, H.J. and Shongwe, M.E., 2016. Evaluation and projections of extreme precipitation over southern Africa from two CORDEX models. Climatic Change, 135(3-4), pp.655-668.

Pizzigalli, C., Palatella, L., Zampieri, M., Lionello, P., Miglietta, M.M. and Paradisi, P., 2012. Dynamical and statistical downscaling of precipitation and temperature in a Mediterranean area. Italian Journal of Agronomy, 7(1), pp.e2-e2.

Reddy, M.A. and Reddy, A., 2008. Textbook of remote sensing and geographical information systems (pp. 4-4). Hyderabad: BS publications.

Riahi, K., Rao, S., Krey, V., Cho, C., Chirkov, V., Fischer, G., Kindermann, G., Nakicenovic, N. and Rafaj, P., 2011. RCP 8.5—A scenario of comparatively high greenhouse gas emissions. Climatic change, 109(1), pp.33-57.

Rummukainen, M., 2010. State-of-the-art with regional climate models. Wiley Interdisciplinary Reviews: Climate Change, 1(1), pp.82-96.

Rwigi, S.K., 2014. Analysis of Potential Impacts of Climate Change and Deforestation on Surface Water Yields from the Mau Forest Complex Catchments in Kenya (Doctoral dissertation, University of Nairobi).

Samuel Kassa, 2016. The impact of land use land cover change on watershed hydrology (a case study of upper awash basin).

Samule Tesfaye, Gebeyehu Taye, Emiru Birhane and S.E van der Zee, 2019. Observed and model simulated twenty-first century hydro-climatic change of Northern Ethiopia. Journal of Hydrology: Regional Studies, 22, p.100595.

Shongwe, M.E., Lennard, C., Liebmann, B., Kalognomou, E.A., Ntsangwane, L. and Pinto, I., 2015. An evaluation of CORDEX regional climate models in simulating precipitation over Southern Africa. Atmospheric Science Letters, 16(3), pp.199-207.

Sisay Nune, Teshome Soromessa and Demel Teketay 2016. Land use and land cover change in the Bale mountain eco region of Ethiopia during 1985 to 2015. Land 5:41 . DOI: 10.3390/land5040041

Soni, S., Garg, P.K., Singh, A. and Maurya, A.K., 2015. Assessment of land use land cover change in Chakrar watershed using geospatial technique. Tropical Plant Research, 2(2), pp.101-107.

Subedi, P., Subedi, K., Thapa, B. (2013): Application of a hybrid cellular automaton Markov (CA-Markov) Model in land-use change prediction: a case study of saddle creek drainage Basin, Florida. – Applied Ecology and Environmental Sciences 1(6): 126-132.

Subramanya, K., 2013. Hydraulic machines. Tata McGraw-Hill Education.

Kassa Tadele, and Gerd Förch, 2007. Impact of land use/cover change on streamflow: the case of Hare River Watershed, Ethiopia. In Catchment and lake research, proceedings 2nd Lake Abaya research symposium (LARS), Arba Minch, Ethiopia.

Wakjira Takala, Tamene Adugna and Dawud Tamam, (2016) Land use and land cover change analysis using multi temporal Landsat data in Gilgel Gibe, Omo Gibe basin, Ethiopia. International journal of science and technology Volume 5 No.7. Center of professional research publications.

Piani, C., Weedon, G.P., Best, M., Gomes, S.M., Viterbo, P., Hagemann, S. and Haerter, J.O., 2010. Statistical bias correction of global simulated daily precipitation and temperature for the application of hydrological models. *Journal of hydrology*, *395*(3-4), pp.199-215.

Tang, F.F., Xu, H.S. and Xu, Z.X., 2012. Model calibration and uncertainty analysis for runoff in the Chao River Basin using sequential uncertainty fitting. Procedia Environmental Sciences, 13, pp.1760-1770.

Tarik Alemayehu, 2017. Modeling the imact of land use/landcover dynamics on stream flow and sediment yield.

Taylor, K.E., Stouffer, R.J. and Meehl, G.A., 2012. An overview of CMIP5 and the experiment design. Bulletin of the American meteorological Society, 93(4), pp.485-498.

Tekalegn Ayele, Nadir Ahmed, L. Ribbe,. and J. Heinrich., 2018. Catchment response to climate and land use changes in the Upper Blue Nile sub-basins, Ethiopia. Science of the total environment, 644, pp.193-206.

Temesgen Gashaw, Taffa Tulu, Mekuria Argaw, Abeyou w., Terefe Tolessa and Mengistie Kindu, 2018. Estimating the impacts of land use/land cover changes on Ecosystem Service Values: The case of the Andassa watershed in the Upper Blue Nile basin of Ethiopia. *Ecosystem Services*, *31*, pp.219-228.

Temesgen Gashaw., Amare Bantider., Abraham Mahari. 2014. Population dynamics and land use/land cover changes in Dera District, Ethiopia. GJBAHS. 3(1):137-140.

Tesfa Gebrie & Bogale Gebremariam, 2015. Impact of Land Use Land Cover Change on Stream Flow and Sediment Yield : A Case Study of Gilgel Abay Watershed, Lake

Tana Sub-basin, Ethiopia. International Journal of Technology Enhancement and Emerging Engineering Research, 3, 28–42.

Tsegazeab Dejene, 2014. Tandem Reservoir Operation of Cascade Hydropower Plants Case of Genale-Dawa River Basin (Doctoral dissertation, Addis Ababa).

Tesfaye Gragn, Asfaw Kebede and Shimelies Berhanu, 2019. Evaluation of Climate Change Impacts on the Water Resources of Awata River Watershed, Genale Dawa Basin: Southern Ethiopia.

Teutschbein, C. and Seibert, J., 2012. Bias correction of regional climate model simulations for hydrological climate-change impact studies: Review and evaluation of different methods. Journal of hydrology, 456, pp.12-29.

Thomson, A.M., Calvin, K.V., Smith, S.J., Kyle, G.P., Volke, A., Patel, P., Delgado-Arias, S., Bond-Lamberty, B., Wise, M.A., Clarke, L.E. and Edmonds, J.A., 2011. RCP4. 5: a pathway for stabilization of radiative forcing by 2100. Climatic change, 109(1), pp.77-94.

Trolle, D., Nielsen, A., Andersen, H.E., Thodsen, H., Olesen, J.E., Børgesen, C.D., Refsgaard, J.C., Sonnenborg, T.O., Karlsson, I.B., Christensen, J.P. and Markager, S., 2019. Effects of changes in land use and climate on aquatic ecosystems: Coupling of models and decomposition of uncertainties. Science of the Total Environment, 657, pp.627-633.

Tufa Negewo and A.K Sarma, 2021. Evaluation of Climate Change-Induced Impact on Streamflow and Sediment Yield of Genale Watershed, Ethiopia.

Umair, M., Kim, D. and Choi, M., 2019. Impacts of land use/land cover on runoff and energy budgets in an East Asia ecosystem from remotely sensed data in a community land model. Science of the Total Environment, 684, pp.641-656.

Van Vuuren, D.P., Lowe, J., Stehfest, E., Gohar, L., Hof, A.F., Hope, C., Warren, R., Meinshausen, M. and Plattner, G.K., 2011. How well do integrated assessment models simulate climate change?. Climatic change, 104(2), pp.255-285.

Van Vuuren, D.P., Stehfest, E., den Elzen, M.G., Kram, T., van Vliet, J., Deetman, S., Isaac, M., Goldewijk, K.K., Hof, A., Beltran, A.M. and Oostenrijk, R., 2011. RCP2. 6: exploring the possibility to keep global mean temperature increase below 2 C. Climatic change, 109(1), pp.95-116.

Wakjira Takala, K. Miegel, and Tamene A. Demissie, 2019. Evaluation of the CORDEX regional climate models performance in simulating climate conditions of two catchments in Upper Blue Nile Basin. Dynamics of Atmospheres and Oceans, 87, p.101104.

Wakjira Takala, K. Miegel, and Tamene A. Demissie, 2020. Watershed hydrological response to combined land use/land cover and climate change in highland Ethiopia: Finchaa catchment. Water, 12(6), p.1801.\aa

Wang, H., Tetzlaff, D. and Soulsby, C., 2018. Modelling the effects of land cover and climate change on soil water partitioning in a boreal headwater catchment. Journal of Hydrology, 558, pp.520-531.

Wayne, J.H., Casper, W.J., Matthews, R.A. and Allen, T.D., 2013. Family-supportive organization perceptions and organizational commitment: The mediating role of work–family conflict and enrichment and partner attitudes. Journal of applied psychology, 98(4), p.606.

Wilby, R.L. and Dawson, C.W., 2013. The statistical downscaling model: insights from one decade of application. International Journal of Climatology, 33(7), pp.1707-1719.

Wise, M., Calvin, K., Thomson, A., Clarke, L., Bond-Lamberty, B., Sands, R., Smith, S.J., Janetos, A. and Edmonds, J., 2009. Implications of limiting CO2 concentrations for land use and energy. Science, 324(5931), pp.1183-1186.

Woldeamlak Bewket and Solomon Abebe, S., 2013. Land-use and land-cover change and its environmental implications in a tropical highland watershed, Ethiopia. International journal of environmental studies, 70(1), pp.126-139.

Wu, F., Zhan, J., Yan, H., Shi, C. and Huang, J., 2013. Land cover mapping based on multisource spatial data mining approach for climate simulation: a case study in the farming-pastoral ecotone of North China. Advances in Meteorology, 2013.

Wuletaw Abera, Lulseged Tamene, Assefa Abegaz and Dawit Solomon, 2019. Understanding climate and land surface changes impact on water resources using Budyko framework and remote sensing data in Ethiopia. Journal of Arid Environments, 167, pp.56-64.

Xu, C.Y., 1999. From GCMs to river flow: a review of downscaling methods and hydrologic modelling approaches. Progress in physical Geography, 23(2), pp.229-249.

Yang, L., Feng, Q., Yin, Z., Wen, X., Si, J., Li, C. and Deo, R.C., 2017. Identifying separate impacts of climate and land use/cover change on hydrological processes in upper stream of Heihe River, Northwest China. Hydrological Processes, 31(5), pp.1100-1112.

Sahalu ,Atalel, 2014. Analysis of urban land use and land cover changes: a case of study in Bahir Dar, Ethiopia (Doctoral dissertation).

Yin, J., He, F., Xiong, Y.J. and Qiu, G.Y., 2017. Effects of land use/land cover and climate changes on surface runoff in a semi-humid and semi-arid transition zone in northwest China. Hydrology and Earth System Sciences, 21(1), pp.183-196.

Zuo, C., Huang, L., Zhang, M., Chen, Q. and Asundi, A., 2016. Temporal phase unwrapping algorithms for fringe projection profilometry: A comparative review. *Optics and lasers in engineering*, *85*, pp.84-103.

Yitea Seneshaw and Van Lanen, 2015. Assessing the impacts of land use-cover change on hydrology of melka Kuntrie subbasin in Ethiopia, using a conceptual hydrological model. Hydrology: Current Research, 6(3), p.1.

Zhang, L., Karthikeyan, R., Bai, Z. and Srinivasan, R., 2017. Analysis of streamflow responses to climate variability and land use change in the Loess Plateau region of China. Catena, 154, pp.1-11.

7. APPENDICES

7.1.Appendix A. Tables

Tables **1:** Mean Monthly Flow for Only LULC under Baseline and future Period

	Past Land Use land cover			Future Land Use land cover	
Month	LULC1985	LULC 2000	LULC2015	LULC 2035	LULC2055
JAN	18.57	18.63	18.12	18.23	18.48
FEB	12.89	12.42	12.12	12.46	12.05
MAR	20.58	20.16	20.87	21.57	21.92
APR	67.58	67.58	66.59	67.75	68.73
MAY	88.32	89.35	89.64	92.06	93.17
JUN	53.82	54.08	54.16	52.26	51.28
JUL	44.75	43.54	42.64	42.45	41.40
AUG	42.13	43.21	44.84	45.67	45.88
SEP	45.26	45.51	46.98	46.37	46.78
OCT	81.17	82.40	82.87	83.46	84.97
NOV	61.06	62.37	65.19	66.22	67.63
DEC	37.77	37.26	37.11	36.39	35.79
Annual	**573.90**	**576.50**	**581.14**	**584.88**	**588.06**

Tables **2:** Major soil type of the watershed

No	Soil Types	Area in (ha)	Area in (KM^2)	Area in %
1	Chromic luvisols	16093.62	160.94	21.95
2	Chromic vertisols	19367.5	193.67	26.42
3	Dystric histosols	784.93	7.85	1.07
4	Eutric cambisols	5004.53	50.05	6.83
5	Eutric fluvisols	11.85	0.12	0.02
6	Eutric nitisols	251.10	2.51	0.34
7	Leptosols	4057.41	40.57	5.53
8	Pellic vertisols	27736.4	277.36	37.84

Tables **3:** Meteorological data used for SWAT model (1985-2015) for Delo Mena Station

description	Jan	Feb	Mar	Apr	May	Jun	Jul	Aug	Sep	Oct	Nov	Dec
PCP_MM	23.81	25.64	95.21	211.58	210.58	38.64	23.99	37.65	86.54	188.94	87.42	29.59
PCPSTD	3.15	3.33	6.67	9.15	8.66	3.16	2.27	3.42	5.43	8.50	6.86	3.43
PCPSKW	6.53	5.88	3.08	1.57	1.65	3.11	4.04	4.77	3.18	1.70	3.25	5.96
PR_W1	0.06	0.07	0.15	0.41	0.44	0.14	0.14	0.16	0.33	0.33	0.17	0.06
PR_W2	0.47	0.54	0.64	0.73	0.70	0.42	0.42	0.46	0.59	0.75	0.66	0.65
PCPD	3.35	3.71	9.32	18.87	19.42	6.23	6.35	7.58	13.87	18.81	10.84	5.45
TMPMX	30.46	31.46	31.27	28.92	27.76	26.91	26.28	28.06	28.61	27.57	28.12	29.27
TMPMN	13.79	14.85	15.9	16.78	16.91	16.31	16.06	16.01	16.36	16.19	14.89	13.44
MPSTDMX1	1.69	1.93	2.39	2.68	1.99	2.15	2.25	1.86	1.80	1.81	1.62	1.50
TMPSTDM	1.59	1.61	1.88	1.01	1.25	1.14	1.40	1.44	1.18	1.13	1.71	1.65
RAINHHMX1	11.91	12.82	47.61	105.79	105.29	19.32	12.00	18.83	43.27	94.47	43.71	14.80
SOLARAV1	24.58	26.18	25.66	23.06	21.83	20.43	19.50	21.18	21.93	21.45	22.70	23.99
DEWPT1	12.46	12.06	14.92	18.65	19.22	17.51	16.58	16.85	16.94	17.72	16.54	14.29
WNDAV1	3.06	3.16	3.02	2.57	2.73	3.29	3.17	2.97	2.41	2.52	2.95	3.04
				Rira Rainfall Station								
PCP_MM	25.95	30.05	71.46	158.44	109.15	52.49	109.29	125.82	97.97	115.22	50.94	28.51
PCPSTD	2.46	3.11	4.29	6.52	4.92	3.65	4.40	4.91	4.04	4.93	3.93	2.40
PCPSKW	4.30	2.99	1.66	1.61	4.29	2.01	1.76	1.53	1.59	3.57	3.46	4.30
PR_W1	0.08	0.09	0.20	0.36	0.27	0.23	0.36	0.41	0.40	0.31	0.17	0.10
PR_W2	0.62	0.71	0.77	0.73	0.61	0.77	0.74	0.72	0.75	0.63	0.67	0.62
PCPD	5.71	5.97	12.97	19.23	16.23	11.94	19.77	20.1	18.74	18.29	9.97	8.1
TMPMX	22.21	23.01	23.01	22.01	21.68	21.57	20.85	20.87	21.02	20.69	20.88	21.4
TMPMN	8.8	9.27	9.55	10.53	10.68	10.3	9.94	9.99	10.13	10.02	9.37	8.75
MPSTDMX1	1.09	1.21	1.53	1.73	1.72	1.53	1.32	1.48	1.42	1.33	1.27	1.14
TMPSTDM	2.04	1.88	2.62	1.46	1.30	1.55	1.62	1.45	1.46	1.55	1.32	1.89
DEWPT1	7.58	6.78	9.15	12.95	13.37	12.77	12.2	12.16	12.28	12.45	11.13	9.14

Tables **4:** Mean monthly flow for Climate Change only simulation under RCP4.5 and RCP8.5

	Land Use Near future period (2021-2050) and Mid future period (2051-2080)			
Month	Near –term RCP4.5	Midterm RCP4.5	Near-term RCP8.5	MidtermRCP8.5
JAN	22.99	25.89	24.23	24.92
FEB	11.94	11.61	11.70	10.97
MAR	27.31	26.06	27.23	24.05
APR	77.08	76.77	71.56	71.95
MAY	126.45	124.00	121.00	120.59
JUN	61.91	58.51	59.52	56.72
JUL	35.14	32.61	33.54	32.15
AUG	16.05	16.69	15.25	17.32
SEP	26.92	20.84	26.42	21.47
OCT	95.13	105.59	95.43	106.25
NOV	83.41	86.06	86.09	85.43
DEC	41.13	44.42	42.66	44.57
Annual	**625.46**	**629.06**	**614.61**	**616.40**

Tables **5:** Mean Monthly Flow for Combined Simulation under RCP4.5 and RCP8.5

	Land Use 2035 (2021-2050)		**Land Use 2055(2051-2080)**	
Month	Near-term RCP4.5	Near-term RCP8.5	Midterm RCP4.5	MidtermRCP8.5
JAN	23.05	24.31	26.54	25.53
FEB	11.92	11.69	11.85	11.15
MAR	27.17	27.09	25.06	23.16
APR	77.20	71.73	74.68	70.22
MAY	127.24	121.81	124.23	121.11
JUN	62.91	60.51	62.00	60.28
JUL	35.66	34.05	34.44	33.99
AUG	16.19	15.36	17.15	17.74
SEP	26.79	26.27	20.30	20.82
OCT	95.07	95.33	103.42	103.73
NOV	83.67	86.33	87.14	86.28
DEC	41.48	43.03	46.42	46.44
Annual	**628.36**	**617.52**	**633.23**	**620.47**

Tables **6:** Projected maximum and minimum Temperature for near and midterm underRCP4.5 and RCP8.5 scenarios

	Baseline Tp Max	**Max Temp RCP4.5**		**Max Temp RCP8.5**	
Month		Near RCP4.5	Mid RCP4.5	Near RCP8.5	MidRCP8.5
JAN	30.46	31.06	27.67	29.79	31.17
FEB	31.46	30.12	28.36	30.10	31.46
MAR	31.27	28.95	29.24	30.11	31.48
APR	28.92	27.79	30.57	29.71	31.21
MAY	27.76	27.21	31.52	29.43	31.00
JUN	26.91	27.16	32.14	29.22	30.55
JUL	26.28	27.65	31.89	28.97	30.07
AUG	28.06	28.67	31.25	28.95	30.07
SEP	28.61	29.72	30.00	29.41	30.46
OCT	27.57	30.99	28.98	28.96	30.19
NOV	28.12	31.55	27.92	29.19	30.37
DEC	29.27	31.64	27.73	29.36	30.60
Annual	**28.72**	**29.38**	**29.77**	**29.43**	**30.72**
	Tpmin	**Min Temp RCP8.5**		**Min Temp RCP8.5**	
JAN	14.29	17.93	14.64	18.03	15.35
FEB	14.85	16.95	15.39	16.96	16.33
MAR	15.9	15.77	16.31	15.76	17.47
APR	16.78	14.62	17.67	14.85	18.96
MAY	16.91	14.13	18.58	14.14	20.01
JUN	16.31	14.12	19.12	14.34	20.20
JUL	16.06	14.68	18.80	14.81	19.88
AUG	16.01	15.77	18.10	15.83	18.94
SEP	16.36	16.85	16.83	17.08	17.71
OCT	16.19	18.12	15.77	18.10	16.49
NOV	15.29	18.62	14.73	18.67	15.47
DEC	15.44	18.63	14.66	18.49	15.23
Annual	**15.87**	**16.35**	**16.72**	**16.42**	**17.67**

Tables 7: Projected mean monthly and % of rainfall under RCP4.5 and RCP8.5.

		RCP4.5				RCP8.5			
Month	**A**	**NRF**	**%**	**MRF**	**%**	**NRF**	**%**	**MRF**	**%**
JAN	23.81	29.10	22.20	29.35	23.28	28.28	18.79	29.42	23.55
FEB	25.64	27.96	9.05	25.15	-1.90	26.76	4.38	25.99	1.38
MAR	95.21	96.84	1.71	91.82	-3.56	95.59	0.40	91.17	-4.24
APR	211.58	197.65	-6.58	198.94	-5.97	191.8	-9.38	199.80	-5.57
MAY	210.58	204.30	-2.98	210.50	-0.04	205.3	-2.50	210.12	-0.22
JUN	38.64	32.68	-15.43	32.51	-15.87	33.42	-13.52	32.99	-14.62
JUL	23.99	26.30	9.64	27.37	14.10	25.95	8.16	27.58	14.95
AUG	37.65	34.49	-8.38	40.56	7.74	31.95	-15.14	41.78	10.98
SEP	86.54	100.97	16.67	86.72	0.21	98.68	14.03	87.92	1.60
OCT	188.94	190.07	0.60	209.22	10.74	192.6	1.94	208.22	10.20
NOV	87.42	93.77	7.27	92.43	5.73	96.35	10.22	93.50	6.96
DEC	29.59	26.83	-9.32	28.27	-4.46	28.10	-5.04	28.65	-3.19

Nate: A= Represent observed rainfall, **NRF** = Near-term Rainfall, **MRF**= midterm rainfall and **%** = percentage change of future rainfall from baseline period.

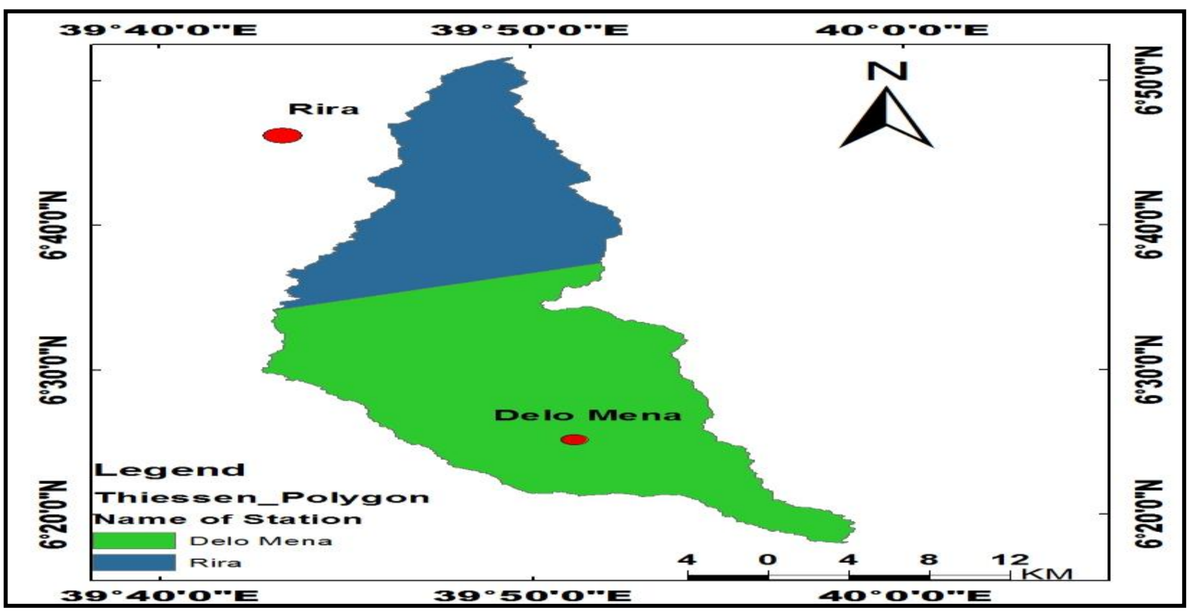

Figures 1: Thiessen polygon of the station